

UNCLASSIFIED

AD NUMBER
ADB198116
NEW LIMITATION CHANGE
TO Approved for public release, distribution unlimited
FROM Distribution authorized to U.S. Govt agencies only; Specific Authority; 11 Apr 95. Other requests shall be referred to RL [OCTM], 26 Electronic Pky, Griffiss AFB, NY 13441-4514.
AUTHORITY
AFRL/IFOIP ltr, 15 Jun 2004

THIS PAGE IS UNCLASSIFIED

RL-TR-95-11
Final Technical Report
February 1995



MULTICHANNEL DETECTION USING HIGHER- ORDER STATISTICS

Scientific Studies Corporation

J.R. Roman and D.W. Davis



*DISTRIBUTION AUTHORIZED TO U.S. GOVERNMENT AGENCIES ONLY; SPECIFIC
AUTHORITY: ~~DDP FAR SUPPLEMENT 252.227-7013, ALT. II.~~ OTHER REQUESTS FOR THIS
DOCUMENT SHALL BE REFERRED TO RL(OCTM), GRIFFISS AFB, NY.*

11 APR 1995

13441-4514

GOVERNMENT PURPOSE LICENSE RIGHTS (SBIR PROGRAM)

Contract No: F30602-93-C-0143

Contractor: Scientific Studies Corporation

For a period of four (4) years after delivery and acceptance of the last deliverable item under the above contract, this technical data shall be subject to the restrictions contained in the definition of "Limited Rights" in DFARS clause at 252.227-7013. After the four-year period, the data shall be subject to the restrictions contained in the definition of "Government Purpose License Rights" in DFARS clause at 252.227-7013. The Government assumes no liability for unauthorized use or disclosure by others. This legend, together with the indications of the portions of the data which are subject to such limitations, shall be included on any reproduction hereof which contains any portions subject to such limitations and shall be honored only as long as the data continues to meet the definition on Government purpose license rights.

19950407 149

Rome Laboratory
Air Force Materiel Command
Griffiss Air Force Base, New York

THIS COPY IS UNCLASSIFIED

RL-TR-95-11 has been reviewed and is approved for publication.

APPROVED:



JAMES H. MICHELS, Ph.D.
Project Engineer

FOR THE COMMANDER:



FRED J. DEMMA
Acting Director
Surveillance & Photonics Directorate

DESTRUCTION NOTICE - For classified documents, follow the procedures in DOD 5200.22M, Industrial Security Manual or DOD 5200.1-R, Information Security Program Regulation. For unclassified limited documents, destroy by any method that will prevent disclosure of contents or reconstruction of the document.

If your address has changed or if you wish to be removed from the Rome Laboratory mailing list, or if the addressee is no longer employed by your organization, please notify RL (^{OCTM}) Griffiss AFB NY 13441. This will assist us in maintaining a current mailing list.

Do not return copies of this report unless contractual obligations or notices on a specific document require that it be returned.

REPORT DOCUMENTATION PAGE

Form Approved
OMB No. 0704-0188

Public reporting burden for this collection of information is estimated to average 1 hour per response, including the time for reviewing instructions, searching existing data sources, gathering and maintaining the data needed, and completing and reviewing the collection of information. Send comments regarding this burden estimate or any other aspect of this collection of information, including suggestions for reducing this burden, to Washington Headquarters Services, Directorate for Information Operations and Reports, 1215 Jefferson Davis Highway, Suite 1204, Arlington, VA 22202-4302, and to the Office of Management and Budget, Paperwork Reduction Project (0704-0188), Washington, DC 20503.

1. AGENCY USE ONLY (Leave Blank)		2. REPORT DATE February 1995		3. REPORT TYPE AND DATES COVERED Final May 93 - Nov 93	
4. TITLE AND SUBTITLE MULTICHANNEL DETECTION USING HIGHER-ORDER STATISTICS				5. FUNDING NUMBERS C - F30602-93-C-0143 PE - 65502F PR - 3005 TA - RD WU - 34	
6. AUTHOR(S) J.R. Roman and D.W. Davis					
7. PERFORMING ORGANIZATION NAME(S) AND ADDRESS(ES) Scientific Studies Corporation 2250 Quail Ridge Palm Beach Gardens FL 33418				8. PERFORMING ORGANIZATION REPORT NUMBER SSC-TR-94-01	
9. SPONSORING/MONITORING AGENCY NAME(S) AND ADDRESS(ES) Rome Laboratory (OCTM) 26 Electronic Pky Griffiss AFB NY 13441-4514				10. SPONSORING/MONITORING AGENCY REPORT NUMBER RL-TR-95-11	
11. SUPPLEMENTARY NOTES Rome Laboratory Project Engineer: James H. Michels, Ph.D./OCTM/(315) 330-4432					
12a. DISTRIBUTION/AVAILABILITY STATEMENT USGO Agencies only; specific authority; DDP FOR CDD 253.227-7019, ALT 11. Other requests RL (OCTM), 26 Electronic Pky, Griffiss AFB NY 13441-4514.				12b. DISTRIBUTION CODE 11 APR 1995	
13. ABSTRACT (Maximum 200 words) A methodology was developed for the detection of an unknown signal observed simultaneously over multiple channels. The model-based approach was adopted, with a binary decision space. In model-based detection, the parameters of a model are identified from the multichannel process, and the identified model is used to facilitate detection of the desired signal. Identification methods based on higher-order statistics were adopted to estimate the model parameters. The formulation developed in this program is generic but, in Phase I, emphasis was placed on airborne surveillance radar array applications. In such systems, the array elements constitute the channel outputs. Ground clutter, interference sources, and noise sources are present in the multiple channel outputs along with the target signal. Applicability of the technique to surveillance radar array systems was established by identifying several radar operational conditions wherein target and/or clutter exhibit non-Gaussian statistics. Additionally, a processing option was identified to modify the channel output data and enhance its non-Gaussian characteristics. Simulation-based analyses were carried out to investigate key technical issues, and to validate fundamental aspects. Results indicate the methodology can discriminate between target-present and target-absent conditions.					
14. SUBJECT TERMS Multichannel, Higher-order statistics, Identification, Detection				15. NUMBER OF PAGES 152	
				16. PRICE CODE	
17. SECURITY CLASSIFICATION OF REPORT UNCLASSIFIED	18. SECURITY CLASSIFICATION OF THIS PAGE UNCLASSIFIED	19. SECURITY CLASSIFICATION OF ABSTRACT UNCLASSIFIED	20. LIMITATION OF ABSTRACT SAR		

Accession For	
NTIS CRA&I	<input type="checkbox"/>
DTIC TAB	<input checked="" type="checkbox"/>
Unannounced	<input type="checkbox"/>
Justification	
By	
Distribution/	
Availability Codes	
Dist	Avail and/or Special
B-3	

TABLE OF CONTENTS

LIST OF FIGURES	v
LIST OF TABLES	vii
LIST OF MNEMONICS	ix
LIST OF MATHEMATICAL SYMBOLS	xi
1.0 INTRODUCTION	1
1.1 Notation.....	5
1.2 Report Overview.....	5
2.0 PROBLEM DEFINITION	7
2.1 Airborne Surveillance Radar.....	11
2.1.1 Alternative Probabilistic Descriptions	14
2.1.2 Non-Gaussian Clutter Scenarios and Probabilistic Models	21
2.1.3 Non-Gaussian Target Probabilistic Models	28
2.1.4 Surveillance Radar Scenarios With Non-Gaussian Signals	30
2.2 Time Series Models.....	32
2.3 Third-Order Cumulants.....	41
2.3.1 Definitions, Properties, and Other Issues	41
2.3.2 Third-Order Cumulant Relations for Time Series Systems	46
3.0 DETECTION METHODOLOGY	63
3.1 Detector Architecture Configurations.....	64
3.2 Detection Domain.....	66

3.3	Pre-Processing Option.....	68
3.4	Detection Rule.....	71
3.5	Digital Realizations For Whitening Filters.....	73
3.5.1	Moving Average System Whitening Filter.....	74
3.5.2	Auto-Regressive System Whitening Filter.....	76
3.5.3	Auto-Regressive Moving Average System Whitening Filter	76
4.0	IDENTIFICATION ALGORITHMS	79
4.1	Third-Order Cumulants Estimation.....	80
4.2	MA Parameter Identification.....	82
4.3	AR Parameter Identification.....	87
4.4	ARMA Parameter Identification.....	89
5.0	SIMULATION-BASED ANALYSES	92
5.1	Non-Gaussian Sequence Generation.....	92
5.2	Identification Algorithms Analyses.....	101
5.2.1	One-Slice MA Identification Algorithm.....	101
5.2.2	Raghuveer AR Identification Algorithm.....	109
5.2.3	Residual Time Series ARMA Identification Method.....	115
5.3	Pseudo-Innovations Sequence Analyses.....	116
6.0	CONCLUSIONS AND RECOMMENDATIONS	119
	REFERENCES	124

LIST OF FIGURES

2-1	Multichannel signal in a coherent surveillance radar array	.11
3-1	Multichannel detector configuration with on-line adaptive filter parameter identification	65
3-2	Multichannel detector off-line architecture configuration (off-line filter design)	66
3-3	Tapped delay line realization for whitening filter corresponding to a MA(M) system	75
3-4	Tapped delay line realization for whitening filter corresponding to an AR(L) system	77
3-5	Tapped delay line realization for whitening filter corresponding to an ARMA(L,M) system (with $L > M$)	78
5-1	Power spectrum of Gaussian AR(2) process	95
5-2	Power spectrum of log of Gaussian AR(2) process	95
5-3	Set-up for logarithmic pre-processing option simulation-based analyses	98
5-4	Auto-correlation of residual for AR(18) model (without pre-processing) of ARMA(3,2) plus GWN data	99
5-5	Auto-correlation of residual for AR(6) model (with log pre-processing) of ARMA(3,2) plus GWN data	100
5-6	Scatter plot for the zeros of all ten realizations in Example 5-1 (Method II)	103
5-7	Scatter plot for the zeros of all ten realizations in Example 5-2 (Method II)	105

5-8	Scatter plot for the zeros of all ten realizations in Example 5-3 (Method II)	107
5-9	Scatter plot for the poles of all ten realizations in Example 5-4 (Method II)	110
5-10	Scatter plot for the poles of all ten realizations in Example 5-5 (Method II)	112
5-11	Normalized average column error for AR matrix parameters as a function of SNR (additive Gaussian noise)	115
5-12	Central segment of pseudo-innovations auto-correlation (H0 data filtered with H0 filter) for Example 5-7	118
5-13	Central segment of pseudo-innovations auto-correlation (H1 data filtered with H0 filter) for Example 5-7	118

LIST OF TABLES

2-1	Baseband vector sequence assumptions under both hypotheses .13
2-2	Non-Gaussian clutter fluctuation PDF models22
2-3	Non-Gaussian target temporal RCS fluctuation PDF models29
2-4	Candidate military surveillance radar problems involving non-Gaussian clutter and/or targets31
2-5	Candidate non-military surveillance radar problems involving non-Gaussian clutter and/or targets31
2-6	Assumptions for the time series models40
2-7	Selected properties of higher-order cumulants45
5-1	Error statistics for the zeros of all ten realizations in the three MA examples (Method II) 108
5-2	Zero estimate errors for the three MA(2) examples using both methods 108
5-3	Error statistics for the poles of all ten realizations in the two AR examples (Method II) 113
5-4	Pole estimate errors for the two AR(2) examples using both methods 113
6-1	List of key technical issues and candidate resolution approaches 121

LIST OF MNEMONICS

AR	Auto-regressive
ARMA	Auto-regressive moving-average
CFAR	Constant false alarm rate
CPI	Coherent processing interval
GC	Gaussian clutter
GCP	Gaussian colored process
GS	Gaussian signal (target)
GWN	Gaussian white noise
HOS	Higher-order statistics
IBDA	Innovations-based detection algorithm
LLR	Log-likelihood ratio
LTI	Linear time-invariant
MA	Moving-average
MFD	Matrix fraction description
MVE	Minimum variance estimate
NGC	Non-Gaussian clutter
NGCP	Non-Gaussian colored process
NGS	Non-Gaussian signal (target)
NGWN	Non-Gaussian white noise
PDF	Probability density function
RCS	Radar cross-section
RL	Rome Laboratory
SIRP	Spherically-invariant random process

SNR	Signal-to-noise ratio
SSC	Scientific Studies Corporation
SVD	Singular value decomposition
VLSI	Very large scale integration
1-D	One-dimensional
2-D	Two-dimensional

LIST OF MATHEMATICAL SYMBOLS

$A(i,j)$	(i,j)th element of matrix A
$E[\bullet]$	Expected value of $[\bullet]$
I_J	J-dimensional identity matrix
O_J	$J \times J$ null (zero) matrix
$O_{J,L}$	$J \times L$ null (zero) matrix
$O(N)$	On the order of N operations
a_{ij}	(i,j)th element of matrix A
$a(i,j)$	(i,j)th element of matrix A
$\det(\bullet)$	Determinant of matrix (\bullet)
$\text{diag}(\bullet)$	Diagonal of matrix (\bullet)
m	Discrete lag index
$\max\{\bullet\}$	Maximum of set or sequence $\{\bullet\}$
$\min\{\bullet\}$	Minimum of set or sequence $\{\bullet\}$
n	Discrete time index
$\delta(n)$	One-dimensional discrete impulse function
$\delta(n_1, n_2)$	Two-dimensional discrete impulse function
δ_{ijk}	Kronecker delta function
$[0]_M$	$M \times M$ null (zero) matrix
$[0]_{N,M}$	$N \times M$ null (zero) matrix
$\underline{0}$	Null (zero) vector of compatible dimensions
$\underline{0}_M$	M-dimensional null (zero) vector
$[\bullet]^*$	Conjugate of $[\bullet]$
$[\bullet]^H$	Hermitian (conjugate) transpose of $[\bullet]$

$[\bullet]^T$	Transpose of $[\bullet]$
$\widehat{(\bullet)}$	Estimate of (\bullet)
$(\bullet)^{-1}$	Inverse of (\bullet)
$(\bullet)^\dagger$	Pseudoinverse of (\bullet)
$\{\bullet\}$	Elements of a sequence or set
$ \bullet $	Absolute value of a real- or complex-valued scalar; magnitude of a vector; determinant of a matrix
:	Separates distinct subscript elements of a vector or matrix
;	Separates distinct arguments of a function; separates distinct indices in a subscript expression
=	Equal to
\approx	Approximately equal to
>	Greater than
\geq	Greater than or equal to
<	Less than
\leq	Less than or equal to
\perp	Is orthogonal to
\in	Is an element of
\forall	For all
\oplus	Direct sum of two vector spaces
\otimes	Kronecker product of matrices and/or vectors

1.0 INTRODUCTION

Various important applications involve the processing of time-tagged streams of data collected over multiple spatially-distributed channels. Such applications arise in the military area as well as in the commercial sector. Military applications include radar, sonar, sensor fusion, communications, and seismic event detection for monitoring of nuclear test ban treaty compliance. Non-military applications include non-destructive evaluation, earthquake activity detection, medical technology, and flood forecasting and control in hydrologic systems. The data can be collected either simultaneously over all channels, or with a time delay between channels. However, in most cases the data exhibits both temporal and spatial correlations. This characteristic offers an opportunity for joint processing of the spatial and temporal domains using techniques that can handle such conditions.

In model-based multichannel detection the objective is to determine the presence (or absence) of a desired signal component in the sensed data. This is carried out by identifying the parameters of an analytic model fit to the observed phenomenology. In this program the model class used to fit the data is a subset of the class of linear systems, and the techniques used to implement the parameter identification are based on processing estimates of the third-order statistics of the multichannel data.

The terminology "higher-order statistics" (HOS) generally denotes all statistics of order higher than two (Brillinger and Rosenblatt, 1967; Mendel, 1991); this usage is adopted in this report. Higher-order statistics are of relevance for data which does not satisfy a Gaussian distribution since, in general, statistics of all orders are required to describe distributions

other than the Gaussian (recall that the Gaussian distribution is described completely by first- and second-order statistics). Cumulants are a special type of statistic with important practical implications due to the fact that cumulants of orders third and higher are identically zero for stationary Gaussian-distributed random processes (for Gaussian-distributed processes, the first-order cumulant is the mean value, and the second-order cumulant is the covariance sequence). Third-order cumulants are of practical interest because their estimation requires significantly less computations than the estimation of cumulants of orders four and higher. Besides, in many cases it is sufficient to process only third-order cumulants in order to determine non-Gaussianity of the data, and to allow effective estimation of model parameters.

As indicated above, model-based multichannel detection methodology and techniques using higher-order statistics have applicability in several areas. However, this report is focused on surveillance radar systems in general, and airborne surveillance radar systems in particular, because it is the application of most interest to the Surveillance Technology Division at Rome Laboratory (RL). Also, by carrying out analyses and simulations in the context of a specific application it is possible to reach a better understanding of the utility and applicability of the algorithms and methodologies.

The fundamental precondition for the applicability of HOS for model-based radar detection is the non-Gaussian nature of the received radar return, since HOS vanish in the case of Gaussian-distributed processes and therefore are useless for model parameter estimation. An important outcome of Phase I is the identification of several surveillance radar operational scenarios wherein target and/or clutter exhibit non-Gaussian statistics. One such scenario is the surveillance of large ocean areas at low

grazing angles to detect long-range cruise missiles flying at low altitudes over the ocean. Other important scenarios are listed in Section 2.1.4.

Utilization of higher-order cumulants in the context of surveillance radar systems is motivated also by the fact that receiver noise and interference sources are usually Gaussian-distributed and statistically-independent from the non-Gaussian clutter and target return, and corrupt the radar signal in an additive manner. Under these conditions the higher-order cumulants of the signal at each channel output are the cumulants of the target and clutter only. That is, noise and interference effects are eliminated from parameter identification algorithms based on higher-order cumulants. In practice, the effects of Gaussian-distributed noise and/or interference sources are mitigated, rather than eliminated completely, because the sequence used to estimate the cumulants is of finite duration.

The model-based multichannel detection methodology for radar arrays can be summarized as follows. Target detection is accomplished by evaluating the output of two multichannel linear time-invariant (LTI) filters, with one filter matched to the condition of clutter and noise only, and the other filter matched to the condition of target embedded in clutter and noise. Each filter is a time series model fitted to observed phenomenology. Filter design can be carried out either off-line or on-line in an adaptive manner. Multichannel filter parameters are estimated using algorithms based on third-order cumulants, where the cumulants of the multichannel data are estimated jointly over the spatial and temporal domains. Such algorithms are well suited for the condition of a desired non-Gaussian target signal embedded in additive non-Gaussian clutter and additive Gaussian noise.

Other detection methodologies are suitable for applications where non-Gaussian signals arise. Of particular interest is the methodology developed by Rangaswamy, Weiner, and Michels (1993). Their approach addresses innovations-based multichannel detection for radar surveillance scenarios in which the spatial behaviour of the return signal over a large number of radar resolution (range-azimuth) cells is described by a non-Gaussian distribution, but the temporal behaviour of the return signal at each individual resolution cell is Gaussian. The spatial return signal in these scenarios belongs to the class of random processes known as spherically invariant random processes (SIRPs). Spatial SIRPs arise in non-homogeneous clutter scenarios where the temporal behaviour of the return signal from each individual radar resolution cell is Gaussian-distributed, but the average return power fluctuates randomly from cell to cell. Thus, in an SIRP clutter model the conditional probability density function (PDF) at each individual resolution cell is Gaussian.

The SIRP-based detection methodology of Rangaswamy, Weiner, and Michels (1993) is an optimal formulation for the case of a known, constant target embedded in SIRP-type clutter. This methodology, however, cannot be applied in scenarios where the temporal behaviour of the return signal from each radar resolution cell is described by a non-Gaussian distribution. For the same reason, SIRPs cannot be used to model the temporal non-Gaussian behaviour of a target in a resolution cell.

The HOS-based detection methodology developed in Phase I can be applied to non-Gaussian temporal as well as spatial clutter scenarios. Additionally, the HOS-based methodology applies in cases where the target behaves according to a non-Gaussian distribution. It follows that the methodology developed in Phase I has broader applicability than the SIRP-based methodology. But

the SIRP-based methodology is optimal for the known, constant target case. Each approach has its merits, and both deserve continued consideration and development.

1.1 Notation

The notation conventions established herein complement the List of Mathematical Symbols. All variables and functions are in Helvetica, Chicago, Symbol, or Zapf Chancery fonts. Vector variables are denoted by underscored lower-case letters (x), including Greek letters (α). Matrices are denoted by upper-case letters (**A**), including Greek letters (**Ω**). Some scalars are denoted also by upper-case letters (for example, **J** denotes the number of channels in a surveillance radar array). Upper-case script letters (*S*) denote sets or linear spaces. The letter *j* is used to denote the imaginary unit, and is used also as an integer index; the intended usage is clear from the context.

1.2 Report Overview

An introduction to the model-based multichannel detection problem is presented in Section 2.0. This section also presents a discussion of surveillance radar problems with emphasis on non-Gaussian operational scenarios (Section 2.1). Time series models, third-order cumulants, and the associated definitions are discussed in Sections 2.2 and 2.3, respectively. The SSC model-based multichannel detection methodology is described in Section 3.0, including an important pre-processing option which allows utilization of third-order cumulants in cases where the PDF of the radar return is symmetric or Gaussian (Section 3.3). HOS-based multichannel time series parameter identification algorithms are discussed in Section 4.0. Some of these algorithms have been modified and/or extended by SSC to handle multichannel complex-

valued sequences. Section 5.0 discusses results from simulation-based analyses carried out in Phase I to investigate key concepts and issues. This includes results which establish the detection methodology potential for discrimination between target-present and target-absent hypotheses. A summary of the key technical issues identified in Phase I is presented in Section 6.0. The main conclusions and recommendations borne out of this study are discussed also in Section 6.0.

2.0 PROBLEM DEFINITION

Within the confines of airborne surveillance radar applications, multichannel formulations arise naturally in various distinct configurations. In a pre-detection radar fusion configuration involving two or more radar systems irradiating the same physical area, each channel is the output of an individual radar with a particular set of operational parameters. The radiated frequency and/or any other operational parameters (such as polarization) may be different from radar to radar (channel to channel). In a radar array configuration each channel is the output of an individual antenna element, or the output of an individual subarray (a subarray is a collection of antenna elements). The methodologies presented herein can be applied to these two configurations as well as to others. Notwithstanding, the radar array configuration is selected as the baseline for discussions.

For the radar applications of interest herein, radar target detection can be posed as a hypothesis testing problem involving the following two hypotheses:

H_0 : Desired target signal is absent

H_1 : Desired target signal is present

where H_0 is the null hypothesis, and H_1 is the alternative hypothesis. The radar detection processor must select between these two hypotheses. Selection of H_1 when H_1 is true is a correct detection, and a common measure of radar detection performance is the probability of detection. Two types of detection errors can occur: (1) selection of H_1 when H_0 is true, which results in a false alarm, and (2) selection of H_0 when H_1 is true, which results

in a missed detection. Each of these two errors has an associated probability measure: probability of false alarm for a type 1 error, and probability of miss for a type 2 error.

Model-based multichannel detection techniques of the type pursued herein are based on the premise that the received radar time sequence (after demodulation to baseband and temporal sampling) can be represented accurately for each hypothesis as the output of an analytic model defined by a unique set of model parameters. It is assumed also that the two parameteric representations (one corresponding to each hypothesis) are sufficiently distinct to allow selection of the correct hypothesis by evaluation of measures that are sensitive to those differences. Linear time-invariant (LTI) models are adopted in this program because such models allow significant modeling freedom while presenting manageable analytical and computational burdens. An important class of LTI models is the so-called time series model class, which includes moving-average (MA), auto-regressive (AR), and auto-regressive moving-average (ARMA) models; this is the model class adopted in this program. The model output is corrupted by additive Gaussian-distributed noise, which is assumed to be uncorrelated in time (white).

In the philosophy summarized above, a time series model is a representation model for the spatial or temporal statistics of the received radar signal; that is, a model which fits experimental and/or simulated statistical data. In contrast, a physical model is the result of a theoretical formulation of the physical phenomenology. Of course, physical models also fit real data. Haykin, Currie, and Kesler (1982), and Metford and Haykin (1985) have demonstrated that time series models provide an excellent fit to surveillance radar data. Their results motivate, in part, the research in this program.

A particular measure that has produced robust analytical and experimental results in the model-based detection context is the log-likelihood ratio (LLR) test. This test is the outcome of solving the hypothesis testing problem using the Neyman-Pearson criterion. The Neyman-Pearson criterion maximizes the probability of detection for a given level of probability of false alarm. The LLR test in the context of model-based detection is calculated using the innovations sequence at the output of each of two LTI filters, one for each hypothesis (of course, only the filter output corresponding to the true hypothesis is a true innovations sequence). Metford and others (Metford et al., 1982; Metford (1984); Metford and Haykin, 1985) have formulated the discrete-time version of the LLR detection test using model-based innovations, and labeled the methodology as the innovations based detection algorithm (IBDA).

In many surveillance scenarios the received radar time series includes at least one component (either target or clutter) described by a non-Gaussian distribution, and corrupted with additive Gaussian-distributed receiver and/or interference noise. An important feature which distinguishes the Gaussian distribution from others is the fact that the Gaussian distribution is defined completely in terms of its first- and second-order statistics. Thus, statistics of order third and higher assume an important role when non-Gaussian distributions are involved. The cumulants of a distribution is a set of statistics of particular interest because higher-order cumulants are zero for the Gaussian distribution, but non-zero for non-Gaussian distributions except that odd-ordered cumulants are zero for distributions with symmetry about the mean value (see, for example, Mendel [1991]).

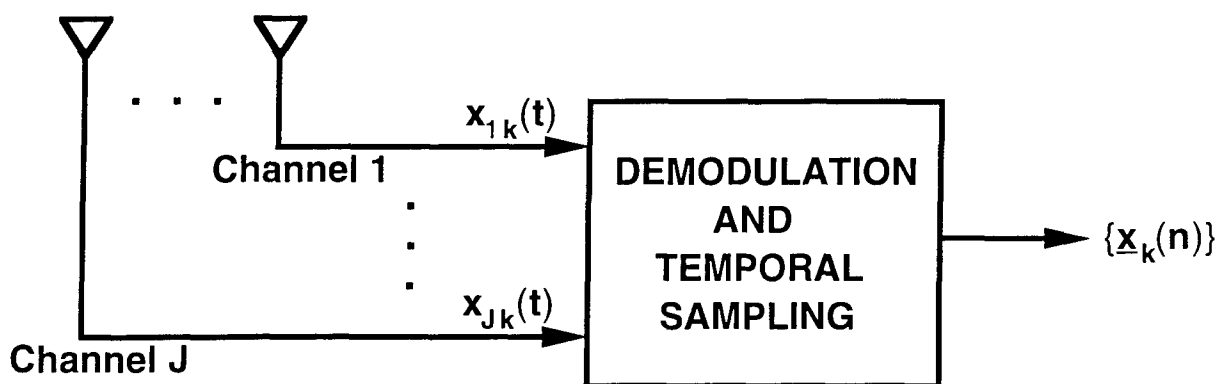
The above discussion suggests that parameter identification techniques based on cumulants can be used for model-based multichannel detection in non-Gaussian scenarios. In the approach pursued herein the parameters of a LTI time series model (MA, AR, or ARMA) are identified using techniques based on processing estimates of third-order cumulants. The effects of additive Gaussian noise are mitigated since the third-order cumulants of a Gaussian-distributed process are zero. Third-order cumulants are preferred because their estimation from data requires fewer computations than the estimation of cumulants of order four and higher. Parameter identification algorithms are developed based on the work of Giannakis, Inouye, and Mendel (1989) and Raghuveer (1986), modified and extended appropriately to handle the case of complex-valued data. An optimal LLR detection rule for the outputs of the LTI filters associated with each hypothesis requires knowledge of the multivariate PDF under each of the hypotheses. In most non-Gaussian cases this information is unavailable. However, Metford (1984) has demonstrated that the LLR detection rule for the Gaussian case is a suboptimal, approximate detection rule for the non-Gaussian case. This approximation was adopted for the work reported herein.

Strictly speaking, the utility of third-order cumulants is restricted to cases where the PDF of the radar return (quadrature components) is asymmetric about the mean value. However, it appears that the cases where the PDF is symmetric can be addressed by first applying a zero-memory nonlinear transformation to the data. Such an approach has been proposed recently by Zheng, McLaughlin, and Mulgrew (1993), with the logarithm function as the zero-memory nonlinear transformation. Their approach is discussed in Section 3.3. Results from simulation-based analyses carried out in Phase I indicate the logarithm is indeed useful for introducing asymmetry in the data PDF (see Section 5.1). This

issue has practical (as well as theoretical) significance because in many radar systems the logarithm function is used to reduce the dynamic range of the radar return.

2.1 Airborne Surveillance Radar

Consider a coherent radar array with J spatial channels (each channel is the output of either an individual array element or a sub-array composed of multiple array elements), as indicated in Figure 2-1. The radar is coherent because both in-phase and out-of-phase quadrature components are generated in each channel. In a surveillance scenario involving a down-looking radar onboard an aircraft (see, for example, Jaffer et al., [1991], or Rangaswamy et al., [1993]), the J -element, discrete-time, baseband, stationary, complex-valued, finite-duration, vector sequence $\{\underline{x}_k(n) | n=0, 1, \dots, N-1\}$ in Figure 2-1 is the return from the k th radar resolution (range-azimuth) cell received at the J channels for the duration of the coherent processing interval (CPI).



$\underline{x}_k(n)$: complex-valued, J -dimensional vector of the return from the k th range gate corresponding to the n th pulse

Figure 2-1. Multichannel signal in a coherent surveillance radar array.

In the context of a hypothesis testing formulation applied to the k th resolution cell, the null hypothesis corresponds to the case of target absent; the alternative hypothesis corresponds to the case of target present. Under the null hypothesis, the baseband vector process $\{\underline{x}_k(n)\}$ contains clutter, interference, and noise. Under the alternative hypothesis, $\{\underline{x}_k(n)\}$ also contains target information. This can be summarized as

$$(2-1a) \quad H_0: \quad \underline{x}_k(n) = \underline{c}_k(n) + \underline{w}_k(n) \quad 0 \leq n \leq N-1$$

$$(2-1b) \quad H_1: \quad \underline{x}_k(n) = \underline{s}_k(n) + \underline{c}_k(n) + \underline{w}_k(n) \quad 0 \leq n \leq N-1$$

where $\{\underline{c}_k(n)\}$ denotes the clutter process, $\{\underline{w}_k(n)\}$ denotes the combination of all noise (receiver noise, etc.) and interference processes, and $\{\underline{s}_k(n)\}$ denotes the desired target signal process. Table 2-1 lists the conditions assumed on the vector process $\{\underline{x}_k(n)\}$. Notice that selection of the initial time as $n=0$ in Equations (2-1) implies no loss of generality since the process is assumed to be stationary (in practice it suffices that the process be stationary at least for the duration of the CPI).

In a typical surveillance application over a large number of resolution cells, the data from each radar resolution cell is processed and a decision is made as to the presence or absence of a target. Various resolution cells can be processed in parallel or sequentially, depending on the design parameters of the radar system. Consider the data $\{\underline{x}_k(n)\}$ from one CPI for a specific resolution cell to which the detection criterion is being applied. This data set is referred to as the primary data. Returns from G cells in the neighborhood of the k th cell are described by the same probability distribution as the k th cell, but it is assumed that a target is not present in those cells. It is further assumed that the data in those cells is statistically independent of the data

in the k th cell. The data from these G range cells is referred to as the secondary data, and is used to set the detection threshold for the k th resolution cell. As the detection process continues, the current primary data becomes part of the secondary data corresponding to a different resolution cell.

BASEBAND VECTOR SEQUENCE ASSUMPTIONS UNDER BOTH HYPOTHESES

- Zero Mean
- Stationary
- Ergodic
- Nyquist Sampling Criterion Is Satisfied
- Noise Process Is Gaussian-Distributed and White
- Target Process Is Non-Gaussian
- Clutter Process Is Non-Gaussian
- Target, Noise, and Clutter Processes Are Independent
- Can Be Modeled as Output of a LTI System

Table 2-1. Baseband vector sequence assumptions under both hypotheses.

From this point on, the subscript k on the baseband vector sequence (this subscript denotes the resolution cell) will be deleted to simplify notation. This is appropriate also because, as discussed above, the data from each resolution cell assumes the status of primary data sometime during the process.

In most of the radar technical literature the terminology "Gaussian-distributed signal" denotes a coherent radar return with Gaussian-distributed quadrature components, Rayleigh-distributed envelope, and exponentially-distributed power (or radar cross-section, RCS). Correspondingly, "non-Gaussian signal" refers to a radar return with either non-Rayleigh envelope or non-exponential

power. This terminology, although common, can be misleading in the context of algorithms and methodologies based on third-order cumulants because the shape of the distribution of the quadrature components is a key issue when third-order cumulants are involved (as well as all odd-ordered cumulants of higher orders). To illustrate this point consider the case of a signal consisting of a constant-frequency sinusoid (representing a constant-velocity moving target) in additive Gaussian white noise. In this case the combined signal (target plus noise) envelope is described by the Rice distribution, the phase is not uniformly-distributed, and the envelope and phase are statistically-dependent (Thomas, 1969). This case is referred to in the literature as non-Gaussian, but such a statement is misleading because the quadrature components are jointly Gaussian-distributed and independent of each other, and the marginal distribution of each is Gaussian with non-zero mean. Estimation of the higher-order cumulants of the quadrature components is carried out after subtracting the mean, which results in zero-mean Gaussian-distributed quadrature components. Thus, for a Rice-distributed envelope all higher-order cumulants of the quadrature components are zero (after mean removal).

2.1.1 Alternative Probabilistic Descriptions

A complete probabilistic model for radar data consists of the multivariate PDF of the received radar time sequence for the full CPI, $\{\mathbf{x}(n) | n = 0, 1, \dots, N\}$. The multivariate PDF model inherently includes the temporal and spatial statistical information (moments, etc.) required to estimate the parameters of a time series model to represent the data. A multivariate PDF model is required also under each of the two hypotheses in order to determine the optimal LLR detection rule. Unfortunately, a temporal multivariate PDF model is available only for a limited number of scenarios and conditions that result in Gaussian-

distributed return signals. In most cases involving non-Gaussian-distributed return signals the available information is a univariate PDF model for either the envelope or the power of each scalar element of $\{\underline{x}(n)\}$ at each discrete instant of time. Some of the available univariate PDF models are physical models, whereas others are representation models.

Multivariate as well as univariate PDF descriptions can be represented in either one of two ways: as a function of complex-valued quantities, or as a function of real-valued quantities. Issues associated with the two representations are considered in this section, with emphasis on those issues that have an impact on model-based multichannel detection for non-Gaussian cases.

Let the complex-valued baseband process $\{\underline{x}(n)\}$ be defined in terms of its real and imaginary components as

$$(2-2) \quad \underline{x}(n) = \underline{x}_I(n) + j \underline{x}_Q(n)$$

where the subscripts I and Q denote in-phase and out-of-phase, respectively. The real-valued vector sequences $\{\underline{x}_I(n)\}$ and $\{\underline{x}_Q(n)\}$ are the quadrature components of $\{\underline{x}(n)\}$. Since the process $\{\underline{x}(n)\}$ is zero-mean, both of these vectors are zero-mean also. The autocovariance and cross-covariance sequences of these two components are defined as

$$(2-3) \quad R_{II}(m) = E[\underline{x}_I(n) \underline{x}_I^T(n-m)]$$

$$(2-4) \quad R_{QQ}(m) = E[\underline{x}_Q(n) \underline{x}_Q^T(n-m)]$$

$$(2-5) \quad R_{IQ}(m) = E[\underline{x}_I(n) \underline{x}_Q^T(n-m)]$$

$$(2-6) \quad R_{QI}(m) = E[\underline{x}_Q(n) \underline{x}_I^T(n-m)]$$

Auto-covariances $R_{II}(m)$ and $R_{QQ}(m)$ are both symmetric and (at least) positive semi-definite. Cross-covariances $R_{IQ}(m)$ and $R_{QI}(m)$ do not exhibit any particular structure, but it is obvious from Equations (2-5) and (2-6) that

$$(2-7) \quad R_{IQ}(m) = R_{QI}^T(m)$$

The covariance sequence of the process $\{\underline{x}(n)\}$ is defined as

$$(2-8a) \quad R_{xx}(m) = E[\underline{x}(n) \underline{x}^H(n-m)]$$

$$(2-8b) \quad R_{xx}(m) = R_{II}(m) + R_{QQ}(m) + j R_{QI}(m) - j R_{IQ}(m)$$

Matrix $R_{xx}(m)$ is Hermitian and (at least) positive semi-definite. Also, the following relationship is true

$$(2-9) \quad R_{xx}(-m) = R_{xx}^H(m) \quad \forall m$$

This covariance sequence constitutes the second-order statistics for the process $\{\underline{x}(n)\}$. Since the process has mean zero, the matrix elements of the covariance sequence are the second-order cumulants of the process.

Now define three JN -dimensional vectors by concatenating all the J -dimensional vectors in the complete CPI as follows:

$$(2-10) \quad \underline{x}_I(0;N-1) = \begin{bmatrix} \underline{x}_I(0) \\ \underline{x}_I(1) \\ \vdots \\ \underline{x}_I(N-1) \end{bmatrix}$$

$$(2-11) \quad \underline{x}_Q(0;N-1) = \begin{bmatrix} \underline{x}_Q(0) \\ \underline{x}_Q(1) \\ \vdots \\ \underline{x}_Q(N-1) \end{bmatrix}$$

$$(2-12) \quad \underline{x}(0;N-1) = \underline{x}_I(0;N-1) + j \underline{x}_Q(0;N-1) = \begin{bmatrix} \underline{x}(0) \\ \underline{x}(1) \\ \vdots \\ \underline{x}(N-1) \end{bmatrix}$$

The vectors in Equations (2-10)-(2-12) contain all the data for a specific resolution cell for one CPI. Define also a $2JN$ -dimensional, real-valued vector as

$$(2-13) \quad \underline{r}(0;N-1) = \begin{bmatrix} \underline{x}_I(0;N-1) \\ \underline{x}_Q(0;N-1) \end{bmatrix}$$

Since the process $\{\underline{x}(n)\}$ is zero-mean, all of the vectors in Equations (2-10)-(2-13) are zero-mean. Vector $\underline{x}(0;N-1)$ contains the same information as vector $\underline{r}(0;N-1)$; however, it turns out that the probabilistic description of the baseband process based on the complex-valued representation of the information is more restrictive.

First it is convenient to introduce additional definitions. The covariance matrix of the JN -dimensional vector $\underline{x}(0;N-1)$, is defined as

$$(2-14) \quad \mathcal{R}_{N,N} = E[\underline{x}(0;N-1) \underline{x}^H(0;N-1)] = \begin{bmatrix} R_{xx}(0) & R_{xx}(-1) & \dots & R_{xx}(1-N) \\ R_{xx}(1) & R_{xx}(0) & \dots & R_{xx}(2-N) \\ \vdots & \vdots & \ddots & \vdots \\ R_{xx}(N-1) & R_{xx}(N-2) & \dots & R_{xx}(0) \end{bmatrix}$$

Matrix $\mathcal{R}_{N,N}$ is Hermitian and block Hermitian, and it exhibits block Toeplitz structure (the (i,j) th block element of a block Toeplitz matrix is a function of $i-j$). The block elements of $\mathcal{R}_{N,N}$ are matrix elements of the covariance sequence $\{R_{xx}(m)\}$. Also relevant is the covariance matrix of $r(0;N-1)$, which is defined as

$$(2-15a) \quad \mathbf{R}_{N,N} = E[r(0;N-1)r^T(0;N-1)]$$

$$(2-15b) \quad \mathbf{R}_{N,N} = \begin{bmatrix} R_{II}(0) & \dots & R_{II}(1-N) & R_{IQ}(0) & \dots & R_{IQ}(1-N) \\ \vdots & \ddots & \vdots & \vdots & \ddots & \vdots \\ R_{II}(N-1) & \dots & R_{II}(0) & R_{IQ}(N-1) & \dots & R_{IQ}(0) \\ R_{QI}(0) & \dots & R_{QI}(1-N) & R_{QQ}(0) & \dots & R_{QQ}(1-N) \\ \vdots & \ddots & \vdots & \vdots & \ddots & \vdots \\ R_{QI}(N-1) & \dots & R_{QI}(0) & R_{QQ}(N-1) & \dots & R_{QQ}(0) \end{bmatrix}$$

Matrix $\mathbf{R}_{N,N}$ is symmetric and block symmetric; however, in general it does not exhibit block Toeplitz structure. The block elements of $\mathbf{R}_{N,N}$ are the real and imaginary matrix components of the covariance sequence, Equation (2-8b).

Having established the relevant notation and correlation matrix definitions, the concept of circular symmetry can be defined. A complex-valued vector process $\{\mathbf{x}(n)\}$ with covariance sequence defined as in Equation (2-8) is circularly symmetric if the following conditions are satisfied (Goodman, 1984; Papoulis, 1984):

$$(2-16) \quad E[\mathbf{x}_I(n)] = E[\mathbf{x}_Q(n)] = \mathbf{0} \quad \forall n$$

$$(2-17a) \quad R_{II}(m) = R_{QQ}(m) \quad \forall m$$

$$(2-17b) \quad R_{IQ}(m) = -R_{QI}(m) \quad \forall m$$

Condition (2-16) requires the radar return to have mean zero, which is satisfied by assumption (see Table 2-1); Conditions (2-17) place structural constraints on the covariance sequence of $\{\underline{x}(n)\}$. Notice that circular symmetry involves only first- and second-order statistics. Thus, most results available in the literature on circular symmetry involve the Gaussian distribution (recall that the Gaussian distribution is defined completely by first- and second-order statistics). One example of such results is the following: if a Gaussian-distributed baseband sequence $\{\underline{x}(n)\}$ is circularly symmetric, then its associated bandpass process $\{\underline{x}(t)\}$ (see Figure 2-1) is a stationary process (Papoulis, 1984). The converse statement is also true. An equivalent result for non-Gaussian processes is unavailable; it seems that such a result may not be possible for non-Gaussian processes because of the role played by higher-order statistics in such processes.

The probabilistic description of the complex-valued vector process $\{\underline{x}(n)\}$ can be represented using either one of two analytic forms. In the first form the multivariate PDF is expressed in terms of the JN -dimensional complex-valued vector $\underline{x}(0;N-1)$, with corresponding complex-valued moments. Alternatively, in the second form the multivariate PDF is expressed in terms of the $2JN$ -dimensional real-valued vector $\underline{r}(0;N-1)$, with corresponding real-valued moments. It is well known that when $\{\underline{x}(n)\}$ is Gaussian-distributed, the two PDF representations are equivalent if the process $\{\underline{x}(n)\}$ is circularly symmetric (see, for example, Goodman [1963]). The above comments and conclusions are valid also for univariate PDF models for each element of the random vector $\underline{x}(n)$ at each time instant n .

Circular symmetry is not satisfied in many cases, even when the quadrature components are Gaussian-distributed. As an example consider a process represented by the Rice envelope PDF model. The quadrature components corresponding to a Rice envelope process are Gaussian-distributed, but the mean is non-zero. Since the process fails Condition (2-16), it is not circularly symmetric. Consequently, this process cannot be represented with a PDF model based on the complex-valued formulation. Similar behaviour can occur for non-Gaussian processes. Furthermore, even if a non-Gaussian process is circularly symmetric, there may not be a valid complex-valued PDF model. In summary, the multivariate PDF representation based on the real-valued vector $\mathbf{r}(0;N-1)$ and its moments is more general than the representation based on the complex-valued vector $\mathbf{x}(0;N-1)$ and its moments (Williams and Johnson, 1993; Michels, 1991). This fact is significant because optimal LLR detection algorithms are developed based on the multivariate PDF model for the sequence.

Based on the discussion presented in this section, it is reasonable to adopt the real-valued probabilistic representation in the formulation of model parameter identification algorithms and detection methodologies for scenarios involving non-Gaussian radar returns. Nevertheless, the methodology and equations were developed in Phase I using the complex-valued probabilistic representation because the form of the resulting equations and diagrams are applicable to both cases (in general, a complex-formulation equation reduces to its real-valued counterpart by setting the imaginary components to zero and replacing the Hermitian operator with the transpose operator). Additionally, the notation for the complex-valued case is more compact than for the real-valued case (compare, for example, Equation (2-14) with Equation (2-15)).

2.1.2 Non-Gaussian Clutter Scenarios and Probabilistic Models

Airborne surveillance radars generally search for moving targets over large areas of ground surface consisting of land, or water (sea, lake, etc.), or both (coastal regions, etc.). Thus, the received radar signal contains land and/or water clutter, and the probabilistic description of these two clutter types is of relevance. The methodology developed in this program is best suited for cases where the return signal is non-Gaussian (unless a transformation is applied to the data first); thus, identification of radar scenarios and/or conditions which result in non-Gaussian clutter is a fundamental issue.

As mentioned in Section 2.1.1, the multivariate PDF of the received radar time sequence for one full CPI is a complete probabilistic model for radar data. However, in most cases of non-Gaussian clutter the available PDF model is a univariate PDF model for either the envelope or the power (equivalently, radar cross-section) at the output of each individual channel and at each discrete instant of time. The univariate PDF is complemented by temporal correlation information. During Phase I of this program a literature review was carried out to identify the various non-Gaussian clutter univariate PDF models and the conditions and/or scenarios where such non-Gaussian clutter arises. A summary of the most common univariate PDF models is presented in Table 2-2. The last column in Table 2-2 describes the clutter type and the conditions under which the PDF model is valid. Several relevant references are provided also in the last column. Most of the references given in this column are texts which discuss clutter issues in detail and provide extensive lists of references for the original experimental and/or analytical work on which the results summarized herein are based.

UNIVARIATE PDF MODEL	MODEL PARAMETER	VARIATION TYPE	CLUTTER TYPE DESCRIPTION
Rice (Non-central gamma)	Envelope (RCS)	Temporal	Terrain with large, fixed scatterers (such as man-made structures) and a large number of small, moving scatterers (Nathanson, 1991; Simkins, 1981).
K-distribution	Envelope	Spatial	Sea clutter at microwave frequencies (Jakeman and Pusey, 1976; Nathanson, 1991).
K-distribution	Envelope	Spatial	Polarimetric scattering from certain types of terrain (Raghavan, 1991).
Gamma	RCS	Spatial	Sea clutter at S-band and C-band radar frequencies; used in RADC model (Simkins, 1991).
Log-normal	RCS	Temporal; Spatial	Sea clutter for high-resolution radar (short-duration pulses and narrow beamwidth), low grazing angles (< 5 deg), and high sea states (Nathanson, 1991; Skolnik, 1980).
Log-normal	RCS	Spatial	Various types of terrain clutter at low grazing angles (< 3 deg); also non-homogeneous (composite) terrain (Currie, 1989; Nathanson, 1991; Skolnik, 1980).
Log-normal	Envelope	Temporal	Rain clutter with millimeter wave radar at rain rates in the 1 mm/hr to 60 mm/hr range (Skolnik, 1980).
Weibull	Envelope	Temporal; Spatial	Sea clutter for high-resolution radar (short-duration pulses and narrow beamwidth), low grazing angles (< 5 deg), and high sea states (Nathanson, 1991; Skolnik, 1980).
Weibull	Envelope	Spatial	Various types of terrain clutter at low grazing angles (< 3 deg), also non-homogeneous (composite) terrain (Currie, 1989; Nathanson, 1991; Skolnik, 1980;).
Weibull	Envelope	Spatial	Weather clutter under stormy conditions at L-band (1.3 GHz) over Tokyo, Japan (Sekine et al., 1979).

Table 2-2. Non-Gaussian clutter fluctuation PDF models.

The univariate PDF models in Table 2-2 provide only part of the information required for the development of optimal detection methodologies and analyses. Minimum additional model information required for suboptimal techniques is a description of the temporal correlation structure. The most commonly adopted

temporal correlation models are those which bound temporal correlation behaviour as defined by Marcum and Swerling (1960): (a) pulse-to-pulse fluctuation, and (b) scan-to-scan (or pulse train-to-pulse train) fluctuation. In multichannel systems spatial correlation models are required also. Analogous to the temporal case, the two models that bound spatial fluctuation behaviour are: (a) channel-to-channel independence, and (b) channel-to-channel full correlation. Multichannel systems offer more degrees of freedom, with the associated performance improvement potential and increased analytical complexity.

A clutter PDF model represents either a temporal or a spatial variation for the model parameter (envelope or RCS), as indicated in Table 2-2. A temporal PDF model describes the instantaneous fluctuations of the envelope (or power) of the baseband radar signal $\{x(n)\}$ at each individual resolution cell. A spatial PDF model describes cell-to-cell fluctuations of the mean envelope or mean power (equivalently, RCS) over a large area covering many resolution cells, and these fluctuations behave according to the listed distribution, except in the case of the K-distribution. The cell-to-cell fluctuations in the K-distribution model behave according to the (un-normalized) chi distribution. In the model referred to in the table, the K-distribution describes the joint fluctuation behaviour of the radar return from all the resolution cells over a CPI (this is discussed in more detail below). Thus, if the same naming convention were to be used in all cases, the correct name for this model would be "chi". However, the K-distribution name for the model is entrenched.

In most spatial model cases the instantaneous envelope fluctuations in each individual radar resolution cell are Rayleigh-distributed, and the instantaneous power fluctuations are exponentially-distributed. This is the Gaussian case. Thus, most

spatial PDF models represent non-homogeneous clutter with Gaussian-distributed behaviour at each individual resolution cell. The spatial vs. temporal distinction is important in the context of higher-order cumulants since all higher-order cumulants are zero for Gaussian-distributed clutter returns. An HOS-based detection formulation can be defined for each case (spatial; temporal), as discussed in Section 3.2.

With exception of the Rice envelope model, each of the PDF models listed in Table 2-2 is incomplete in the sense that information is unavailable in the literature which is essential to determine the unqualified feasibility of time series model parameter estimation using third-order cumulants of the quadrature components ("unqualified" implies without the pre-processing step introduced in Section 3.3). Specifically, the following information is unavailable for each of the listed PDF models (except Rice envelope):

- (a) joint distribution of the envelope and phase,
- (b) marginal distribution of the phase,
- (c) joint distribution of the quadrature components, and
- (d) marginal distribution of the quadrature components.

Of these four items, the key model information (in the context of third-order cumulants of the quadrature components) is the marginal distribution of the quadrature components. Given the marginal PDF, the asymmetry of the distribution about the mean value can be determined. An effective measure of univariate PDF asymmetry is the coefficient of skewness, η_3 , which is defined as

$$(2-18) \quad \eta_3 = \frac{\mu_3}{\sigma^3}$$

where μ_3 is the third moment about the mean and σ is the standard deviation of the PDF model (Hastings and Peacock, 1974). For a symmetric distribution, $\mu_3 = 0$; a highly asymmetric PDF has a large

coefficient of skewness. Variants of the definition in Equation (2-18) have been introduced in the literature for specific objectives. Maffett (1989) uses a modified coefficient of skewness, where the modification consists of replacing σ^3 in the denominator by the product $\mu\sigma^2$, with μ the mean of the process.

Often it is assumed that the clutter return phase corresponding to the temporal distributions in Table 2-2 is uniformly-distributed and independent of the envelope (or RCS). Sometimes these two assumptions are made to simplify the generation of simulated data. Other times they are introduced in order to simplify analyses. However, the validity of these two assumptions has not been justified via experimental and/or analytical means. In fact, the Rice envelope is an example of the opposite: in the Rician envelope model the phase and the envelope are dependent, and the phase marginal PDF is not uniform (Thomas, 1969). The quadrature components of the Rice envelope model are independent and Gaussian-distributed, though. The validity (or lack thereof) of the two assumptions on phase (uniformly-distributed and independence of phase and envelope) for any of the non-Gaussian cases in Table 2-2 (except Rice envelope) has significant implications in the context of third-order cumulants. This is so because it can be shown that if the phase is uniformly-distributed and independent of the envelope (or RCS), then the marginal PDF of each of the two quadrature components is symmetric about the mean. Furthermore, it is reasonable to conjecture that the marginal PDF of each of the quadrature components is symmetric about the mean if the phase is independent of the envelope (or RCS) and the phase distribution is symmetric about its mean (but not necessarily uniform). In summary, it is important to keep in mind the potential impact of any assumption made with respect to the distribution of the phase and/or the dependence (or lack thereof) between the phase and envelope processes.

For the temporal distributions in Table 2-2 there are several open questions of relevance to the approach pursued in this Phase I. Two of those questions are:

- (1) Is the phase distribution always symmetric about the mean, irrespective of the corresponding envelope PDF?
- (2) Is the marginal PDF of the quadrature components symmetric about the mean irrespective of the envelope PDF?

These questions are difficult to answer. One reason is the fact that the temporal PDF models in Table 2-2 are models of representation, except for the Rice envelope model. Nevertheless, it is relevant to pursue the answers to these and other related questions because the unqualified feasibility of using third-order cumulants in a model-based detection algorithm is determined by such issues.

The discussion thus far has centered on the temporal PDF models in Table 2-2 due to the fact that cumulant-based techniques are better suited to such cases. It is appropriate to consider the cases involving spatial fluctuations of the clutter parameters. Non-Gaussian spatial fluctuations arise as a result of non-homogeneities of the ground (land or water) clutter over an area which covers a large number of radar resolution (range-azimuth) cells. Clutter temporal fluctuations in each resolution cell are Gaussian-distributed, but the average RCS fluctuates from cell to cell in a random manner. This condition is modeled using a compound distribution to describe the overall clutter return covering a large number of resolution cells, in contrast to a local neighborhood of resolution cells (Lewinski, 1983; Nathanson, 1991). A compound distribution model for the clutter envelope is a PDF model of the form

$$(2-19) \quad p(a) = \int_0^{\infty} p(a|r) p(r) dr$$

where $p(a)$ is the overall spatial clutter envelope PDF, $p(a|r)$ is the clutter envelope PDF at each individual resolution cell, and $p(r)$ is the PDF of the cell-to-cell mean envelope fluctuations. The sea clutter envelope model listed in the second row of Table 2-2 is an example of a spatial variation model generated from a compound distribution. The overall clutter envelope is K-distributed, the conditional PDF is Rayleigh, and the cell-to-cell mean envelope fluctuations behave according to the (un-normalized) chi distribution (Watts, 1987).

The K-distributed PDF model discussed above is a physical model. Such a scenario can be modeled effectively using SIRPs, for which a wealth of results is available (see, for example, Rangaswamy [1992] and the references therein). In particular, for a K-distributed SIRP the marginal PDF of each of the quadrature components is the so-called generalized Laplace PDF, which is symmetric about the mean. The spatial multivariate K-distribution PDF model is well defined for complex-valued as well as real-valued formulations.

In summary, key aspects of the probabilistic description (the marginal PDF of the quadrature components, in particular) of the non-Gaussian clutter types listed in Table 2-2 are unavailable, and may remain so for a long time. Nevertheless, it can be stated that detection techniques based on higher-order cumulants can be applied to the multichannel detection problem for the following two reasons. First, even-ordered cumulants are non-zero for all non-Gaussian PDFs, whether symmetric or asymmetric. This implies

that the methodology developed in Phase I can be applied using fourth-order cumulants. Second, the SSC detection methodology can be applied in the cases where the quadrature components are symmetrically-distributed by introducing a pre-processing step, as discussed in Section 3.3. In essence, symmetrically-distributed clutter is transformed by a zero-memory nonlinearity to induce asymmetry in the PDF of the quadrature components, while introducing tolerable distortion to the temporal correlation function (or, equivalently, the frequency-domain spectrum). The pre-processing step considered in Section 3.3 is the logarithmic function, which is applied to the clutter process prior to processing. The degree of distortion depends on the dynamic range and the frequency content of the quadrature components, as well as on the operating region in the logarithm function. After the transformation the clutter process is characterized by a different univariate PDF with a larger-valued coefficient of skewness (see Section 5.1).

2.1.3 Non-Gaussian Target Probabilistic Models

In a typical surveillance scenario the target's physical dimensions are small in relation to the radar footprint; thus, in general the target is illuminated completely by the radar beam and is present in the return from only one resolution cell. This is in contrast with the clutter, which has a large spatial extent that covers many resolution cells. As a result, the target RCS fluctuations in a surveillance scenario of the type considered herein arise only in the temporal sense.

During Phase I SSC searched the literature for non-Gaussian target models. This activity led to the realization that the radar return from many surveillance targets is characterized by non-Gaussian statistics. As in the case of clutter, the most

common probabilistic models for targets are in the form of a univariate PDF which characterizes the instantaneous RCS fluctuations, and a temporal correlation function. Table 2-3 lists several univariate PDF models for the temporal RCS fluctuations and the target types which can be represented by each PDF model. This table has been adapted from the text by Nathanson (1991), and enhanced by SSC with the entry for the beta distribution. Notice that aircraft, missiles, and similar targets are listed, which indicates that most of the airborne targets of interest exhibit non-Gaussian statistical features.

TEMPORAL RCS FLUCTUATION PDF	TARGET TYPE DESCRIPTION
Non-central gamma (Rice envelope)	Targets composed of one large reflector and many small reflectors (the sum of the RCS of all the small reflectors can be different than the RCS of the large reflector).
Beta	Complex targets such as aircraft and missiles; postulated as a physical model as well as a representation model (Maffett, 1989).
Log-normal	Targets with large mean-to-median ratios (> 1.44); this includes battleships, missiles, satellites, and aircraft (at near broadside).
Chi-squared of degree 4 (Swerling cases 3 and 4)	Targets composed of one large reflector and many small reflectors (the sum of the RCS of all the small reflectors is equal to the RCS of the large reflector). In general, the Rice PDF is a better model.
Chi-squared of degree $2m$ (for $m > 2$)	Short-term (or reduced-aspect viewing) statistics of several types of aircraft. The degree is an inverse function of the level of the fluctuations about the mean RCS. Equivalent to gamma distribution for non-integer values of m .
Weinstock	This model is included in the chi-squared PDF of degree $2m$ for $0.3 < m < 2.0$.

Table 2-3. Non-Gaussian target temporal RCS fluctuation PDF models.

Other non-Gaussian target models have been developed for parameters different than the RCS. For example, Novak, Sechtin, and Cardullo (1989) have demonstrated that the polarimetric return fluctuations from complex ground targets such as tanks and trucks can be modeled accurately and effectively using the K-

distribution. Their approach is analogous to the modeling of spatial variation using the compound distribution model as summarized in Section 2.1.2, with target aspect angle variability playing the role of spatial ocean surface variability.

The issues and open questions identified in Section 2.1.2 are just as relevant to radar return from targets. In particular, the PDF models for targets are deficient in the same manner as for clutter:

- multivariate quadrature component PDF for each of the non-Gaussian models (except Rice envelope);
- phase model information (joint PDF with envelope; marginal phase distribution; symmetry of marginal phase PDF);
- univariate marginal PDF of the quadrature components.

In the same manner, candidate resolution approaches identified for clutter are relevant also for targets. This includes the use of a zero-memory nonlinear transformation to skew the marginal PDF of the quadrature components.

2.1.4 Surveillance Radar Scenarios With Non-Gaussian Signals

Based on the clutter and target PDF models presented in Sections 2.1.2 and 2.1.3, several military and non-military surveillance scenarios and/or detection problems for radar arrays can be identified wherein at least one non-Gaussian component is part of the radar return. A variety of generic scenarios and detection problems wherein non-Gaussian components arise are presented in Table 2-4 for military applications, and in Table 2-5 for non-military applications. The first two scenarios in Table 2-4 cover the type of detection problems that arise in programs such as the Space-Time Processing Program at RL.

RADAR ARRAY PLATFORM	SURVEILLANCE COVERAGE	TARGETS OF INTEREST
High-altitude aircraft	Ocean	<ul style="list-style-type: none"> • Missiles (cruise) • Aircraft (bombers, fighters)
High-altitude aircraft	Ground	<ul style="list-style-type: none"> • Aircraft (bombers, fighters) • Missiles (cruise)
Large ships	Airborne threats	<ul style="list-style-type: none"> • Missiles (cruise, short-range) • Aircraft (bombers, fighters)
Aircraft	Ground	<ul style="list-style-type: none"> • Land vehicles (tanks, trucks, etc.) • Aircraft (fighters, helicopters)

Table 2-4. Candidate military surveillance radar problems involving non-Gaussian clutter and/or targets.

RADAR ARRAY PLATFORM	FUNCTION	TARGETS OF INTEREST
Ground-based system	Air traffic control	Aircraft, including helicopters
Ground-based system	Weather radar	Weather phenomenology

Table 2-5. Candidate non-military surveillance radar problems involving non-Gaussian clutter and/or targets.

The radar return $\{x(n)\}$ for each of the radar surveillance scenarios summarized in Tables 2-4 and 2-5 can be represented by at least one of the first three cases listed next (presented here assuming the alternative hypothesis is true):

(2-20a) $x(n): \text{NGS} + \text{NGC} + \text{GWN}$

$$(2-20b) \quad \underline{x}(n): \text{NGS} + \text{GC} + \text{GWN}$$

$$(2-20c) \quad \underline{x}(n): \text{GS} + \text{NGC} + \text{GWN}$$

$$(2-20d) \quad \underline{x}(n): \text{GS} + \text{GC} + \text{GWN}$$

where GS and NGS denote Gaussian and non-Gaussian target signal, respectively; GC and NGC denote Gaussian and non-Gaussian clutter, respectively; and GWN denotes Gaussian white noise. The methodologies discussed in this report address Case (2-20a). It appears that Cases (2-20b) and (2-20c) may be handled via modifications and/or extensions to the approach defined herein. This will be investigated in Phase II. HOS-based identification and detection methods are inappropriate for Case (2-20d), because all three components are Gaussian-distributed. Use of the log transformation may allow the handling of Case (2-20d) also.

2.2 Time Series Models

The time series model class is adopted in this program to represent the target and clutter components in the radar return, $\{\underline{x}(n)\}$. Specifically, it is presumed herein that Cases (2-20a)-(2-20c) can be expressed in the form

$$(2-21) \quad \underline{x}(n) = \underline{y}(n) + \underline{w}(n)$$

where the process $\{\underline{y}(n)\}$ is the output of a time series system that represents the target and/or clutter components, depending upon which hypothesis is valid. For the data in one CPI,

$$(2-22a) \quad H_0: \quad \underline{y}(n) = \underline{c}(n) \quad 0 \leq n \leq N-1$$

$$(2-22b) \quad H_1: \quad \underline{y}(n) = \underline{s}(n) + \underline{c}(n) \quad 0 \leq n \leq N-1$$

MA, AR, and ARMA models are adopted herein to generate the process $\{y(n)\}$, with emphasis on MA and AR models because their use leads to simpler algorithms with reduced analytical and computational complexity. Haykin and co-workers have shown that these models provide accurate representation of single-channel radar signals, specially clutter return (Haykin, Currie, and Kesler [1982]; Metford and Haykin [1985]). Michels (1991) has demonstrated the value of model-based multichannel detection using AR models and second-order statistics for Gaussian conditions, Case (2-20d).

Moving-Average Process. A J-dimensional, zero-mean, stationary, complex-valued sequence $\{y(n)\}$ is referred to as a moving-average vector process of order M, and is denoted as MA(M), if it satisfies a vector recursion of the form

$$(2-23) \quad y(n) = \sum_{k=0}^M B_k^H u(n-k)$$

where M is a non-negative integer, and $\{B_k | k=0,1,\dots,M\}$ are $J \times J$, time-invariant, complex-valued matrices. Equation (2-23) is a linear system, with $\{u(n)\}$ as the input, $\{y(n)\}$ as the output, and $\{B_k\}$ as the system parameters. In the context of this program the output sequence is non-Gaussian; however, an MA(M) process can be Gaussian-distributed.

Auto-Regressive Process. A J-dimensional, zero-mean, stationary, complex-valued sequence $\{y(n)\}$ is referred to as an auto-regressive vector process of order L, and is denoted as AR(L), if it satisfies a vector recursion of the form

$$(2-24) \quad y(n) = - \sum_{k=1}^L A_k^H y(n-k) + u(n)$$

where L is a non-negative integer, and $\{A_k | k=1, 2, \dots, L\}$ are $J \times J$, time-invariant, complex-valued matrices. Equation (2-24) is a linear system, with $\{\underline{u}(n)\}$ as the input, $\{\underline{y}(n)\}$ as the output, and $\{A_k\}$ as the system parameters. The output sequence is non-Gaussian.

Auto-Regressive Moving-Average Process. A J -dimensional, zero-mean, stationary, complex-valued sequence $\{\underline{y}(n)\}$ is referred to as an auto-regressive moving-average vector process of order (L, M) , and is denoted as $\text{ARMA}(L, M)$, if it satisfies a vector recursion of the form

$$(2-25) \quad \underline{y}(n) = - \sum_{k=1}^L A_k^H \underline{y}(n-k) + \sum_{k=0}^M B_k^H \underline{u}(n-k)$$

here L and M are non-negative integers with $L \geq M$, and $\{A_k | k=1, 2, \dots, L\}$ and $\{B_k | k=0, 1, \dots, M\}$ are $J \times J$, time-invariant, complex-valued matrices. Equation (2-25) is a linear system, with $\{\underline{u}(n)\}$ as the input, $\{\underline{y}(n)\}$ as the output, and $\{A_k\}$, $\{B_k\}$ as the system parameters. The output sequence is non-Gaussian.

Characteristics and Properties of Time Series Models. The material presented in the remainder of this subsection applies to all three time series models; distinctions specific to individual models are noted. The input process $\{\underline{u}(n)\}$ is a J -dimensional, zero-mean, stationary, complex-valued, non-Gaussian, white noise sequence with finite cumulants at least up to sixth-order (this last assumption is required in Section 4.1). The second-order statistics of the input noise are established as (for all n because the sequence is stationary),

$$(2-26a) \quad R_{uu}(0) = \Sigma_u = E[\underline{u}(n)\underline{u}^H(n)]$$

$$(2-26b) \quad R_{uu}(m) = E[\underline{u}(n)\underline{u}^H(n-m)] = [0] \quad m \neq 0$$

$$(2-26c) \quad R_{uu}(m) = E[\underline{u}(n) \otimes \underline{u}^H(n-m)] = E \begin{bmatrix} u_1(n)\underline{u}^H(n-m) \\ u_2(n)\underline{u}^H(n-m) \\ \vdots \\ u_J(n)\underline{u}^H(n-m) \end{bmatrix} = [0] \quad m \neq 0$$

here Σ_u is a $J \times J$ Hermitian matrix. The symbol \otimes denotes the Kronecker matrix product (see, for example, Pease [1965]), which is defined implicitly in Equation (2-26c). Kronecker product notation simplifies analytical expressions in many cases, such as those involving third-order cumulants. Since the mean of the input sequence is zero, Equations (2-26) define the covariance sequence of the input process, and matrix Σ_u is the covariance of $\underline{u}(n)$. The matrix elements of the covariance sequence are the second-order cumulants of the process (Mendel, 1991). Equations (2-26) can be combined into one equation of the form,

$$(2-27) \quad R_{uu}(m) = E[\underline{u}(n) \otimes \underline{u}^H(n-m)] = \Sigma_u \delta(m) \quad \forall m$$

where $\delta(m)$ is the one-dimensional (1-D) discrete impulse function,

$$(2-28) \quad \delta(m) = \begin{cases} 1 & m = 0 \\ 0 & m \neq 0 \end{cases}$$

The third-order statistics of the input noise sequence are given as (for all n since $\{\underline{u}(n)\}$ is stationary)

$$(2-29a) \quad C_{u;k}(0,0) = \Gamma_k = E[\underline{u}(n)\underline{u}^H(n)u_k^*(n)] \quad k = 1, 2, \dots, J$$

$$(2-29b) \quad C_{u;k}(m_1, m_2) = E[\underline{u}(n)\underline{u}^H(n-m_1)u_k^*(n-m_2)] = [0] \quad m_1, m_2 \neq 0 \\ k = 1, 2, \dots, J$$

where $\{\Gamma_k | k=1, 2, \dots, J\}$ are $J \times J$, time-invariant, complex-valued matrices. Using the two-dimensional (2-D) discrete impulse function (which attains unity value only at the origin of the 2-D plane), these two sets of equations can be combined into one set of equations of the form

$$(2-30) \quad C_{u;k}(m_1, m_2) = E[\underline{u}(n)\underline{u}^H(n-m_1)u_k^*(n-m_2)] = \Gamma_k \delta(m_1, m_2) \quad \forall m_1, m_2 \\ k=1, 2, \dots, J$$

Finally, the set of Equations (2-30) can be compacted into a single equation using Kronecker product notation; this results in

$$(2-31a) \quad C_u(m_1, m_2) = E[\underline{u}^*(n-m_2) \otimes \underline{u}(n) \otimes \underline{u}^H(n-m_1)] \quad \forall m_1, m_2$$

$$(2-31b) \quad C_u(m_1, m_2) = \begin{bmatrix} \Gamma_1 \\ \Gamma_2 \\ \vdots \\ \Gamma_J \end{bmatrix} \delta(m_1, m_2) \quad \forall m_1, m_2$$

Since the input sequence is zero-mean, Equations (2-31) constitute the third-order cumulants of the input process, and matrices $\{\Gamma_k\}$ are the non-zero third-order cumulants of the input process (Mendel, 1991).

In general, the complex-valued cumulants do not have a special structure. However, when the input noise is spatially-independent the covariance and the third-order cumulants $\{\Gamma_k\}$ become diagonal matrices. The covariance of a spatially-independent noise vector $\underline{u}(n)$ is

$$(2-32) \quad \Sigma_u = \text{diag}[\sigma_i^2] = \begin{bmatrix} \sigma_1^2 & 0 & \dots & 0 \\ 0 & \sigma_2^2 & \dots & 0 \\ \vdots & \vdots & \ddots & \vdots \\ 0 & 0 & \dots & \sigma_J^2 \end{bmatrix}$$

with σ_i^2 representing the variance of the i th element of $\underline{u}(n)$. The k th cumulant matrix of a spatially-independent noise vector $\underline{u}(n)$ is diagonal also, with only one non-zero element located at the k th diagonal position:

$$(2-33a) \quad \Gamma_k = \begin{matrix} & \begin{matrix} \text{kth column} \\ \downarrow \end{matrix} & \\ \begin{bmatrix} 0 \dots 0 & 0 & 0 \dots 0 \\ \vdots & \vdots & \vdots & \vdots & \vdots \\ 0 \dots 0 & 0 & 0 \dots 0 \\ 0 \dots 0 & \gamma_k & 0 \dots 0 \\ 0 \dots 0 & 0 & 0 \dots 0 \\ \vdots & \vdots & \vdots & \vdots & \vdots \\ 0 \dots 0 & 0 & 0 \dots 0 \end{bmatrix} & \begin{matrix} \leftarrow \text{kth row} \end{matrix} \end{matrix}$$

$$(2-33b) \quad E[u_i(n)u_j^*(n)u_k^*(n)] = \gamma_k \delta_{ijk}$$

here the complex-valued scalar γ_k denotes the third-order cumulant of $u_k(n)$, and δ_{ijk} denotes the Kronecker delta, which is defined as

$$(2-34) \quad \delta(m) = \begin{cases} 1 & i=j=k \\ 0 & \text{otherwise} \end{cases}$$

Thus, the third-order statistics of a J -dimensional, zero-mean, complex-valued, spatially-independent, non-Gaussian, white noise sequence are the complex-valued scalars $\{\gamma_k | k=1, 2, \dots, J\}$.

For the models in Equations (2-23)-(2-25) the input noise and the output sequence are both non-Gaussian. However, it is important to note that in general the PDF of the output belongs to a different family than the PDF family of the input. In all three models the input process is transformed into the output process, and these transformations alter the PDF. Furthermore, the output process tends to become Gaussian for rather general conditions dictated by the central limit theorem (Thomas [1969] discusses one of the various versions of the theorem). Consider, for example, the MA model as in Equation (2-23). For an MA(M) system, the output process tends to be Gaussian-distributed for large values of the system model order, M, and/or large values of the dimension of the input noise vector, J. If a sufficiently large number of elements of the parameter matrices have non-negligible magnitude, then Gaussianity may be approximated at smaller values for M and/or J. Analogous comments apply to the AR and ARMA models.

The fact that (for the three time series models) the linear operations on the input sequence transform the PDF of the input sequence creates significant difficulties in the generation of simulated data for algorithm performance evaluation (Section 5.1). This fact also has significant implications in the formulation of real-time multichannel detection architectures.

An important construct associated with the time series systems (2-23)-(2-25) is the system transfer function. For a time series the system transfer function is determined using the Z-transform (Oppenheim and Schaffer, 1975). The discrete-time system transfer functions for the systems (2-23)-(2-25) are given as,

$$(2-35) \quad T_{MA}(z) = B(z)$$

$$(2-36) \quad T_{AR}(z) = A^{-1}(z)$$

$$(2-37) \quad T_{ARMA}(z) = A^{-1}(z) B(z)$$

where $A(z)$ and $B(z)$ are the following matrix polynomials in z ,

$$(2-38a) \quad A(z) = \sum_{k=0}^L A_k^H z^{-k}$$

$$(2-38b) \quad A_0 = I_J$$

$$(2-39) \quad B(z) = \sum_{k=0}^M B_k^H z^{-k}$$

Definition (2-38b) follows trivially from Equations (2-24)-(2-25). The determinants of the two polynomial matrices, $A(z)$ and $B(z)$, are defined as

$$(2-40) \quad \alpha(z) = |A(z)|$$

$$(2-41) \quad \beta(z) = |B(z)|$$

The properties of these scalar polynomials determine, in part, the behaviour of the time series. The matrix pair $\{A(z), B(z)\}$ is referred to as a matrix polynomial representation for the system (including the MA and AR cases, where $A(z) = I_J$ and $B(z) = I_J$, respectively). The pair $\{A(z), B(z)\}$ is referred to also as a matrix fraction description (MFD) for the system.

The conditions satisfied by the time series models are listed in Table 2-6. With respect to Table 2-6, Assumptions (a), (b), and (d) insure that each of the scalar polynomials $\alpha(z)$ and $\beta(z)$ is of maximum possible order: $\alpha(z)$ is of order JL , and $\beta(z)$ is of order

JM. A time series system (MA, AR, or ARMA) for which Assumptions (c) and/or (e) are satisfied is referred to as a minimum phase system, and is said to have a minimum phase transfer function (all the finite multivariable system poles and zeros of a minimum phase system are inside the unit circle). A minimum phase system (MA, AR, or ARMA) and its inverse system are both asymptotically stable (Oppenheim and Schaffer, 1975). In model-based detection using innovations the identified model must be minimum phase in order for the whitening filter (model inverse) to be well behaved (the output of an unstable system grows unbounded). Assumption (f) insures that the ARMA system is irreducible; that is, there are no pole-zero cancelations in the transfer function $T_{ARMA}(z)$ (Rosenbrock, 1970). A system which admits pole-zero cancelations can be represented as an irreducible system of lower model order.

ASSUMPTIONS FOR THE TIME SERIES MODELS

MA and ARMA

- (a) B_0 Has Full Rank**
- (b) B_M Has Full Rank**
- (c) Zeros of $\beta(z)$ Are Inside the Unit Circle**

AR and ARMA

- (d) A_L Has Full Rank**
- (e) Zeros of $\alpha(z)$ Are Inside the Unit Circle**

ARMA

- (f) $\{A(z), B(z)\}$ is relatively prime from the left**

Table 2-6. Assumptions for the time series models.

2.3 Third-Order Cumulants

The cumulants of the output of a time series model possess several general properties of interest, and satisfy constraints due to the structure imposed by the system model. Those constraints are the basis for cumulant-based model parameter identification algorithms.

2.3.1 Definitions, Properties, and Other Issues

The third-order cumulants of a J -dimensional, zero-mean, stationary, complex-valued, discrete-time process $\{\underline{x}(n)\}$ are the following complex-valued matrices:

$$(2-42a) \quad C_{x;k}(m_1, m_2) = E[\underline{x}(n)\underline{x}^H(n-m_1)x_k^*(n-m_2)] \quad \forall m_1, m_2$$

$$k = 1, 2, \dots, J$$

$$(2-42b) \quad C_x(m_1, m_2) = E[\underline{x}^*(n-m_2) \otimes \underline{x}(n) \otimes \underline{x}^H(n-m_1)] \quad \forall m_1, m_2$$

here $x_k(n)$ is the k th element of $\underline{x}(n)$, matrix $C_{x;k}(m_1, m_2)$ is $J \times J$, and matrix $C_x(m_1, m_2)$ is $J^2 \times J$. The second expression is the compact form of the definition using Kronecker matrix product notation (the J cumulants for a fixed lag pair are concatenated into a $J^2 \times J$ matrix). This definition has been introduced already in Section 2.2 for two special cases (a white noise vector sequence, and a spatially-independent white noise vector sequence). The cumulants $\{C_x(m_1, m_2)\}$ can be interpreted as a 2-D matrix sequence, analogous to the 1-D covariance matrix sequence. A 1-D slice of $\{C_x(m_1, m_2)\}$ is a subset of the third-order cumulants defined by a set of lag pairs constrained to satisfy a fixed linear relation between the lag indices. For example, one possible "vertical slice" is defined by $m_1 = 0$ and $m_2 = \{\dots -1, 0, 1, \dots\}$; a possible "diagonal slice" is defined by $m_1 = m_2$ and $m_2 = \{\dots -1, 0, 1, \dots\}$.

The (i,j) th element of the k th cumulant matrix $C_{x;k}(m_1, m_2)$ is a complex-valued scalar denoted as

$$(2-43) \quad c_{x;ijk}(m_1, m_2) = E[x_i(n)x_j^*(n-m_1)x_k^*(n-m_2)]$$

Lower-case notation is used for the cumulant in this equation to emphasize that it is a scalar. In contrast to second-order cumulants (covariances) for complex-valued vector processes, the third-order cumulants defined in Equation (2-42) do not satisfy symmetry conditions. However, third-order cumulants for scalar and/or real-valued processes do satisfy symmetry conditions, as discussed thoroughly in the literature (real-valued scalar: Raghuveer and Nikias [1985]; complex-valued scalar: Jouny and Moses [1992]; real-valued vector: Raghuveer [1986]). For example, based on definition (2-43) it is easy to verify that for a complex-valued scalar sequence $\{h(n)\}$,

$$(2-44) \quad c_h(m_2, m_1) = c_h(m_1, m_2)$$

Other equivalences can be established for complex-valued scalar sequences. A greater number of equivalences can be established for real-valued sequences (vector and scalar).

Alternative definitions for third-order cumulants are possible in the complex-valued vector case, with the number and placement of conjugate operators as the major factors which determine the definitions. Each valid definition can lead to a different set of cumulant constraints as a result of the structure imposed by the time series models. SSC is unaware of open literature work involving cumulants for complex-valued vector processes, and the approach and results presented herein address only a subset of all possible issues that can be identified. The

complex-valued scalar case, however, has been considered by Jouny and Moses (1992) and by Jelonnek and Kammeyer (1992).

Jouny and Moses (1992) have shown that the third-order cumulants must be defined appropriately in the context of AR models for a process defined as the sum of harmonically-related complex sinusoids with uniformly-distributed phase and quadratic phase coupling (three frequencies are harmonically-related when the highest frequency is the sum of the other two; three harmonically-related frequencies have quadratic phase coupling when the phase associated with the highest frequency is equal to the sum of the phases associated with each of the other two frequencies). As indicated by Raghuveer and Nikias (1985), phase-coupled harmonically-related complex sinusoids have non-zero third-order cumulants, whereas the third-order cumulants are zero if the phase coupling is zero. Jouny and Moses (1992) demonstrate that for such processes some of the alternative definitions for third-order cumulants lead to incorrect AR parameter estimates, in the sense that the scalar AR model transfer function does not generate the true bispectrum, which is known to be the sum of pairs of impulse functions (the bispectrum of a scalar discrete-time process is the 2-D Fourier transform of the third-order cumulants).

The Jouny-Moses third-order cumulants for a complex-valued scalar process $\{h(n)\}$ are defined as

$$(2-45) \quad \mathbf{c}_h(m_1, m_2) = E[\{h^*(n)h(n-m_1)h(n-m_2)\} + \{h(n)h^*(n-m_1)h(n-m_2)\} + \{h(n)h(n-m_1)h^*(n-m_2)\}] \quad \forall m_1, m_2$$

A different font element is used in this definition to emphasize the fact that $\mathbf{c}_h(m_1, m_2)$ is not equal to $c_h(m_1, m_2)$. Notice that cumulant $\mathbf{c}_h(m_1, m_2)$ is defined as the sum of three terms, and that

each of the individual terms can be used by itself to establish another alternative definition for complex-valued scalar third-order cumulants. The extension of the Jouny-Moses definition to the vector case is obvious. However, the vector version of Equation (2-45) leads to intractable expressions in the derivation of recursions for the cumulants of the output of a time series model as a function of the cumulants of the input. Furthermore, satisfactory model parameter estimation results have been obtained to date for non-sinusoidal time series processes using Definition (2-42). This indicates that the problems observed by Jouny and Moses (1992) may be restricted to sums of pairs of coupled complex-valued sinusoids with uniformly-distributed phase (the bandwidth of a complex sinusoid is infinitesimally narrow). Therefore, the cumulant definition in Equation (2-42) is adopted for this program (a deviation is indulged upon in Section 2.3.2 for the sake of notational simplicity in a special context).

Cumulants possess several properties which motivate the approach of this Phase I program. Mendel (1991) presents an extensive list of properties of cumulants, with their associated proofs. He also points out that cumulants can be treated as an operator, much like the expectation operator. The properties most relevant to the work herein are listed in Table 2-7.

It is appropriate to consider the implications of these properties to radar surveillance problems. Properties (A)-(C) in Table 2-7 provide the major justification for the application of higher-order cumulants to the surveillance radar problem in scenarios with non-Gaussian clutter and/or targets. Based on these properties and on the formulation established in the preceding sections, it follows that the third-order cumulants of the process $\{x(n)\}$ are equal to the cumulants of the process which represents the non-Gaussian clutter and/or target,

$$(2-46) \quad C_x(m_1, m_2) = C_y(m_1, m_2) + C_w(m_1, m_2) = C_y(m_1, m_2)$$

This equation states that the Gaussian-distributed noise is eliminated from formulations and computations based on third-order cumulants. Elimination of the Gaussian-distributed noise effects is only approximated in practice because the presence of Gaussian noise generates inaccuracies in the estimates of the cumulants, and in the subsequent estimates of model parameters. Furthermore, even if the true cumulants are utilized to generate the filter parameters, noise residuals are present in the filter output.

SELECTED PROPERTIES OF HIGHER-ORDER CUMULANTS

- (A) Cumulants of a sum of independent random variates equal the sum of the cumulants of the individual variates.
- (B) Cumulants of a set of random variates of which at least two variates are pairwise independent are equal to zero.
- (C) Cumulants of a Gaussian-distributed scalar random sequence are equal to zero.
- (D) Odd-ordered cumulants of a scalar random sequence distributed according to a symmetric PDF are equal to zero.
- (E) Cumulants of a set of scalar random variates are invariant to permutations in the order of the arguments.

Table 2-7. Selected properties of higher-order cumulants.

Properties (C) and (D) have been referred to in the preceding sections. These properties restrict the utilization of cumulants to cases involving non-Gaussian clutter and/or targets distributed according to asymmetric PDFs. Lastly, Property (E) is the basis for the equivalence in Equation (2-44). This property is useful also in the generation of cumulant recursions, as indicated next in Section 2.3.2.

2.3.2 Third-Order Cumulant Relations for Time Series Systems

Third-order cumulants of the output sequence of time series systems satisfy algebraic expressions which involve the input sequence parameters and the model parameters in a manner analogous to the relations satisfied by output covariances (second-order cumulants). Those relations are developed in this section for MA, AR, and ARMA systems. The material presented in this section extends the multichannel work of Giannakis, Inouye, and Mendel (1989) and Raghuveer (1986) to the complex-valued case, with the appropriate modifications to account for the specific cumulant definition adopted in this program, Equation (2-42).

MA System. Consider the MA(M) process relation, Equation (2-23), and let $\underline{b}_{j;k}$ and $b_{ij;k}$ denote the j th column and the (i,j) th element of matrix \underline{B}_k , respectively. That is,

$$(2-47) \quad \underline{B}_k = [\underline{b}_{1;k} \quad \underline{b}_{2;k} \quad \cdots \quad \underline{b}_{J;k}] = \begin{bmatrix} b_{11;k} & b_{12;k} & \cdots & b_{1J;k} \\ b_{21;k} & b_{22;k} & \cdots & b_{2J;k} \\ \vdots & \vdots & \ddots & \vdots \\ b_{J1;k} & b_{J2;k} & \cdots & b_{JJ;k} \end{bmatrix}$$

It follows from Equations (2-23) and (2-47) that the j th element of vector $\underline{y}(n)$ can be expressed as

$$(2-48) \quad y_j(n) = \sum_{s=0}^M \underline{b}_{j;s}^H \underline{u}(n-s) = \sum_{s=0}^M \sum_{i=1}^J b_{ij;s}^* u_i(n-s)$$

Given these definitions, the j th third-order cumulant sequence of $\{y(n)\}$ is obtained as

$$(2-49) \quad C_{y;j}(m_1, m_2) = E \left[\left(\sum_{k=0}^M B_k^H \underline{u}(n-k) \right) \left(\sum_{r=0}^M \underline{u}^H(n-m_1-r) B_r \right) \left(\sum_{s=0}^M \sum_{i=1}^J b_{ij;s}^* u_i(n-m_2-s) \right) \right]$$

In this equation the order of the expectation and finite summations can be interchanged. Carrying out this interchange and re-ordering terms results in the expression

$$(2-50) \quad C_{y;j}(m_1, m_2) = \sum_{k=0}^M \sum_{r=0}^M \sum_{s=0}^M \sum_{i=1}^J B_k^H E[\underline{u}(n-k) \underline{u}^H(n-m_1-r) u_i^*(n-m_2-s)] B_r b_{ij;s}$$

The expected value inside the summations is recognized as the third-order cumulants of the input noise. Thus, substitution of Equation (2-30) into Equation (2-50) leads to

$$(2-51a) \quad C_{y;j}(m_1, m_2) = \sum_{k=0}^M \sum_{r=0}^M \sum_{s=0}^M \sum_{i=1}^J B_k^H \Gamma_i \delta(m_1+r-k, m_2+s-k) B_r b_{ij;s}$$

$$0 \leq m_1, m_2 \leq M$$

$$(2-51b) \quad C_{y;j}(m_1, m_2) = [0]$$

$$m_1 > M; \quad m_2 > M$$

Notice that Equation (2-51a) is defined for a limited range of values of the two lags, m_1 and m_2 , and that the cumulants are zero for all lag value pairs where at least one of the two lags is greater than the model order, M . This is a result of the temporal independence (whiteness) of the input sequence and of the finite order of the MA process (finite summation limit).

The remaining steps in the derivation apply only to the non-zero cumulants, Equation (2-51a). The 2-D discrete delta function in Equation (2-51a) assumes the value of unity only when both of its arguments are equal to zero simultaneously. This implies that in the summation over r all the terms are eliminated except the term corresponding to $r = k - m_1$; similarly, in the summation over s all the terms are eliminated except the term corresponding to $s = k - m_2$. Thus, Equation (2-51) reduces to

$$(2-52a) \quad C_{y,j}(m_1, m_2) = \sum_{k=m}^M \sum_{i=1}^J B_k^H \Gamma_i B_{k-m_1} b_{ij;k-m_2} \quad 0 \leq m_1, m_2 \leq M$$

$$(2-52b) \quad C_{y,j}(m_1, m_2) = \sum_{k=m}^M B_k^H \left[\sum_{i=1}^J \Gamma_i b_{ij;k-m_2} \right] B_{k-m_1} \quad 0 \leq m_1, m_2 \leq M$$

$$(2-52c) \quad m = \max(m_1, m_2)$$

Notice that the lower limit in the summation for k is now determined according to Equation (2-52c). This reflects the fact that the MA model parameter matrices, $\{B_r\}$, are defined only for indices in the range $0 \leq r \leq M$, with $r = k - m_l$ and $l = 1, 2$. The expressions in Equations (2-52a) and (2-52b) are equivalent; however, the second expression is preferred because it collects all the terms of the summation for i . Notice that each of the terms in the i summation is a matrix; it is convenient to represent this sum of matrices as the following matrix

$$(2-53) \quad B_j(k-m_2) = \sum_{i=1}^J \Gamma_i b_{ij;k-m_2} \quad m_2 \leq M; \quad 0 \leq k \leq m; \quad 1 \leq j \leq J$$

The letter "**B**" is selected to represent the summation in this definition in order to maintain association with the MA model

parameters $\{b_{ij,k}\}$; a different font type is selected to emphasize that matrices $\{\mathbf{B}_j(k-m_2)\}$ are distinct from the MA model matrices $\{\mathbf{B}_k\}$.

Substituting Definition (2-53) into Equation (2-52b) leads to the desired final expression,

$$(2-54a) \quad C_{y,ij}(m_1, m_2) = \sum_{k=m}^M \mathbf{B}_k^H \mathbf{B}_j(k-m_2) \mathbf{B}_{k-m_1} \quad 0 \leq m_1, m_2 \leq M; \quad 1 \leq j \leq J$$

$$(2-54b) \quad m = \max(m_1, m_2)$$

$$(2-54c) \quad C_{y,ij}(m_1, m_2) = [0] \quad m_1 > M; \quad m_2 > M; \quad 1 \leq j \leq J$$

Notice that Equations (2-51b) and (2-52c) are repeated as Equations (2-54c) and (2-54b), respectively, to emphasize the link that exists among these expressions.

Equation (2-54a) relates the model matrix parameters $\{\mathbf{B}_k\}$ and the matrix cumulants of the input noise process $\{\Gamma_k\}$ to the matrix cumulants of the MA(M) model output $\{C_{y,ij}(m_1, m_2)\}$ in a nonlinear manner. This equation is similar to the result derived by Giannakis, Inouye, and Mendel (1989) for the real-valued multichannel case, and is the basis for the MA model parameter identification algorithm presented in Section 4.2. Equation (2-54c) provides a guideline for MA model order selection in the algorithm.

AR System: Standard Cumulant Formulation. Consider the AR(L) process relation, Equation (2-24), and let $\underline{a}_{j,k}$ and $a_{ij,k}$ denote the j th column and the (i,j) th element of matrix \mathbf{A}_k , respectively. That is,

$$(2-55) \quad A_k = [a_{1;k} \ a_{2;k} \ \dots \ a_{J;k}] = \begin{bmatrix} a_{11;k} & a_{12;k} & \dots & a_{1J;k} \\ a_{21;k} & a_{22;k} & \dots & a_{2J;k} \\ \vdots & \vdots & \ddots & \vdots \\ a_{J1;k} & a_{J2;k} & \dots & a_{JJ;k} \end{bmatrix}$$

As in the MA case, the definition introduced in Equation (2-55) can be used to express the j th element of the AR vector $y(n)$ as

$$(2-56) \quad y_j(n) = - \sum_{s=1}^L a_{j;s}^H y(n-s) + u_j(n) = - \sum_{s=1}^L \sum_{i=1}^J a_{ij;s}^* y_i(n-s) + u_j(n)$$

Substitution of Equation (2-24) for $y(n-m_1)$ into the j th third-order cumulant definition, Equation (2-42a), results in the following expression,

$$(2-57) \quad C_{y,j}(m_1, m_2) = E \left[y(n) \left\{ - \sum_{k=1}^L y^H(n-m_1-k) A_k \right\} y_j^*(n-m_2) \right] \\ + E \left[y(n) u^H(n-m_1) y_j^*(n-m_2) \right]$$

The order of the expectation and finite summation on the first term on the right-hand-side of this equation can be interchanged. Also, the second term on the right-hand-side can be expanded by substitution of Equation (2-24). These manipulations lead to the expression

$$(2-58) \quad C_{y,j}(m_1, m_2) = - \sum_{k=1}^L E \left[y(n) y^H(n-m_1-k) y_j^*(n-m_2) \right] A_k \\ + E \left[\left\{ - \sum_{k=1}^L A_k^H y(n-k) \right\} u^H(n-m_1) y_j^*(n-m_2) \right] \\ + E \left[u(n) u^H(n-m_1) y_j^*(n-m_2) \right]$$

The expectation inside the summation on the first term on the right-hand-side of this equation is the j th third-order cumulant at lags (m_1+k, m_2) , and the order of the expectation and finite summation can be interchanged on the second term. Also, Equation (2-56) can be substituted for $y_j(n-m_2)$ on the third term. These operations result in

$$\begin{aligned}
 (2-59) \quad C_{y_{ij}}(m_1, m_2) = & - \sum_{k=1}^L C_{y_{ij}}(m_1+k, m_2) A_k \\
 & - \sum_{k=1}^L A_k^H E \left[y(n-k) \underline{u}^H(n-m_1) y_j^*(n-m_2) \right] \\
 & + E \left[\underline{u}(n) \underline{u}^H(n-m_1) \left\{ - \sum_{s=1}^L \sum_{i=1}^J a_{ij;s} y_i^*(n-m_2-s) \right\} \right] \\
 & + E \left[\underline{u}(n) \underline{u}^H(n-m_1) u_j^*(n-m_2) \right]
 \end{aligned}$$

The order of the expectation and finite summations can be interchanged on the third term on the right-hand-side of this equation. Also, the last term is recognized as the j th third-order cumulant of the input noise sequence. Carrying out these manipulations leads to (after re-ordering the terms)

$$\begin{aligned}
 (2-60) \quad C_{y_{ij}}(m_1, m_2) = & - \sum_{k=1}^L C_{y_{ij}}(m_1+k, m_2) A_k + \Gamma_j \delta(m_1, m_2) \\
 & - \sum_{k=1}^L A_k^H E \left[y(n-k) \underline{u}^H(n-m_1) y_j^*(n-m_2) \right] \\
 & - \sum_{s=1}^L \sum_{i=1}^J E \left[\underline{u}(n) \underline{u}^H(n-m_1) y_i^*(n-m_2-s) \right] a_{ij;s} \quad 1 \leq j \leq J
 \end{aligned}$$

Equation (2-60) is a general expression which is valid for all values of the lags m_1 and m_2 . Further substitutions of the AR expression into Equation (2-60) do not lead to a simpler form. However, an alternative approach results in a simplified relation, as indicated next.

The number of terms on the right-hand-side of Equation (2-60) can be reduced by selecting a subset of all possible lag values such that Property (B) in Table 2-7 applies. Specifically, for lags $m_1 = m_2 = 0$ the last two terms in the right-hand-side are equal to zero, and for lags in the range $0 < m_1 < m_2$ the last three terms in the right-hand-side are equal to zero. That is,

$$(2-61a) \quad C_{y,j}(0,0) = - \sum_{k=1}^L C_{y,j}(k,0) A_k + \Gamma_j \quad 1 \leq j \leq J$$

$$(2-61b) \quad C_{y,j}(m_1, m_2) = - \sum_{k=1}^L C_{y,j}(m_1+k, m_2) A_k \quad 0 < m_1 < m_2; \quad 1 \leq j \leq J$$

These equations can be written in a form which emphasizes their recursive structure and is related to covariance formulations. In order to do so it is convenient to first define a $JL \times J$ block column matrix \mathbf{A} as

$$(2-62) \quad \mathbf{A} = \begin{bmatrix} A_1 \\ A_2 \\ \vdots \\ A_L \end{bmatrix}$$

Now it is possible to write Equations (2-61a) in the form of a single block equation as

$$(2-63) \quad C_y(0,0) + [C_y(1,0) \ C_y(2,0) \ \dots \ C_y(L,0)] \mathbf{A} = C_u(0,0)$$

where the definitions in Equations (2-31) and (2-42b) have been used. The block row matrix which pre-multiplies \mathbf{A} in Equation (2-63) is dimensioned $J^2 \times JL$. Consider now Equations (2-61b) for a 1-D slice defined by $m_1 = 0$ and $m_2 = \{1, 2, \dots, S\}$, with $S \geq L$. For this 1-D slice Equations (2-61b) can be expressed in expanded form as

$$(2-64) \quad \begin{bmatrix} C_y(1,1) & C_y(2,1) & \dots & C_y(L,1) \\ C_y(1,2) & C_y(2,2) & \dots & C_y(L,2) \\ \vdots & \vdots & \ddots & \vdots \\ C_y(1,S) & C_y(2,S) & \dots & C_y(L,S) \end{bmatrix} \begin{bmatrix} A_1 \\ A_2 \\ \vdots \\ A_L \end{bmatrix} = - \begin{bmatrix} C_y(0,1) \\ C_y(0,2) \\ \vdots \\ C_y(0,S) \end{bmatrix}$$

Now define a $J^2 \times JL$ block row matrix $\mathbf{C}_{y:1,L}$, a $J^2 S \times JL$ block matrix $\mathbf{C}_{y:S,L}$, and a $J^2 S \times J$ block column matrix $\mathbf{C}_{y:S,1}$ as

$$(2-65) \quad \mathbf{C}_{y:1,L} = [C_y(1,0) \ C_y(2,0) \ \dots \ C_y(L,0)]$$

$$(2-66) \quad \mathbf{C}_{y:S,L} = \begin{bmatrix} C_y(1,1) & C_y(2,1) & \dots & C_y(L,1) \\ C_y(1,2) & C_y(2,2) & \dots & C_y(L,2) \\ \vdots & \vdots & \ddots & \vdots \\ C_y(1,S) & C_y(2,S) & \dots & C_y(L,S) \end{bmatrix}$$

$$(2-67) \quad \mathbf{C}_{y:S,1} = \begin{bmatrix} C_y(0,1) \\ C_y(0,2) \\ \vdots \\ C_y(0,S) \end{bmatrix}$$

Combining the definitions in Equations (2-62)-(2-67), it follows that

$$(2-68) \quad \mathbf{C}_{y:S,L} \mathbf{A} = -\mathbf{C}_{y:S,1}$$

$$(2-69) \quad \mathbf{C}_u(0,0) = \mathbf{C}_y(0,0) + \mathbf{C}_{y:1,L} \mathbf{A}$$

Equation (2-68) is referred to as the third-order cumulant normal equation, and the $J^2 S \times J L$ matrix $\mathbf{C}_{y:S,L}$ is the normal matrix. This normal matrix does not have a particular structure.

Equation (2-68) is used to identify the AR matrix parameters (Section 4.3). Given the $\mathbf{AR}(L)$ matrix coefficients, Equation (2-68) is used to generate an estimate of the input noise third-order cumulants. AR model recursions of this type are discussed by Mendel (1991) and others for the real-valued scalar case.

The form of Equations (2-68) and (2-69) results from the approach adopted for the derivation, and from the specific 1-D slice selected to constrain the lag values. Different choices (for the approach and/or the 1-D slice) result in different expressions with distinct analytical and numerical properties. An option of interest leads to a normal matrix with block Toeplitz structure, as summarized next.

Recursive equations with a structure different from that of Equations (2-61) can be generated by changing the steps in the derivation presented above. Specifically, consider the third-order cumulant definition, Equation (2-42a), and substitute the AR system expression for $\mathbf{y}(n)$, instead of for $\mathbf{y}(n-m_1)$ as in Equation (2-57). After a few manipulations similar to those carried above, the following expressions are obtained:

$$(2-70a) \quad \mathbf{C}_{y;j}(0,0) = - \sum_{k=1}^L \mathbf{A}_k^H \mathbf{C}_{y;j}(-k,-k) + \mathbf{\Gamma}_j \quad 1 \leq j \leq J$$

$$(2-70b) \quad C_{y,ij}(m_1, m_2) = - \sum_{k=1}^L A_k^H C_{y,ij}(m_1-k, m_2-k) \quad m_1, m_2 > 0; \quad 1 \leq j \leq J$$

These equations are analogous to Equations (2-61), but exhibit a different structure (it is important to note that in Equation (2-70b) it suffices that either $m_1 > 0$ or $m_2 > 0$). As before, the J Equations (2-70a) can be combined into a single expression. Also, for Equations (2-70b) select the diagonal 1-D slice defined by $m_1 = m_2 = \{1, 2, \dots, L\}$, and combine all J equations into a single expression. Finally, define the following three block matrices:

$$(2-71) \quad \mathbf{C}_{y:L,1} = \begin{bmatrix} C_y(-1,-1) \\ C_y(-2,-2) \\ \vdots \\ C_y(-L,-L) \end{bmatrix} = \begin{bmatrix} C_{y,1}(-1,-1) & \dots & C_{y,J}(-1,-1) \\ C_{y,1}(-2,-2) & \dots & C_{y,J}(-2,-2) \\ \vdots & & \vdots \\ C_{y,1}(-L,-L) & \dots & C_{y,J}(-L,-L) \end{bmatrix}$$

$$(2-72) \quad \mathbf{C}_{y:L,L} = \begin{bmatrix} C_y(0,0) & C_y(1,1) & \dots & C_y(L-1,L-1) \\ C_y(-1,-1) & C_y(0,0) & \dots & C_y(L-2,L-2) \\ \vdots & \vdots & \ddots & \vdots \\ C_y(-L+1,-L+1) & C_y(-L+2,-L+2) & \dots & C_y(0,0) \end{bmatrix}$$

$$(2-73) \quad \mathbf{C}_{y:1,L} = [C_y(1,1) \quad C_y(2,2) \quad \dots \quad C_y(L,L)]$$

$\mathbf{C}_{y:L,1}$ is a $JL \times J^2$ block column matrix, $\mathbf{C}_{y:L,L}$ is a $JL \times J^2 L$ block matrix, and $\mathbf{C}_{y:1,L}$ is a $J \times J^2 L$ block row matrix. Given these definitions, Equations (2-70) are expressed compactly as

$$(2-74) \quad \mathbf{C}_{y:L,L}^H \mathbf{A} = - \mathbf{C}_{y:1,L}^H$$

$$(2-75) \quad C_u(0,0) = [\Gamma_1 \quad \Gamma_2 \quad \dots \quad \Gamma_J] = C_y(0,0) + \mathbf{A}^H \mathbf{C}_{y:L,1}$$

where \mathbf{A} is as defined in Equation (2-62). The Hermitian operator is used in Equation (2-74) so that this equation can be compared directly with Equation (2-68). Notice that matrix $\mathbf{C}_{y:L,L}$ is block Toeplitz and block square. Also notice that the arrangement of the matrix elements as a block row in $\mathbf{C}_y(m,m)$ and in $\mathbf{C}_u(0,0)$ differs from the definition used heretofore (block column arrangement). This notational deviation is introduced to obtain compact block matrices in Equations (2-74) and (2-75), instead of sparse, higher-dimensioned matrices. The fact that an alternative notation is preferable when a different derivation approach is pursued provides another indication of the richness of options available when HOS for vector processes are involved.

Equations (2-74) and (2-75) contain equivalent information as Equations (2-68) and (2-69) with $\mathbf{S}=\mathbf{L}$. However, it is likely that each of these two pairs of equations will lead to different results in the practical solution of modeling, identification, and related problems. An extended version of Equation (2-74) is obtained by using $\mathbf{S} > \mathbf{L}$ index pairs (m_1, m_2) in the diagonal 1-D slice. The resulting matrix corresponding to Equation (2-72) has block Toeplitz structure, but is not block square.

AR System: Raghuveer Cumulant Formulation. Raghuveer (1986) has proposed an AR model recursion based on a subset of the full set of third-order cumulants for the real-valued multichannel case. SSC extended Raghuveer's formulation to the complex-valued multichannel case. Raghuveer's formulation requires fewer computations than the normal equations approach (since fewer scalar cumulants are estimated), and the matrix generated by the recursion, although not a normal matrix, has Toeplitz structure.

Raghuveer's formulation is based on a "reduced" cumulant matrix. Given the AR(L) system output sequence $\{y(n)\}$, define a $J \times J$ matrix $Y(n)$ as

$$(2-76) \quad Y(n) = \text{diag}[y_i(n)] = \begin{bmatrix} y_1(n) & 0 & \dots & 0 \\ 0 & y_2(n) & \dots & 0 \\ \vdots & \vdots & \ddots & \vdots \\ 0 & 0 & \dots & y_J(n) \end{bmatrix}$$

Let $C_y(m)$ denote a $J \times J$ matrix of third-order cumulants defined as

$$(2-77) \quad C_y(m) = E[y(n)y^H(n-m)Y^*(n-m)] \quad \forall m$$

The elements of this matrix are a subset of the third-order cumulants of the process $\{y(n)\}$. Thus, matrix $C_y(m)$ is not equal to the third-order cumulants, $C_y(m_1, m_2)$, as defined in Equation (2-42); in fact, matrix $C_y(m_1, m_2)$ has J^3 elements (third-order scalar moments) whereas matrix $C_y(m)$ has only J^2 elements. Furthermore, matrix $C_y(m)$ is different than matrix $C_y(m_1, m_2)$ restricted to the 1-D slice defined by $m_1 = 0$ and $m_2 = m$.

For an AR(L) process $\{y(n)\}$, cumulant matrix $C_y(m)$ restricted to lag values in the set $1 \leq m \leq L$ results in

$$(2-78) \quad C_y(m) = E \left[\left\{ - \sum_{k=1}^L A_k^H y(n-k) \right\} y^H(n-m) Y^*(n-m) \right] \\ + E[u(n) y^H(n-m) Y^*(n-m)] \quad 1 \leq m \leq L$$

In this equation the order of expectation and finite summation can be interchanged on the first term to the right of the equal sign. Also, for the selected range of lags the second term on the right-

hand-side is equal to zero (past outputs are independent of future inputs). Thus, Equations (2-78) reduce to

$$(2-79) \quad C_y(m) = - \sum_{k=1}^L A_k^H E[y(n-k) y^H(n-m) Y^*(n-m)] \quad 1 \leq m \leq L$$

Since the AR process is stationary, each of the three factors inside the expectation operator can be shifted forward in time by k integer steps; the result is recognized as $C_y(m-k)$. Equations (2-79) become

$$(2-80) \quad C_y(m) = - \sum_{k=1}^L A_k^H C_y(m-k) \quad 1 \leq m \leq L$$

In expanded form, Equations (2-80) are expressed as

$$(2-81) \quad [C_y(1) \ C_y(2) \ \dots \ C_y(L)] = -\mathbf{A}^H \begin{bmatrix} C_y(0) & C_y(1) & \dots & C_y(L-1) \\ C_y(-1) & C_y(0) & \dots & C_y(L-2) \\ \vdots & \vdots & \ddots & \vdots \\ C_y(-L+1) & C_y(-L+2) & \dots & C_y(0) \end{bmatrix}$$

where \mathbf{A} is the $JL \times J$ block matrix defined in Equation (2-62). Now define a $JL \times JL$ block matrix $\mathbf{C}_{y:L,L}$ and a $J \times JL$ block row matrix $\mathbf{C}_{y:1,L}$ as (bold type is used to emphasize that these matrices are distinct from their counterparts in Equations (2-68) and (2-69),

$$(2-82) \quad \mathbf{C}_{y:L,L} = \begin{bmatrix} C_y(0) & C_y(1) & \dots & C_y(L-1) \\ C_y(-1) & C_y(0) & \dots & C_y(L-2) \\ \vdots & \vdots & \ddots & \vdots \\ C_y(-L+1) & C_y(-L+2) & \dots & C_y(0) \end{bmatrix}$$

$$(2-83) \quad \mathbf{C}_{y:1,L} = [C_y(1) \ C_y(2) \ \dots \ C_y(L)]$$

By applying the definitions in Equations (2-62) and (2-82)-(2-83), the following compact expression is obtained for Equation (2-81),

$$(2-84) \quad \mathbf{C}_{y:L,L}^H \mathbf{A} = -\mathbf{C}_{y:1,L}^H$$

The Hermitian operator has been applied in Equation (2-84) so that this expression can be compared directly with Equations (2-68) and (2-74). The \mathbf{JLxJL} block matrix $\mathbf{C}_{y:L,L}$ has block Toeplitz structure.

ARMA System: Standard Cumulant Formulation. Consider the output process, $\{\mathbf{y}(n)\}$, of an ARMA(L,M) system, Equation (2-25), and the third-order cumulant definition in Equation (2-42). Substitution of the ARMA definition for $\mathbf{y}(n)$ into Equation (2-42a) results in

$$(2-85) \quad C_{y,ij}(m_1, m_2) = E \left[\left\{ - \sum_{k=1}^L A_k^H \mathbf{y}(n-k) \right\} \mathbf{y}^H(n-m_1) \mathbf{y}_j^*(n-m_2) \right] \\ + E \left[\left\{ \sum_{s=0}^M B_s^H \mathbf{u}(n-s) \right\} \mathbf{y}^H(n-m_1) \mathbf{y}_j^*(n-m_2) \right]$$

The order of the expectation and finite summation operations can be interchanged in each of the two terms on the right-hand-side of this equation. This leads to

$$(2-86) \quad C_{y,ij}(m_1, m_2) = - \sum_{k=1}^L A_k^H E \left[\mathbf{y}(n-k) \mathbf{y}^H(n-m_1) \mathbf{y}_j^*(n-m_2) \right] \\ + \sum_{s=0}^M B_s^H E \left[\mathbf{u}(n-s) \mathbf{y}^H(n-m_1) \mathbf{y}_j^*(n-m_2) \right]$$

Since both the input and output processes are stationary, the factors inside the first expectation operator can be shifted forward in time by k integer steps, and the factors inside the

second expectation operator can be shifted forward in time by s integer steps. Thus, Equations (2-86) become

$$(2-87) \quad C_{y,ij}(m_1, m_2) = - \sum_{k=1}^L A_k^H E[y(n) y^H(n-m_1+k) y_j^*(n-m_2+k)] \\ + \sum_{s=0}^M B_s^H E[u(n) y^H(n-m_1+s) y_j^*(n-m_2+s)]$$

The expected value factors in the first summation are recognized as $C_{y,ij}(m_1-k, m_2-k)$. Similarly, it is recognized that the expected value factors in the second summation are equal to zero for $m_1 > M$ and $m_2 > 0$ (or equivalently, for $m_1 > 0$ and $m_2 > M$). Therefore, a subset of Equations (2-87) is obtained as

$$(2-88) \quad C_{y,ij}(m_1, m_2) = - \sum_{k=1}^L A_k^H C_{y,ij}(m_1-k, m_2-k) \quad m_1 > M; \quad m_2 > 0; \quad 1 \leq j \leq J$$

The structure of this equation is identical to that of Equation (2-70b). However, the range of applicable values for m_1 is less in Equation (2-88) than in Equation (2-70b). Proceeding as in the discussion following Equation (2-70b), the final result of Equation (2-75) is valid for this case also, with the provision for the different range of values for m_1 . Namely,

$$(2-89) \quad \mathbf{C}_{y:L,L}^H \mathbf{A} = - \mathbf{C}_{y:1,L}^H \quad m_1 > M; \quad m_2 > 0$$

Block matrices $\mathbf{C}_{y:L,L}$ and $\mathbf{C}_{y:1,L}$ have structure analogous to the structure defined in Equations (2-72) and (2-73). As an example, for a 1-D slice defined by $m_1 = m_2 = \{L+1, L+2, \dots, 2L\}$, matrices $\mathbf{C}_{y:L,L}$ and $\mathbf{C}_{y:1,L}$ are given as

$$(2-90) \quad \mathbf{C}_{y:L,L} = \begin{bmatrix} C_y(L,L) & C_y(L+1,L+1) & \dots & C_y(2L-1,2L-1) \\ C_y(L-1,L-1) & C_y(L,L) & \dots & C_y(2L-2,2L-2) \\ \vdots & \vdots & \ddots & \vdots \\ C_y(1,1) & C_y(2,2) & \dots & C_y(L,L) \end{bmatrix}$$

$$(2-91) \quad \mathbf{C}_{y:1,L} = [C_y(L+1,L+1) \ C_y(L+2,L+2) \ \dots \ C_y(2L,2L)]$$

For the selected 1-D slice, the conditions on m_1 and m_2 expressed in Equation (2-89) are satisfied because $L \geq M$. Notice that matrix $\mathbf{C}_{y:L,L}$ is block Toeplitz. The real-valued scalar ARMA case has been discussed by Mendel (1991) and others.

ARMA System: Raghuveer Cumulant Formulation. Consider the third-order cumulant definition in Equation (2-77), applied to an ARMA(L,M) process $\{y(n)\}$, Equation (2-25). Substitution of the ARMA definition into Equation (2-77) restricted to lag values in the range $m \geq 1$ results in

$$(2-92) \quad C_y(m) = E \left[\left\{ - \sum_{k=1}^L A_k^H y(n-k) \right\} y^H(n-m) Y^*(n-m) \right] \\ + E \left[\left\{ \sum_{s=0}^M B_s^H u(n-s) \right\} y^H(n-m) Y^*(n-m) \right] \quad m \geq 1$$

Following the approach established earlier, it is possible to show that Equations (2-92) reduce to the following

$$(2-93) \quad C_y(m) = - \sum_{k=1}^L A_k^H C_y(m-k) + \sum_{s=0}^M B_s^H E[u(n) y^H(n-m+s) Y^*(n-m+s)] \quad m \geq 1$$

Notice that the second summation is equal to zero for lag values in the range $m > M$ (since past outputs are independent of future inputs). Therefore, an important subset of Equations (2-93) is

$$(2-94) \quad C_y(m) = - \sum_{k=1}^L A_k^H C_y(m-k) \quad m > M$$

This equation is identical to Equation (2-80), except that the range of applicable lag values for m in Equation (2-80) is $m \geq 1$, instead of $m > M$. Proceeding as in the discussion following Equation (2-80), the final result of Equation (2-84) is valid for this case also, with the different range of values for m . Namely,

$$(2-95) \quad \mathbf{C}_{y:L,L}^H \mathbf{A} = -\mathbf{C}_{y:1,L}^H \quad m > M$$

Block matrices $\mathbf{C}_{y:L,L}$ and $\mathbf{C}_{y:1,L}$ have structure analogous to the structure defined in Equations (2-82) and (2-83). For the case where the range of lag values is $m = \{L+1, L+2, \dots, 2L\}$, matrices $\mathbf{C}_{y:L,L}$ and $\mathbf{C}_{y:1,L}$ are given as

$$(2-96) \quad \mathbf{C}_{y:L,L} = \begin{bmatrix} C_y(L) & C_y(L+1) & \dots & C_y(2L-1) \\ C_y(L-1) & C_y(L) & \dots & C_y(2L-2) \\ \vdots & \vdots & \ddots & \vdots \\ C_y(1) & C_y(2) & \dots & C_y(L) \end{bmatrix}$$

$$(2-97) \quad \mathbf{C}_{y:1,L} = [C_y(L+1) \quad C_y(L+2) \quad \dots \quad C_y(2L)]$$

Notice that the constraint on m stated in Equation (3-47) is satisfied because $L \geq M$. Also, matrix $\mathbf{C}_{y:L,L}$ is block Toeplitz. These results extend Raghuveer's formulation to complex-valued multichannel ARMA systems.

3.0 DETECTION METHODOLOGY

The detection case considered in this report is Case (2-20a), wherein the baseband sequence $\{\underline{x}(n)\}$ is composed of a spatially-unresolved non-Gaussian target embedded in additive non-Gaussian clutter and additive Gaussian noise. Several issues associated with Case (2-20a) are addressed in this section, and possible detection options are presented.

Define the set of vectors $\{\underline{x}(n-1), \underline{x}(n-2), \dots\}$ as the past of the sequence $\{\underline{x}(n)\}$, and denote as $X^-(n)$ the vector space covering all possible linear combinations of the elements of the past of $\{\underline{x}(n)\}$. The minimum variance estimate (MVE) of $\underline{x}(n)$ is the conditional expectation $E[\underline{x}(n)|X^-(n)]$. Determination of the MVE and of the LLR detector requires availability of the multivariate PDF, and in the case of a non-Gaussian sequence the MVE and the LLR detector may be nonlinear functions of the data. As mentioned in Sections 2.1.2 and 2.1.3, the multivariate PDF is unavailable in most non-Gaussian cases; also, nonlinear functions can be difficult to implement. Thus, suboptimal linear approximations to the MVE and to the LLR detector were adopted in Phase I.

Let $\hat{\underline{x}}(n|n-1; H_i)$ for $i=0, 1$, denote a linear estimate of $\underline{x}(n)$ based on $X^-(n)$ and conditioned on hypothesis H_i being true. The linear estimates referred to are as defined in Section 3.5 using model parameters estimated as described in Section 4.0. Now define a conditional pseudo-innovations sequence, $\{\underline{g}(n|H_i)\}$ for $i=0, 1$, as

$$(3-1) \quad \underline{g}(n|H_i) = \underline{x}(n) - \hat{\underline{x}}(n|n-1; H_i) \quad i=0, 1$$

The conditional pseudo-innovations is a zero-mean sequence because both the baseband process and its linear estimate are zero-mean. This sequence is not a true innovations sequence because the

estimate $\hat{x}(n|n-1;H_i)$ as determined in Section 3.5 is not the MVE, and because the noise sequence $\{w(n)\}$ is non-zero (if $w(n)=0$ for all n , then the estimate generated as in Section 3.5 is a linear MVE). For these same reasons a detector which uses the pseudo-innovations (3-1) is not the LLR detector. In place of the true, but unavailable, LLR detector for the non-Gaussian case, the approximate, suboptimal detector proposed by Metford (1984) can be used. The pseudo-innovations of Equation (3-1) is used in such a configuration, as discussed in Section 3.4. In a minor abuse of notation, $g(n|H_0)$ and $g(n|H_1)$ are used herein to denote the output of the null hypothesis filter and the alternative hypothesis filter, respectively. At each resolution cell only the output of one of the two filters is a valid pseudo-innovations.

3.1 Detector Architecture Configurations

Two basic configurations can be defined for detection architectures: (a) adaptive on-line, and (b) off-line. The adaptive on-line configuration is illustrated in Figure 3-1. In this configuration the parameters of the two filters (one filter corresponding to each hypothesis) and covariance matrices required for detection rule calculations are determined in real-time by processing the multichannel baseband sequence for at least one CPI. Filter order may be estimated on-line also to provide complete adaptability. Order determination is, however, a difficult task. Alternatively, the orders of the two filters may be pre-stored in the radar processor memory. The order of the alternative hypothesis filter is always higher than the order of the null hypothesis filter because the radar return contains more information (the target component) when the alternative hypothesis is true. An on-line configuration provides the most adaptability, but presents a large computational burden even if filter order is pre-stored as a function of scenario conditions.

Higher-order cumulants can be used to adapt other aspects of the radar processor. As an example, estimates of higher-order cumulants can be used to assess the extent of deviation of the radar return from a Gaussian-distributed sequence. Such knowledge can be used to select the detection rule most appropriate for the identified conditions.

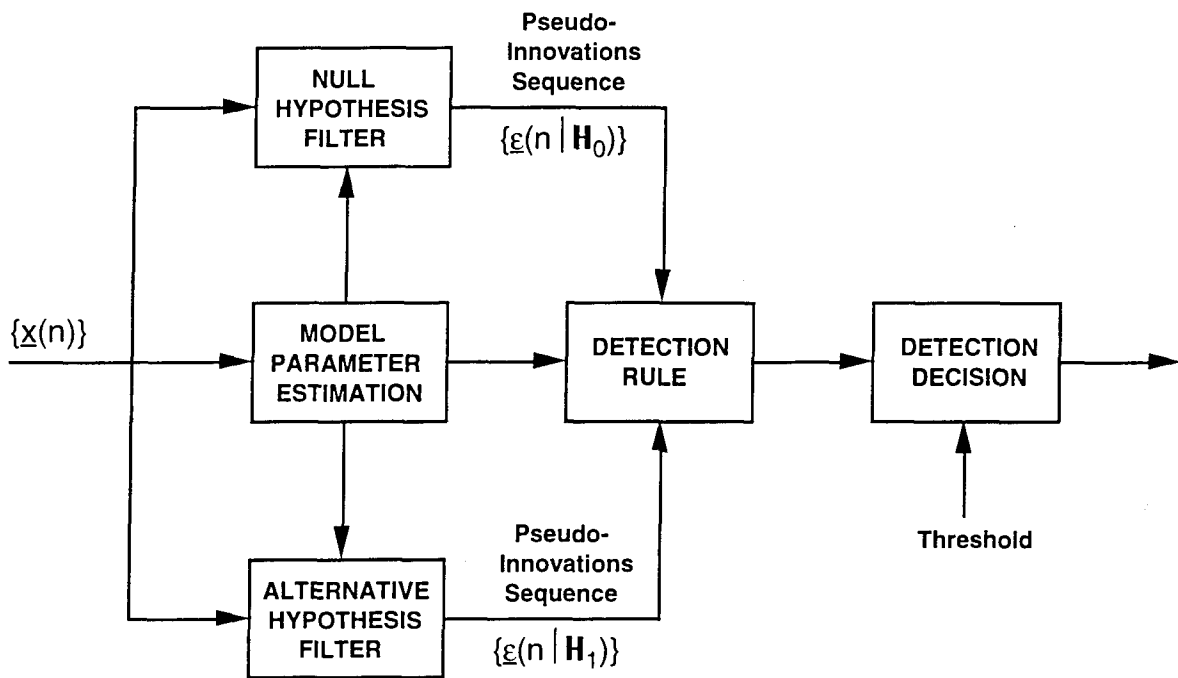


Figure 3-1. Multichannel detector configuration with on-line adaptive filter parameter identification.

The second configuration is illustrated in Figure 3-2. The major differences between the two configurations involve the central block in each of the two diagrams. In this configuration each filter is designed off-line using simulated and/or true radar data, and the resulting filter designs are implemented in the radar processor. Multiple filter pairs may be designed off-line, with each filter pair tuned to a distinct set of operational

conditions. This provides a partial degree of adaptability. The multichannel baseband sequence is used to estimate covariance matrices required for detection rule calculations, and to select the filter pair which best matches the scenario conditions if more than one filter pair is pre-stored in the radar processor memory. Careful off-line design of the filters can lead to acceptable performance.

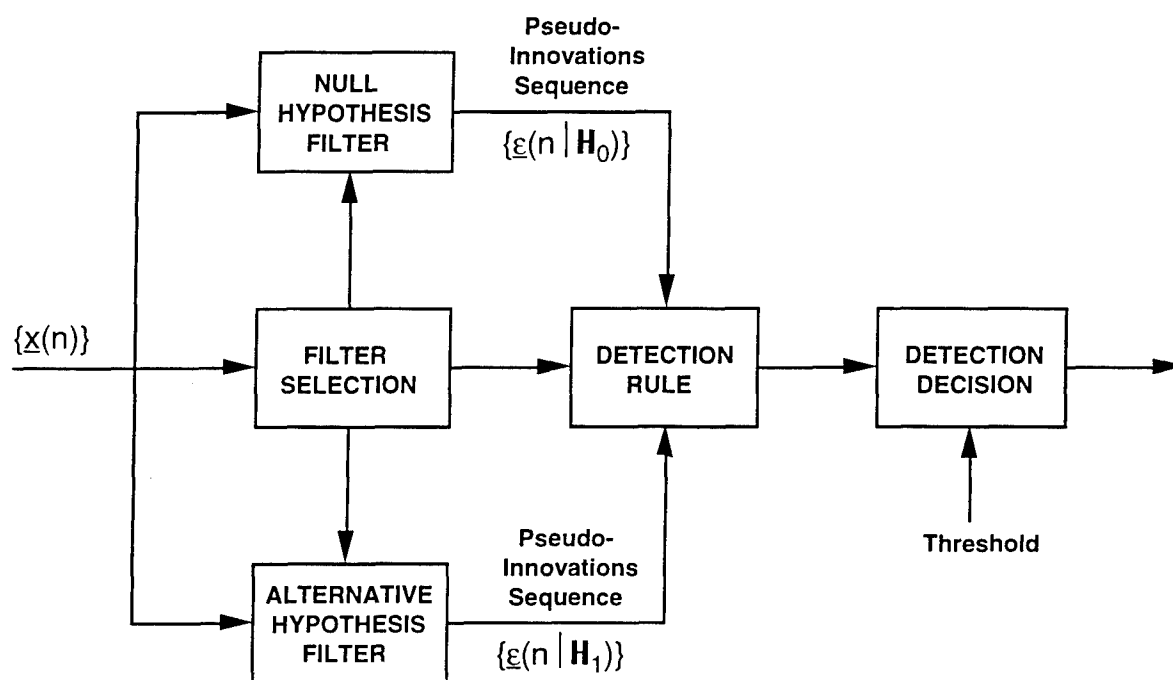


Figure 3-2. Multichannel detector off-line architecture configuration (off-line filter design).

3.2 Detection Domain

As discussed in Section 2.1.2, a non-Gaussian temporal clutter PDF model represents the conditions wherein the instantaneous fluctuations of the clutter signal at each individual resolution cell behave according to a non-Gaussian distribution. In turn, a non-Gaussian spatial clutter PDF model

represents conditions wherein the clutter is non-homogeneous over a large physical area which includes many resolution cells, but the instantaneous temporal fluctuations in each individual resolution cell behave according to a Gaussian distribution. A cumulant-based detection architecture can be designed for each of these two conditions.

Consider first a scenario wherein the non-Gaussian temporal clutter PDF model is valid, and the filter parameters are estimated on-line. In such a scenario, at each individual resolution cell the third-order cumulants of the multichannel baseband sequence are non-zero and can be estimated for each CPI using time averages (recall from Table 2-1 that $\{x(n)\}$ is ergodic). In turn, the estimated cumulants are used in the identification algorithms to estimate the model parameters of a whitening filter tuned to the particular resolution cell. The procedure is repeated for each resolution cell, and it is likely that the estimated filter varies from cell to cell. The domain in which this procedure is carried out is a local domain; more specifically, it is a single-cell domain. A detection architecture defined for a single resolution cell is referred to herein as a single-cell detection architecture.

In an off-line architecture configuration the whitening filter design is done off-line. In this case the non-Gaussian characteristic of the radar return in individual cells is taken into account in the estimation of third-order cumulants and in the design of the filters for use at each individual resolution cell.

Consider now a scenario in which the non-Gaussian spatial clutter PDF model is applicable. In this case all higher-order cumulants determined at individual cells over a CPI are zero. However, since the clutter process is non-Gaussian for the total

region, the ensemble of radar returns for all resolution cells over a CPI represents a non-Gaussian process. An ensemble estimate (as opposed to a time-average estimate) of third-order cumulants can be obtained, and the estimated cumulants can be used to identify the parameters of a whitening filter which is tuned to all resolution cells in the region. This procedure has a global domain, and a detection architecture defined for a whole region with a large number of resolution cells is referred to herein as a global detection architecture.

A global detection architecture can be configured either as an adaptive on-line or an off-line architecture. In a global detection architecture a single filter pair is used for a large number of resolution cells. This is a simple architecture with significantly reduced computational requirements in relation to the requirements of a single-cell detection architecture, specially for an off-line configuration. The detection architecture proposed by Rangaswamy, Weiner, and Michels (1993) for SIRPs is a global detection architecture. It is different, however, from the cumulant-based global detection architecture introduced herein.

3.3 Pre-Processing Option

As stated in Sections 2.1.2 and 2.1.3, it is unknown whether the marginal PDF of the quadrature components is symmetric or asymmetric about the mean because the marginal PDFs are unavailable for the non-Gaussian temporal clutter and target PDF models in Tables 2-2 and 2-3. Since the degree of asymmetry of the marginal PDFs is an open question, it is appropriate to define candidate options to handle each of the two possibilities. If the marginal PDF is asymmetric, then the third-order cumulants are non-zero and the cumulant-based procedures defined in this report can be applied directly. On the other hand, if the marginal PDF

is symmetric, then the third-order cumulants are zero. This case can be handled via two different approaches, as discussed next.

One approach is to formulate the procedures in this report using fourth-order (or higher-order) cumulants instead of third-order cumulants. This approach is feasible because many non-Gaussian symmetric PDFs often have fourth-order cumulants with large magnitude. However, in the multichannel case estimation of fourth-order cumulants requires significantly more computations than estimation of third-order cumulants. Furthermore, parameter identification algorithms based on fourth-order cumulants are computationally more intensive than equivalent algorithms based on third-order cumulants.

The second approach is motivated by the fact that the marginal PDF of the quadrature components can be altered (skewed) significantly, while the temporal correlation sequence is affected to a tolerable degree, by the application of some zero-memory nonlinear transformations to each of the two real-valued quadrature components prior to any cumulant-based processing. One such nonlinear transformation is the logarithm function, as indicated by Zheng, McLaughlin, and Mulgrew (1993). The logarithm of $\{x(n)\}$ is computed as a pre-processing step preceding the block diagrams in Figures 3-1 and 3-2. That is, the following operations are carried out on the multichannel baseband sequence,

$$(3-2a) \quad z_I(n) = \log_b[x_I(n) + a_I]$$

$$(3-2b) \quad z_Q(n) = \log_b[x_Q(n) + a_Q]$$

$$(3-2c) \quad \mu = E[z_I(n) + j z_Q(n)]$$

$$(3-2d) \quad \underline{z}(n) = z_I(n) + j z_Q(n) - \mu$$

where b denotes the logarithm base, μ is the complex-valued mean of the sequence $z_I(n) + jz_Q(n)$, and \underline{a}_I and \underline{a}_Q are real-valued vectors determined as

$$(3-3a) \quad \underline{a}_I = \lfloor \min\{\underline{x}_I(n)\} \rfloor + ci$$

$$(3-3b) \quad \underline{a}_Q = \lfloor \min\{\underline{x}_Q(n)\} \rfloor + ci$$

$$(3-3c) \quad c \geq 1$$

with c a real-valued scalar, and j is a J -dimensional vector with all elements equal to unity. The function of the vectors \underline{a}_I and \underline{a}_Q is to bias the sequence $\{\underline{x}(n)\}$ so that the argument of the logarithm function in Equations (3-2a) and (3-2b) is greater than or equal to unity for all n (recall that the sequence $\{\underline{x}(n)\}$ has zero mean). In a hardware implementation the sample mean of $z_I(n) + jz_Q(n)$ is used in place of the unavailable true mean. Notice that sequence $\{z(n)\}$ has zero mean, as required for cumulant estimation. If this pre-processing option is used, the transformed sequence $\{z(n)\}$ replaces $\{\underline{x}(n)\}$ in the detection procedure. However, in order to avoid confusion $\{\underline{x}(n)\}$ will continue to denote the multichannel baseband sequence in the remainder of this report.

The use of the logarithmic transformation has several features of interest. The log transformation is instantaneous (zero-memory), and can be implemented as a table look-up in a digital processor. In some radar systems the logarithm is an inherent function in the analog portion of the receiver, applied to the radar return signal in order to reduce its dynamic range (see, for example, Nathanson [1991]). The effect of the logarithmic transformation on simulated data is examined in Section 5.0. The results discussed therein indicate that the log

transformation can be used effectively for data generation as well as a pre-processor in the cases where the PDF of the quadrature components is symmetric about the mean.

3.4 Detection Rule

Metford (1984) (see also Metford, Haykin, and Taylor [1982]) has demonstrated that the LLR detection rule for the Gaussian case, Case (2-20d), can be used in an approximate sense as the detection rule for the case of detecting a non-Gaussian sequence embedded in additive Gaussian noise. Furthermore, acceptable results can be obtained for the cases where the true innovations sequence is unavailable (or equivalently, where only a suboptimal estimate of the non-Gaussian sequence is available). These conditions are similar to the conditions for Case (2-20a), as described in Sections 2.0-4.0 of this report. Additionally, SSC has noticed in simulation-based analyses that the pseudo-innovations generated using the whitening filters for time series models tend to be Gaussian-distributed as the model order and/or the number of channels increases. This is a manifestation of the central limit theorem: a linear combination of a large number of non-Gaussian random variates tends to be Gaussian-distributed. It is likely that the pseudo-innovations tend to be Gaussian-distributed also when there is some model mismatch (the true system differs from the model adopted for the filter design). A degree of model mismatch is present when real radar data is concerned because the time series models are inherently models of representation. For these reasons the Gaussian LLR is adopted in this program as an approximate, suboptimal detection rule for non-Gaussian sequences.

The innovations-based multichannel LLR detection rule for the complex-valued Gaussian case has been derived by Michels (1991).

Also, Rangaswamy, Weiner, and Michels (1993) have demonstrated recently that the methodology can be extended to include non-Gaussian SIRPs (recall that the SIRP model is appropriate for the spatial non-Gaussian clutter conditions as described in Section 2.1.2). Based on the above discussion, Michels' multichannel LLR detection methodology is adopted in this program, with the conditional pseudo-innovations used in place of the conditional innovations. For brevity, only the final LLR expression is presented here.

Consider the conditional pseudo-innovations in Equations (3-1), and let $\Omega(\mathbf{H}_i)$ denote the covariance matrix of the pseudo-innovations,

$$(3-4) \quad \Omega(\mathbf{H}_i) = E[\underline{\varepsilon}(n|\mathbf{H}_i) \underline{\varepsilon}^H(n|\mathbf{H}_i)] \quad i = 0, 1$$

This is a true covariance matrix because the pseudo-innovations sequence is zero-mean. Now let $\Theta(\mathbf{H}_0, \mathbf{H}_1)$ denote the multichannel likelihood ratio for Case (2-20d), the Gaussian case. Then, the complex-valued multichannel LLR as defined by Michels (1991) is

$$(3-5) \quad \ln[\Theta(\mathbf{H}_0, \mathbf{H}_1)] = \sum_{n=0}^{N-1} \left[\ln \left[\frac{|\Omega(\mathbf{H}_0)|}{|\Omega(\mathbf{H}_1)|} \right] + \underline{\varepsilon}^H(n|\mathbf{H}_0) \Omega^{-1}(\mathbf{H}_0) \underline{\varepsilon}(n|\mathbf{H}_0) - \underline{\varepsilon}^H(n|\mathbf{H}_1) \Omega^{-1}(\mathbf{H}_1) \underline{\varepsilon}(n|\mathbf{H}_1) \right]$$

As indicated in Figures 3-1 and 3-2, the LLR is compared to a threshold, \mathcal{T} , which is calculated adaptively to maintain a constant false alarm rate (CFAR),

$$(3-6) \quad \ln[\Theta(\mathbf{H}_0, \mathbf{H}_1)] = \begin{cases} \geq \mathcal{T} & \text{select } \mathbf{H}_1 \\ < \mathcal{T} & \text{select } \mathbf{H}_0 \end{cases}$$

A candidate CFAR approach with demonstrated good performance consists of calculating the median of a set of the LLR values from a number of adjacent range cells (at the same azimuth) on both sides of the cell in question, and then scaling the calculated median value by a pre-determined constant to provide the desired false alarm rate (Metford and Haykin, 1985).

Alternative expressions for the LLR can be generated based on factorization of the pseudo-innovations covariance matrix and spatial whitening of the pseudo-innovations sequence. Applicable covariance factorization methods include Cholesky factorization, LDU decomposition, and singular value decomposition (SVD); all three lead to simplified LLR expressions. The first two techniques have been described by Michels (1991), and the SVD technique is described by Román and Davis (1993).

3.5 Digital Realizations For Whitening Filters

The cumulant-based model parameter identification algorithms presented in Section 4.0 generate the parameters of a time series model for the multichannel baseband sequence, $\{x(n)\}$. Given the matrix parameters for a time series model, the whitening filter which generates the pseudo-innovations is obtained as the inverse system of the time series model. Specifically, the whitening filter for a MA(M) system is an AR(M) filter; the whitening filter for an AR(L) system is a MA(L) filter; and the whitening filter for an ARMA(L,M) system is an ARMA(L,L) filter.

A time series whitening filter can be implemented with various distinct digital realizations, such as tapped delay line (or direct form), parallel, and cascade. These three types of digital realizations are minimal (or canonical) because their implementation requires the minimum number of delay operations.

The tapped delay line realization is of particular interest because it can be generated by inspection of the time series system expressions. In general, cascade and parallel digital filter realizations offer the best numerical performance (minimization of parameter quantization effects), but require knowledge of the system poles and/or zeros (Oppenheim and Schafer, 1975). The system poles and zeros are the roots of the polynomials $\alpha(z)$ and $\beta(z)$, respectively, as defined in Equations (2-40) and (2-41). Time series systems which satisfy the assumptions in Table 2-6 have JL poles and/or JM zeros. Computation of the polynomials $\alpha(z)$ and $\beta(z)$ and their roots imposes a large computational load and is difficult to implement on-line. It is feasible, however, in the off-line case.

In the remainder of this section the conditional notation is dropped from the argument set of the pseudo-innovations, estimates, and other variates for notational simplicity. The figures and equations presented are applicable for both hypotheses with the stipulation that the system model order is larger for the alternative hypothesis (the target forces additional modeling degrees-of-freedom).

3.5.1 Moving Average System Whitening Filter

A tapped delay line realization for the whitening filter of a MA(M) system is presented in Figure 3-3. In this figure, as well as in the next two figures, each of the blocks labeled "DELAY" represents a J-dimensional column of scalar delay operators because the input to each block is a J-dimensional vector. This is a minimal realization, with a total of JM delays. The linear estimate and the pseudo-innovations for this case are

$$(3-7) \quad \hat{x}(n|n-1) = \sum_{k=1}^M B_k^H \varepsilon(n-k)$$

$$(3-8) \quad \varepsilon(n) = x(n) - \hat{x}(n|n-1) = - \sum_{k=1}^M B_k^H \varepsilon(n-k) + x(n)$$

From Equation (3-8), the whitening filter is an AR(M) system with $x(n)$ as the input, $\varepsilon(n)$ as the output, and $\{B_k\}$ as the AR matrix parameters. The MA system zeros are the poles of the whitening filter; the whitening filter does not have any finite-value zeros.

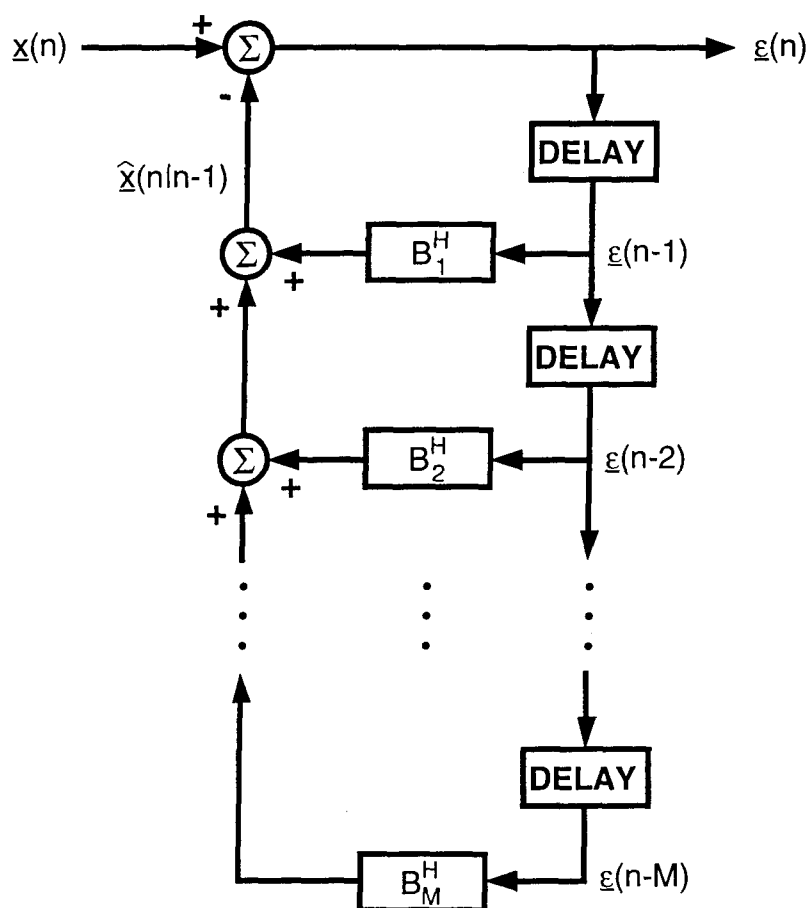


Figure 3-3. Tapped delay line realization for whitening filter corresponding to a MA(M) system.

3.5.2 Auto-Regressive System Whitening Filter

A tapped delay line minimal realization (JL delays) for the whitening filter of an $AR(L)$ system is presented in Figure 3-4. The linear estimate and the pseudo-innovations for this case are

$$(3-9) \quad \hat{x}(n|n-1) = - \sum_{k=1}^L A_k^H x(n-k)$$

$$(3-10a) \quad \varepsilon(n) = x(n) - \hat{x}(n|n-1) = x(n) + \sum_{k=1}^L A_k^H x(n-k) = \sum_{k=0}^L A_k^H x(n-k)$$

$$(3-10b) \quad A_0 = I_J$$

Thus, the whitening filter is a $MA(L)$ system with $x(n)$ as the input, $\varepsilon(n)$ as the output, and $\{A_k\}$ as the MA matrix parameters. The AR system poles are the zeros of the whitening filter; all the whitening filter poles assume the value zero.

3.5.3 Auto-Regressive Moving-Average System Whitening Filter

A tapped delay line minimal realization for the whitening filter of an $ARMA(L,M)$ system is presented in Figure 3-5. This realization has a total number of JL delays. The linear estimate and the pseudo-innovations for this case are

$$(3-11) \quad \hat{x}(n|n-1) = - \sum_{k=1}^L A_k^H x(n-k) + \sum_{k=1}^M B_k^H \varepsilon(n-k)$$

$$(3-12a) \quad \varepsilon(n) = x(n) - \hat{x}(n|n-1) = - \sum_{k=1}^L B_k^H \varepsilon(n-k) + \sum_{k=0}^L A_k^H x(n-k)$$

$$(3-12b) \quad A_0 = I_J$$

$$(3-12c) \quad B_k = [0]$$

$$k = M+1, \dots, L$$

From Equation (3-12), the whitening filter is an ARMA(L,L) system with $\underline{x}(n)$ as the input, $\underline{g}(n)$ as the output, $\{A_k\}$ as the MA parameters, and $\{B_k\}$ as the AR parameters. The ARMA system zeros are the poles of the whitening filter, and the ARMA system poles are the zeros of the whitening filter. When $L > M$, the extra poles in the whitening filter assume the value zero.

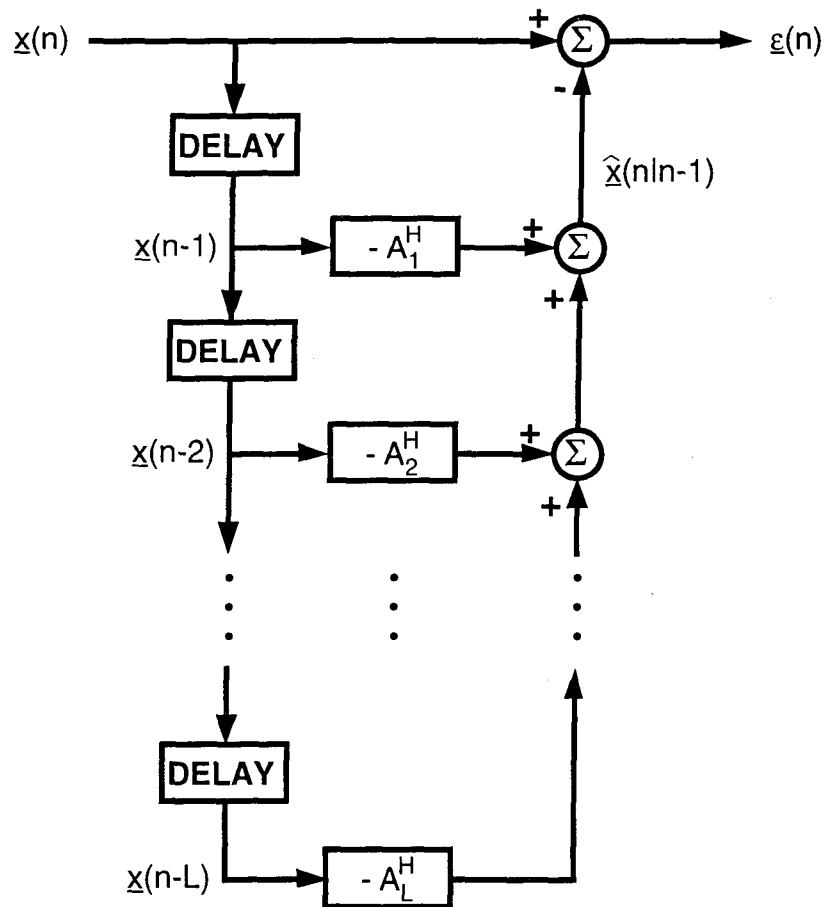


Figure 3-4. Tapped delay line realization for whitening filter corresponding to an AR(L) system.

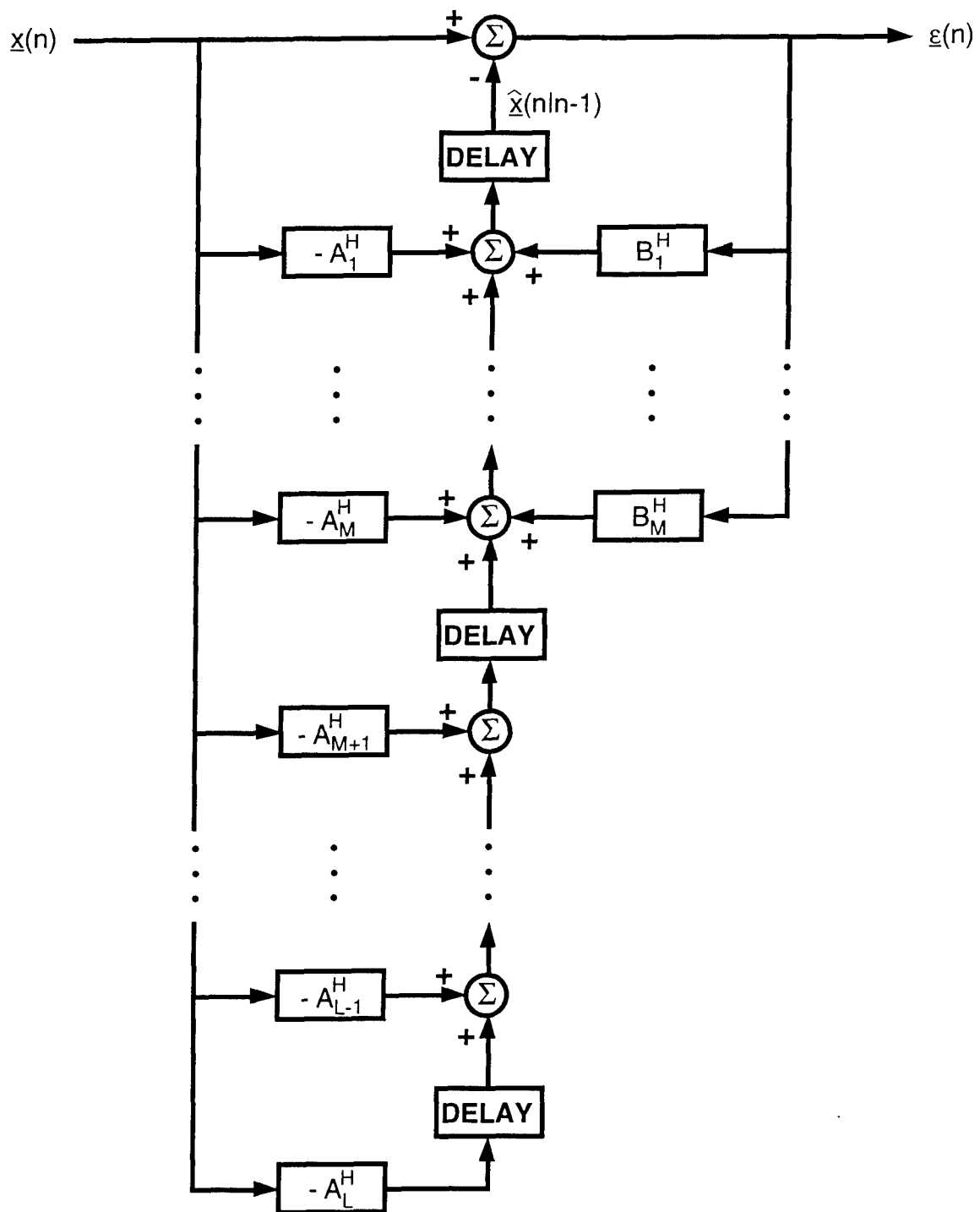


Figure 3-5. Tapped delay line realization for whitening filter corresponding to an ARMA(L,M) system (with $L > M$).

4.0 IDENTIFICATION ALGORITHMS

Identification of the model parameter matrices, $\{A_k\}$ and/or $\{B_k\}$, for the whitening filters is carried out based on the third-order cumulant relations for time series systems presented in Section 2.3.2. The MA and AR identification algorithms presented herein can be categorized as linear algebra algorithms because in these methods the key step in the estimation of the unknown matrix parameters is the solution of a system of equations which are linear in a set of parameters. In comparison with optimization algorithms (which require the iterative solution to a nonlinear system of equations), linear algebra algorithms are simpler to implement in software and/or hardware, and do not involve convergence issues directly. Optimization algorithms do provide more accurate results at an increased computational cost. Thus, linear algebra algorithms are better candidates for on-line implementation, and optimization algorithms are better candidates for off-line analyses and design. The identification algorithms summarized herein require the third-order cumulants of the multichannel baseband sequence; since the true cumulants are unavailable, an estimate is obtained and used in the algorithms.

Stability of the identified model and the associated whitening filter is an issue of relevance to all known identification algorithms based on higher-order cumulants. Specifically, none of the identification algorithms based on higher-order cumulants can guarantee that the estimated parameters correspond to a stable system. This is due, in part, to the fact that third-order cumulants contain phase information (unlike the covariance sequence), which allows the use of third-order cumulants to identify minimum-phase as well as non-minimum phase models (recall that if a system is minimum-phase, then it is stable, and its whitening filter is stable also). Analyses

carried out to date by SSC indicate that all the algorithms considered in Phase I can identify non-minimum phase models even when a stable system is used to generate the data. However, this occurs only in a limited number of cases. SSC has observed also that MA algorithms are more prone to generate unstable system estimates than AR algorithms. Further analyses are required during Phase II in order to establish MA, AR, and ARMA algorithm performance with respect to stability.

In the context of multichannel detection for radar surveillance, model stability is an issue only for adaptive on-line detector configurations. Two possible approaches to address this potential problem for on-line configurations have been identified. The first approach is to average several estimates of model parameters obtained over a homogeneous region. The second approach is to extend the detection rule formulation to handle non-causal whitening filters, and to assign the unstable poles and/or zeros to the non-causal component of the filter. Stability is not an issue if causality is not a requirement. Since in an airborne radar processor the received data can be stored at least for one CPI, it is possible to consider a non-causal processing approach.

4.1 Third-Order Cumulants Estimation

Each of the two detector architectures mentioned in Section 3.2 requires a different cumulant estimator. The first estimator is a time average estimator for a single-cell domain detector formulation and is defined as

$$(4-1a) \quad \hat{C}_{x_{ij}}(m_1, m_2) = \frac{1}{N-m} \sum_{n=m}^{N-1} x(n) x^H(n-m_1) x_j^*(n-m_2) \quad j = 1, 2, \dots, J$$

$$(4-1b) \quad \hat{C}_x(m_1, m_2) = \frac{1}{N-m} \sum_{n=m}^{N-1} \underline{x}^*(n-m_2) \otimes \underline{x}(n) \otimes \underline{x}^H(n-m_1)$$

$$(4-1c) \quad m = \max(m_1, m_2)$$

In this estimator the time average is taken over one CPI. If appropriate, it is possible to include data for more than one CPI. Estimator (4-1) provides an unbiased estimate of the multichannel baseband sequence third-order cumulants since the temporal process is assumed to be ergodic and zero mean (Table 2-1). The estimate (4-1) converges in probability to the true third-order cumulants because $\{\underline{x}(n)\}$ is assumed to be exponentially stable, and the model input noise process $\{\underline{u}(n)\}$ is assumed to be stationary with finite cumulants at least up to sixth-order. The condition of finite cumulants at least up to sixth-order guarantees that the first six cumulants of the input noise process are absolutely summable, which is the actual requirement for convergence in probability (see Mendel [1991] and the references therein).

The second estimator is an ensemble estimator for a global domain detector formulation and is defined as

$$(4-2a) \quad \hat{C}_{x;j}(m_1, m_2) = \frac{1}{K} \sum_{k \in \mathcal{K}} \underline{x}_k(n) \underline{x}_k^H(n-m_1) \underline{x}_{jk}^*(n-m_2) \quad j = 1, 2, \dots, J$$

$$(4-2b) \quad \hat{C}_x(m_1, m_2) = \frac{1}{K} \sum_{k \in \mathcal{K}} \underline{x}_k^*(n-m_2) \otimes \underline{x}_k(n) \otimes \underline{x}_k^H(n-m_1)$$

The subscript k denotes the radar resolution cell (as in Section 2.1 and Figure 2-1), \mathcal{K} denotes the set of selected ensemble resolution cells, and K denotes the number of resolution cells included in \mathcal{K} . The number K must be large in order to insure that the global non-Gaussian features are represented well. If the

selected resolution cells are independent, then a smaller number of cells suffices. The time n is fixed at an instant in the CPI for each resolution cell in the ensemble. The ensemble mean must be estimated and, if non-zero, subtracted from the ensemble samples prior to estimation of the cumulants. Estimator (4-2) is an unbiased estimator of the true third-order cumulants; also, the estimate converges in probability to the true third-order cumulants for the same reasons as Estimator (4-1).

The following approximations are adopted implicitly in all equations and discussions where cumulants appear and the true cumulants are unavailable,

$$(4-3a) \quad C_{x,j}(m_1, m_2) \approx \hat{C}_{x,j}(m_1, m_2) \quad j = 1, 2, \dots, J$$

$$(4-3b) \quad C_x(m_1, m_2) \approx \hat{C}_x(m_1, m_2)$$

That is, the appropriate estimate (either (4-1) or (4-2)) is used in place of the unknown true third-order cumulants.

4.2 MA Parameter Identification

The MA parameter identification algorithm presented herein is a modification of the algorithm proposed by Giannakis, Inouye, and Mendel (1989). The modifications made by SSC include extension of the algorithm to the complex-valued case, and simpler expressions for the identification equations. In this report, this algorithm is referred to as the one-slice MA algorithm.

One-Slice MA Algorithm. The one-slice identification algorithm for MA systems is based on two key decisions involving the third-order cumulant relations for MA systems, Equations (2-54). First, a specific 1-D slice of Equations (2-54a) is selected so that the

summation on the right-hand-side has only one non-zero term. The selected 1-D slice is defined by $0 \leq m_1 \leq M$ and $m_2 = M$. For the lag pairs in this slice the summation on the right-hand-side of Equations (2-54a) includes only one non-zero term. Second, matrix B_M is taken to be equal to the J -dimensional identity matrix. This does not imply a loss of generality because matrix B_M has full rank (Table 2-6), and because the basis in which the noise input $\{u(n)\}$ is identified is irrelevant with respect to detection performance (recall also that the MA model is a representation model).

Consider the third-order cumulant relations for MA systems derived in Section 2.3.2, and let $m_2 = M$ in Equations (2-54a). Also, concatenate Equations (2-54a) for $j=1,2,\dots,J$, to obtain

$$(4-4) \quad C_x(m_1, M) = [I_J \otimes B_M^H] B(0) B_{M-m_1} \quad 0 \leq m_1 \leq M$$

where $C_x(m_1, M)$ and $B(0)$ are $J^2 \times J$ matrices defined as

$$(4-5) \quad C_x(m_1, M) = \begin{bmatrix} C_{x,1}(m_1, M) \\ C_{x,2}(m_1, M) \\ \vdots \\ C_{x,J}(m_1, M) \end{bmatrix} \quad 0 \leq m_1 \leq M$$

$$(4-6) \quad B(0) = \begin{bmatrix} B_1(0) \\ B_2(0) \\ \vdots \\ B_J(0) \end{bmatrix}$$

Now let $m_1 = 0$ in Equation (4-4), and use the fact that B_M has full rank to obtain

$$(4-7) \quad [I_J \otimes B_M^H] \mathbf{B}(0) = C_x(0,M) B_M^{-1}$$

This expression is substituted into Equation (4-4) to eliminate matrix $\mathbf{B}(0)$, which results in

$$(4-8) \quad C_x(m_1, M) = C_x(0, M) B_M^{-1} B_{M-m_1} \quad 0 \leq m_1 \leq M$$

Since the basis adopted to represent the input noise sequence $\{\underline{u}(n)\}$ is arbitrary with respect to detection performance, matrix B_M can be assumed to be an identity matrix. Given this assumption and Equation (4-8), the MA matrix parameters are obtained as

$$(4-9a) \quad B_M = I_J$$

$$(4-9b) \quad B_{M-m_1} = C_x^\dagger(0, M) C_x(m_1, M) \quad 0 < m_1 \leq M$$

where the dagger (\dagger) denotes the pseudoinverse operator.

To identify the third-order cumulants of the input noise the MA matrix parameters are estimated first according to Equation (4-9). Next, let $m_1 = M$ and $m_2 = 0$ in Equations (2-54a) to obtain

$$(4-10) \quad C_{x,j}(M, 0) = B_j(M) B_0 \quad j = 1, 2, \dots, J$$

with Equation (4-9a) taken into account. From Definition (2-53),

$$(4-11) \quad B_j(M) = \sum_{i=1}^J \Gamma_i b_{ij,M} \quad j = 1, 2, \dots, J$$

Since $b_{ij,M}$ is the (i,j) th element of B_M , it follows from Equation (4-9a) that

$$(4-12) \quad b_{ij;M} = \delta_{ij}$$

Consequently, Equation (4-11) reduces to

$$(4-13) \quad \mathbf{B}_j(M) = \Gamma_j \quad j = 1, 2, \dots, J$$

And Equations (4-10) become

$$(4-14) \quad \mathbf{C}_{x;j}(M,0) = \Gamma_j \mathbf{B}_0 \quad j = 1, 2, \dots, J$$

Matrix \mathbf{B}_0 is determined using Equation (4-9b) for $m_1 = M$, and is a full rank matrix (Table 2-6). Therefore, the parameters $\{\Gamma_j\}$ are identified according to the expression

$$(4-15) \quad \Gamma_j = \mathbf{C}_{x;j}(M,0) \mathbf{B}_0^{-1} = \mathbf{C}_{x;j}(M,0) [\mathbf{C}_x^\dagger(0,M) \mathbf{C}_x(M,M)]^{-1} \quad j = 1, 2, \dots, J$$

These cumulants are not required for the detection rule. Computation of the pseudoinverse in Equation (4-9b) and of the inverse in Equation (4-15) can be carried out via the SVD.

An alternative multichannel MA identification algorithm has been proposed by Tong, Inouye, and Liu (1992). Their algorithm converges in a finite number of steps, but is significantly more complicated than the one-slice algorithm presented above. The Tong-Inouye-Liu algorithm should be considered in Phase II, including evaluation of its capability to generate correct parameter estimates for minimum-phase systems.

Model Order Determination. Model order for an MA(M) system can be determined based on Equation (2-54c). Assume that the true model order is less than a given upper bound, denoted as M_T . Then compute as many 1-D slices as possible of the third-order

cumulants $C_x(m_1, m_2)$. At least two 1-D slices should be computed. Two convenient 1-D slices are the horizontal and vertical slices, defined as $\{0 \leq m_1 \leq M_T, m_2 = 0\}$ and $\{m_1 = 0, 0 \leq m_2 \leq M_T\}$, respectively. In theory, the cumulants for lag pairs with either $m_1 > M$ or $m_2 > M$ are zero, but in practice all cumulants are likely to be non-zero. However, if good estimates of the cumulants $C_x(m_1, m_2)$ are available, then a discontinuity in the magnitude of the elements of the estimated cumulant matrices can be expected at lag pairs with either $m_1 = M+1$ or $m_2 = M+1$. The next step in the procedure is to apply the principle of a matrix norm to each of the estimated cumulant matrices (a matrix norm is useful in assessing relative magnitude between square matrices [Faddeeva, 1959]). The set of computed norms is a 2-D function of m_1 and m_2 . This 2-D function is examined to determine the points of discontinuities, which provide an estimate of model order. A candidate matrix norm, referred to herein as matrix norm A, is defined for a $J \times J$ matrix C with elements $\{c_{ij}\}$, as

$$(4-16) \quad \|C\|_A = \max_j \left[\sum_{i=1}^J |c_{ij}| \right]$$

Since the cumulant matrices are rectangular ($J^2 \times J$), matrix norm A cannot be applied directly. However, matrix norm A can be applied to a $J \times J$ matrix computed as

$$(4-17) \quad C = C_x^H(m_1, m_2) C_x(m_1, m_2)$$

Other matrix norms are available (such as the Euclidean matrix norm [Faddeeva, 1959]), but matrix norm A is attractive because squaring operations are not involved (by Equation (4-17), the elements of the cumulants are squared already).

4.3 AR Parameter Identification

The AR parameter identification algorithms summarized herein are discussed by Mendel (1991) for the real-valued scalar case, and Raghuveer (1986) for the real-valued multichannel case. The algorithms are based on the recursive relations for cumulants derived by SSC for the complex-valued multichannel case and presented in Section 2.3.2. Two distinct, but similar, algorithms are summarized. The first algorithm is based on the standard cumulant formulation, and the second algorithm is based on the Raghuveer cumulant formulation.

AR Model Identification Using the Standard Cumulant Formulation.

Consider the third-order cumulant recursions presented as Equations (2-68) and (2-69), and recall that $S \geq L+1$. Equation (2-68) can be viewed as a collection of J linear systems of equations (corresponding to the J columns of \mathbf{A}), with each system consisting of $JS \times JL$ equations in JL unknowns (the total number of scalar unknowns is J^2L). Thus, Equation (2-68) is an over-determined system if the rank of the $J^2S \times JL$ matrix $\mathbf{C}_{x:S,L}$ is equal to JL . Matrix $\mathbf{C}_{x:S,L}$ has full rank in most cases if $S \geq L+1$ (see Mendel [1991] and the references therein), as selected herein. The linear system of Equations (2-68) is solved via the pseudoinverse operator to result in

$$(4-18) \quad \mathbf{A} = -\mathbf{C}_{x:S,L}^{\dagger} \mathbf{C}_{x:S,1}$$

Using the matrix parameters obtained via Equation (4-18), the input noise third-order cumulants are estimated using Equation (2-69) directly, repeated here as

$$(4-19) \quad C_u(0,0) = C_x(0,0) + \mathbf{C}_{x:1,L} \mathbf{A}$$

(recall that $C_u(0,0)$ is a block column matrix with Γ_j as the j th block element). The pseudoinverse in Equation (4-18) can be implemented using the SVD or another robust technique.

The SVD can be used also to determine model order. As in the case of the MA system, assume that an upper bound for the true model order is known, and denote this upper bound as L_T . Let $\{s_i | i = 1, 2, \dots, L_T\}$ denote the singular values of matrix $C_{x,s,L}$, arranged in decreasing order of magnitude (as usual). In ideal circumstances, only the first JL singular values are non-zero, but in practical cases all singular values are likely to be non-zero. Given good estimates of the cumulants, a significant discontinuity in the magnitude of the singular values can be expected after s_L . Thus, the SVD-based model order estimate is the number of significant non-zero singular values.

Equations (2-74) and (2-75) can be used instead to obtain the AR model matrix parameters and to determine the model order following the same approach outlined above. However, the normal matrix in Equation (2-74) is block Toeplitz, and a wider set of alternative algorithms can be used to solve for the matrix parameters (Marple, 1987). These two alternative systems of equations (Equations (2-68) and (2-69) vs. Equations (2-74) and (2-75)) can provide distinct results from numerical and algebraic viewpoints. This issue should be evaluated during Phase II.

AR Model Identification Using the Raghuveer Cumulant Formulation.
Consider now Equation (2-84), Raghuveer's linear system of equations for the AR(L) model parameters $\{A_k\}$. As in the preceding case, Equation (2-84) can be viewed as a collection of J linear systems of equations (corresponding to the J columns of \mathbf{A}). In this case, however, each system consists of $JL \times JL$ equations in JL

unknowns, and the $JL \times JL$ matrix $C_{x:L,L}$ has full rank and block Toeplitz structure. The linear system of Equations (2-84) can be solved using any applicable Toeplitz equation solver algorithm (for example, Michels [1991]; Marple [1987]). Alternatively, Equation (2-84) can be solved via the pseudoinverse operator implemented using the SVD. The SVD approach is preferred in cases where model order is unknown because the model order determination procedure outlined for the AR Standard Cumulant Formulation (which is based on the SVD) can be applied in this case also.

4.4 ARMA Parameter Identification

One approach to multichannel ARMA parameter estimation is the residual time series method. In this approximate method the AR model order and matrix parameters are identified first, and the whitening filter corresponding to the AR model is applied to the multichannel baseband sequence. In theory, the whitening filter output (or residual) is an MA sequence. The residual sequence is processed further to estimate the MA model order and matrix parameters. And the whitening filter corresponding to the MA model is applied to the residual output of the first whitening filter. Also in theory, the residual of the second whitening filter is a white sequence. AR model order and matrix parameter estimation is accomplished as described in Section 4.3, except that Equations (2-89) and (2-95) are used instead of Equations (2-68) and (2-84), respectively. MA model order and matrix parameter estimation is accomplished as described in Section 4.2.

The residual time series method involves a simple concept. However, it requires significant computations since two distinct identification problems are solved in sequence. SSC has simulated the residual time series method, and has carried out various simulation-based analyses. In most cases this method does not

produce good results. Specifically, SSC has observed that the AR portion of the procedure generates good matrix parameter estimates, while the MA portion generates poor estimates (Section 5.0). This agrees with the observed performance of the one-slice MA algorithm applied to MA-generated sequences.

SSC has considered also the higher-order AR approximation method, which has been used most recently by Michels (1991) for complex-valued vector sequences. It consists of fitting a higher-order AR model to an ARMA sequence. Preliminary simulation results suggest that the higher-order AR approximation method generates better estimates than the residual time series method (see Section 5.1).

Swami, Giannakis, and Mendel (1989) have proposed the multichannel M-slice algorithm for ARMA matrix parameter identification. This algorithm generates an estimate of the matrix parameters using linear algebra, without generating a residual sequence. The algorithm generates a segment of the impulse response sequence as an intermediate result.

For an ARMA process as defined in Equation (2-25), the impulse response matrix sequence $\{G(n)\}$ is defined as

$$(4-20) \quad y(n) = \sum_{k=-\infty}^{\infty} G(n-k) u(k) = \sum_{k=-\infty}^{\infty} G(k) u(n-k)$$

These impulse response parameters are related to the MA matrix parameters according to

$$(4-21) \quad B_k^H = \sum_{s=0}^k A_s^H G(k-s) \quad k = 1, 2, \dots, M$$

where $B_0 = I_J$ and $A_0 = I_J$ (recall that $L \geq M$, and that B_0 has full rank). It follows that $G(0) = I_J$.

The multichannel M -slice algorithm proceeds in two steps. First the $AR(L)$ matrix parameters, $\{A_k\}$, and the first $M+1$ impulse response matrices, $\{G(n) | n = 0, 1, \dots, M\}$, are estimated using a generalized form of Equation (2-89). In this first step M 1-D slices of the output cumulants are used, thus giving rise to the algorithm's name. Next the MA matrix parameters are obtained using Equation (4-21). This algorithm will be evaluated in Phase II.

5.0 SIMULATION-BASED ANALYSES

In Phase I SSC generated software routines to carry out selected analyses and validate important aspects of the HOS-based multichannel detection methodology formulated in the program. The software was programmed in an Apple II MacIntosh processor using FORTRAN 77. Several routines, including SVD and other matrix operations for complex-valued matrices, were adapted from the LINPACK software package (Dongarra et al., 1979). The software was generated to carry out the analyses listed next.

- (A) Non-Gaussian sequence generation
- (B) Identification algorithm analyses
 - 1. One-slice MA identification algorithm
 - 2. Raghuveer AR identification algorithm
 - 3. Residual time series ARMA identification method
- (C) Pseudo-innovations sequence analyses

Results and conclusions derived from the analyses are summarized herein.

5.1 Non-Gaussian Sequence Generation

Two methods were considered for generating colored (spatial and temporal) non-Gaussian vector sequences. The first method is referred to herein as the nonlinear-linear method. In this method a Gaussian white noise (GWN) vector sequence (zero spatial and temporal correlation) is generated and then a zero-memory nonlinearity is applied to each element of the GWN vector sequence to obtain a non-Gaussian white noise (NGWN) vector sequence. Then the NGWN vector sequence is colored, in space and time, by filtering with a time series model. The result is a non-Gaussian colored process (NGCP). This method produces a time series with known true correlation (spectrum) and true third-order cumulants, but the true PDF of the sequence is unknown. The linear filtering

process correlates the sequence and alters the PDF in a manner such that the univariate PDF of each element of the NGCP is more symmetric, in general, than the univariate PDF of the NGWN. Furthermore, the univariate PDF of each element of the NGCP tends to become Gaussian as the filter order increases. This method is useful for identification algorithm evaluation when used with low-order shaping filters. As the filter order increases, longer-duration sequences are required in order to have reliable estimates of the third-order cumulants to use as inputs to the parameter identification algorithms. This is due to the fact that third-order cumulants of approximately symmetric (or approximately Gaussian) PDFs have small magnitudes.

The second method is referred to as the linear-nonlinear method. In this method a GWN vector sequence is generated and then colored, in space and time, by filtering with a time series model to obtain a Gaussian colored process (GCP). Then a zero-memory nonlinearity is applied to each element of the GCP vector to obtain a NGCP. This method produces a time series with a known true univariate PDF, but the true correlation (spectrum) and the true third-order cumulants of the sequence are unknown. The zero-memory nonlinearity distorts the spatial and temporal statistics (of all orders) of the sequence. As a result, the "true" linear model that represents the signal is unknown. This method is useful for evaluation of cumulant estimation techniques. The method is useful also for whitening filter performance evaluation, specially for short-duration sequences because the sequence can be generated to have large third-order moments that are estimated more accurately. Also, some zero-memory nonlinear transformations induce tolerable distortion in the univariate second-order statistics (correlation sequence) of the vector process. This is important for detection-related analyses because the detection rule used in this program is based on second-order statistics.

The logarithm is a zero-memory nonlinear transformation with the feature mentioned above. Figure 5-1 presents the power spectrum of a scalar sequence generated by filtering a GWN sequence with an AR(2). The skewness coefficient for the GCP at the filter output is 0.015, indicating a Gaussian process. Figure 5-2 presents the power spectrum of the sequence after application of the logarithm operator. A comparison of the two spectra indicates that the power distribution varies little over the frequency range (these figures represent single-realization spectra); also, Figure 5-2 shows that the log operator did not introduce high-frequency components. The skewness coefficient of the NGCP with spectrum as shown in Figure 5-2 is -1.039, indicating its non-Gaussian character.

Other results obtained by SSC support the utility of the log transformation in the context of HOS. In a relevant set of analyses, a NGWN sequence was used to drive a two-channel ARMA(3,2) model, and GWN was added to the ARMA system output (after decay of initial transients). Raghuveer's AR algorithm was used to identify the matrix parameters of AR(8), AR(10), . . . , and AR(18) models. An associated inverse filter was defined for each of the identified AR models, and the data was processed with each inverse filter. None of the inverse filters generated a white sequence. This is due to symmetry in the PDF of the ARMA(3,2) output induced by the ARMA transformation itself. As a separate procedure, the log transformation described in Section 3.3 was applied to the noisy ARMA(3,2) sequence, and Raghuveer's AR algorithm was applied to the transformed sequence to identify the parameters of an AR(6) model. The inverse filter associated with the AR(6) model was used to process the transformed data, and generated a white residual sequence. Further details on the analyses and representative results are presented next.

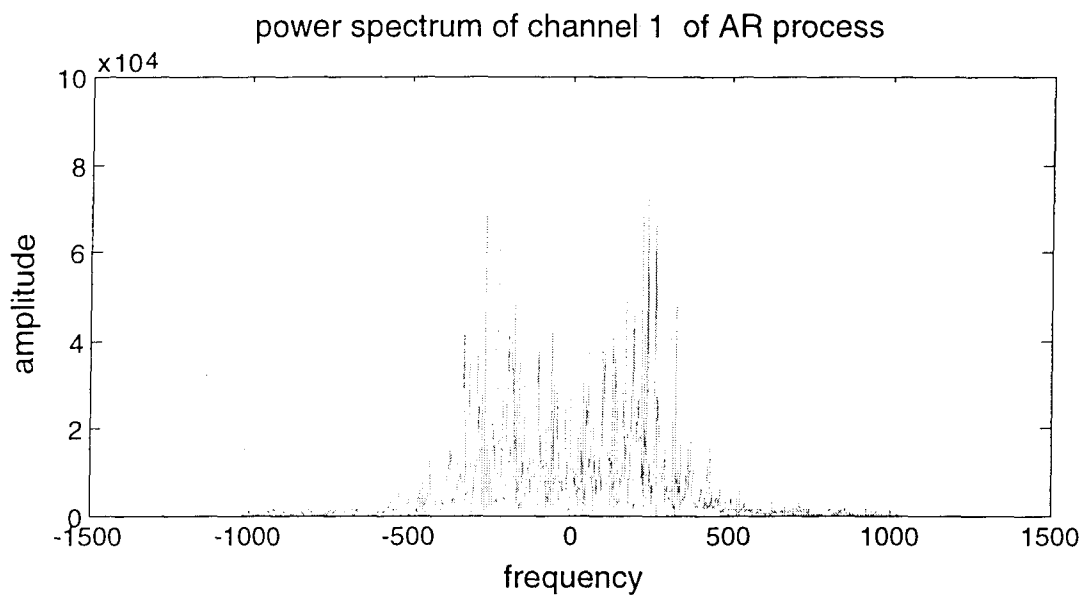


Figure 5-1. Power spectrum of Gaussian AR(2) process.

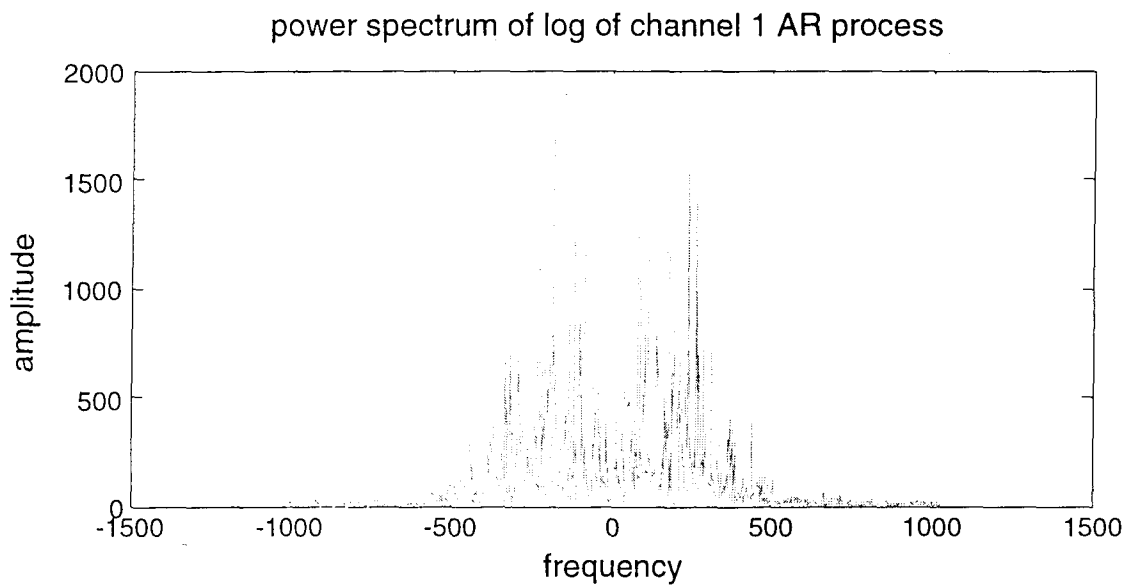


Figure 5-2. Power spectrum of log of Gaussian AR(2) process.

Figure 5-3 presents the procedure followed in the logarithm pre-processing option simulation-based analyses. The NGWN process used as input to the Data Generation step is a zero-mean vector (two-channel) sequence of independent variables sampled from a one-degree-of-freedom chi-squared distribution (the sample mean is estimated and removed from the chi-squared sequence). This sequence has a theoretical skewness coefficient of $2^{1.5} \approx 2.83$. The sample skewness coefficient values for the realization selected for presentation herein are 2.75 and 3.01 for channels 1 and 2, respectively. A 2,048-point segment is selected from the steady-state output $\{y(n)\}$ of the ARMA(3,2) system (the true system parameters are defined below). Analysis runs were made also with 1,024 data points, and the results are similar to those presented herein. The sample skewness coefficient values for the $\{y(n)\}$ realization selected for presentation herein are -0.024 and 0.03 for channels 1 and 2, respectively. These values indicate the loss of asymmetry induced by the linear system. A 2,048-point zero-mean GWN vector sequence is added to the steady-state ARMA(3,2) output. The noise variance in each channel is selected to result in 0 dB SNR.

Model Identification is carried out via the higher-order AR approximation method using Raghuveer's AR algorithm. Furthermore, this step is carried out with and without the logarithm pre-processing option, as indicated in Figure 5-3. The results presented herein correspond to the case where a two-channel AR(18) model is selected for the case where pre-processing is not used. In general, an AR(18) model is more than sufficient to represent adequately an ARMA(3,2) system. The logarithm function modifies the distribution that describes the transformed data. The sample skewness coefficient values for the transformed data segment for the realization selected for presentation herein are -2.05 and -1.86 for channels 1 and 2, respectively. These values are close

to the values that describe the input data. A two-channel AR(6) model is selected for the case with logarithm pre-processing.

Residual Generation is accomplished in both cases using the corresponding inverse filter. Both inverse filters are two-channel MA systems (see Section 3.5.2).

The true ARMA(3,2) parameters are (with $A_0 = I_2$ and $B_0 = I_2$):

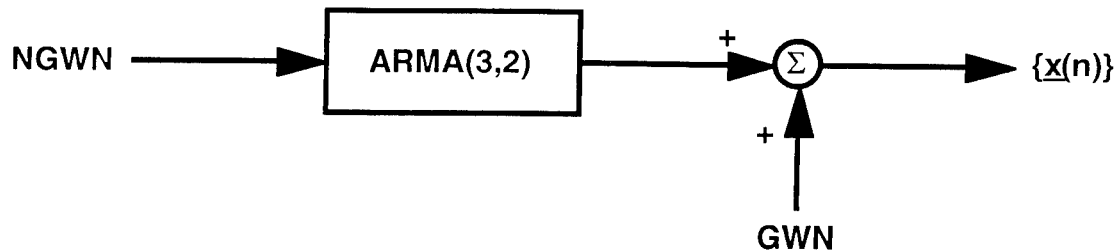
$$A_1^H = \begin{bmatrix} 0.410 & -0.200 \\ 0.120 & 0.405 \end{bmatrix} \quad A_2^H = \begin{bmatrix} 0.22 & 0.24 \\ -0.65 & 0.34 \end{bmatrix} \quad A_3^H = \begin{bmatrix} 0.15 & 0.10 \\ 0.10 & -0.20 \end{bmatrix}$$

$$B_1^H = \begin{bmatrix} -1.40 & 0 \\ 0 & -1.40 \end{bmatrix} \quad B_2^H = \begin{bmatrix} 0.49 & 0 \\ 0 & 0.49 \end{bmatrix}$$

This system has six poles (number of poles = number of channels x AR order) and six finite multivariable system zeros (Rosenbrock, 1970). The system poles are located at: $\{0.289, -0.436, -0.552 \pm j0.778, 0.218 \pm j0.549\}$, and the system zeros are located at: $\{0.7, 0.7, 0.7, 0.7, 0.0, 0.0\}$. This system is minimum phase since all the poles and zeros are inside the unit circle. Thus, the true inverse system (whitening filter) is stable also.

Residual auto-correlation sequences for a single realization of the channel 1 output for each of the two cases are presented in Figures 5-4 and 5-5. Channel 2 residual auto-correlations are similar. In each figure the complete 4,096-point auto-correlation sequence is shown. The central segment of the auto-correlation is shown also in order to highlight the correlation detail. Notice that the residual is colored for the case without pre-processing (Figure 5-4), and white for the case with logarithm pre-processing (Figure 5-5). These figures are representative of all the realizations generated in the analysis.

DATA GENERATION

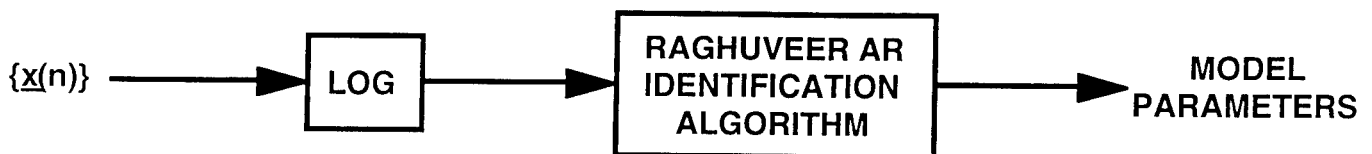


MODEL IDENTIFICATION

NO PRE-PROCESSING:



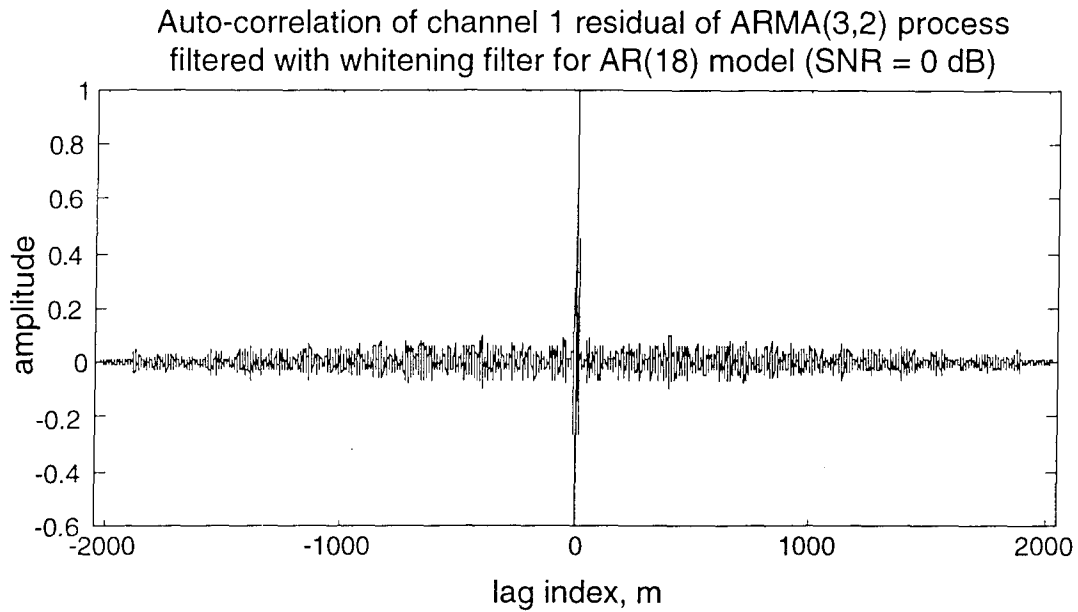
LOGARITHM PRE-PROCESSING:



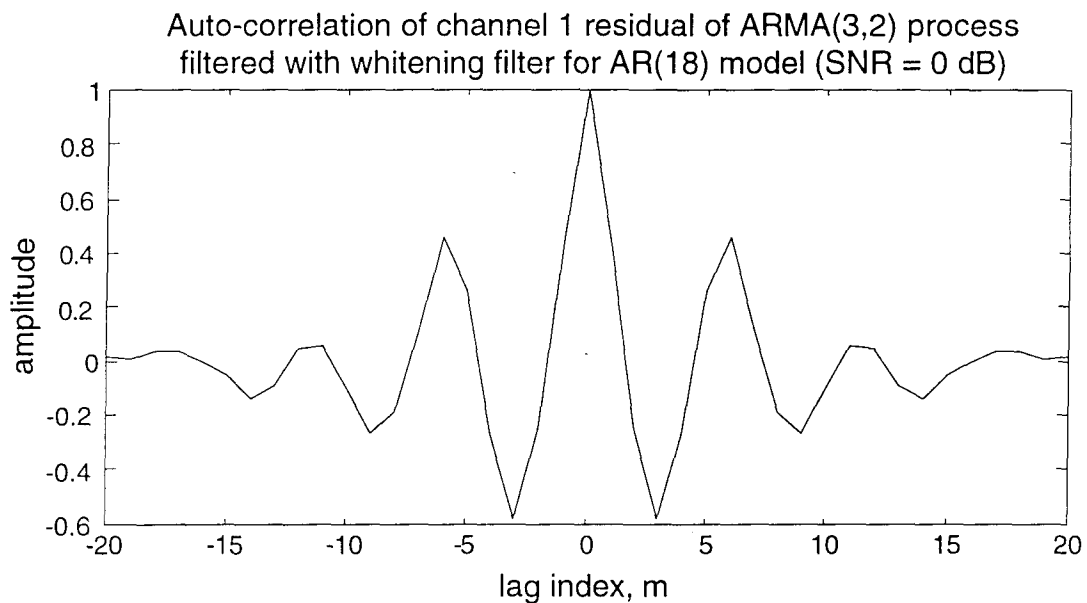
RESIDUAL GENERATION (BOTH CASES)



Figure 5-3. Set-up for logarithmic pre-processing option simulation-based analyses.

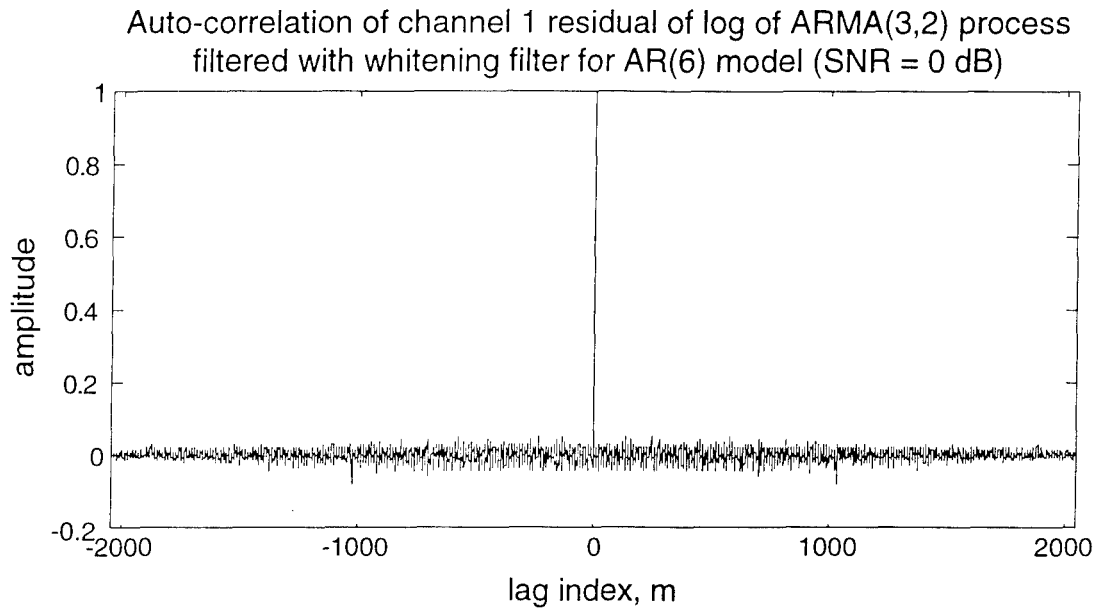


(a) Complete auto-correlation sequence for Channel 1 residual.

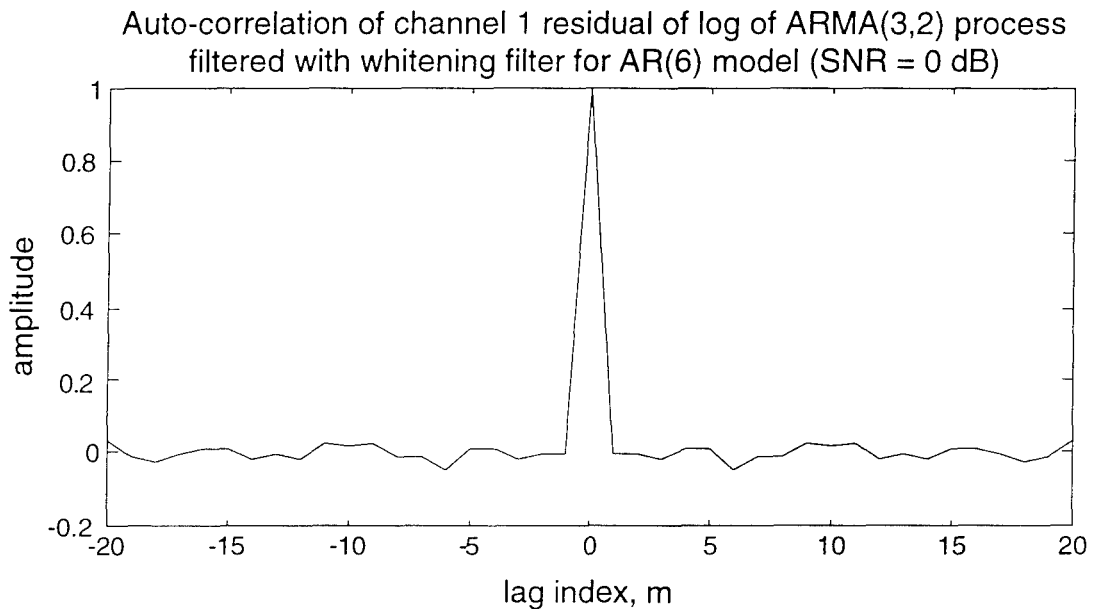


(b) Central segment of auto-correlation sequence for channel 1 residual.

Figure 5-4. Auto-correlation of residual for AR(18) model
(without pre-processing) of ARMA(3,2) plus GWN data.



(a) Complete auto-correlation sequence for Channel 1 residual.



(b) Central segment of auto-correlation sequence for channel 1 residual.

Figure 5-5. Auto-correlation of residual for AR(6) model (with log pre-processing) of ARMA(3,2) plus GWN data.

5.2 Identification Algorithms Analyses

Software-based analyses were carried out to validate analytical derivations and to determine algorithm performance. The results presented herein are representative of all the results obtained in Phase I. The additive noise, $\{\underline{w}(n)\}$, is zero for Examples 5-1 through 5-5.

5.2.1 One-Slice MA Identification Algorithm

In most of the test cases considered the MA algorithm performed poorly in an absolute sense, as well as in comparison with the AR algorithm. The MA algorithm generates non-minimum-phase zeros more often than the AR algorithm, even when the true zeros are minimum-phase. This performance is evidenced in the examples presented next for a MA(2) model (the results can be compared directly with the results from the AR examples presented in Section 5.2.2).

Two different methods are used to obtain the matrix parameter estimates in the examples. In the first method (Method I), the MA parameter estimates are obtained using a single realization of 10^4 time samples. In the second method (Method II), ten realizations of 10^3 time samples each are processed to obtain ten sets of estimated MA parameters; the average of the ten sets of parameters is calculated and presented herein. Notice that the total number of samples used is the same in both methods.

With respect to whitening filter performance, the locations of the zeros of the transfer function of the identified MA model determine the system dynamics. In these examples, the values listed as "zeros" are the roots of the polynomial $\beta(z)$, as defined

in Equation (2-41). Also, the normalized error in the estimate of the i th zero, denoted as δz_i , is defined as

$$(5-1) \quad \delta z_i = \frac{|z_i - \hat{z}_i|}{|z_i|}$$

where z_i denotes the true i th zero and \hat{z}_i denotes its estimate. This error is converted to a percent error by multiplication by 100%.

Example 5-1. The true MA(2) parameters are (with $B_0 = I_2$):

$$B_1^H = \begin{bmatrix} -1.0 & 0 \\ 0 & -1.0 \end{bmatrix} \quad \text{zeros: } \{0.5, 0.5, 0.5, 0.5\}$$

$$B_2^H = \begin{bmatrix} 0.25 & 0 \\ 0 & 0.25 \end{bmatrix}$$

Method I Estimates (single realization):

$$B_1^H = \begin{bmatrix} -0.9991 & 0.0078 \\ 0.0073 & -1.0383 \end{bmatrix} \quad \text{zeros: } \{0.388, 0.435, 0.577, 0.637\}$$

$$B_2^H = \begin{bmatrix} 0.2425 & -0.0071 \\ -0.0080 & 0.2561 \end{bmatrix}$$

The errors in the location of the four real-valued zeros in the order listed above are: 22.4%, 13.0%, 15.4%, and 27.4%.

Method II Estimates (average of ten realizations):

$$B_1^H = \begin{bmatrix} -0.9968 & 0.0111 \\ -0.0007 & -0.8993 \end{bmatrix} \quad \text{zeros: } \{0.445 \pm j 0.154, 0.503 \pm j 0.232\}$$

$$B_2^H = \begin{bmatrix} 0.3036 & 0.0094 \\ -0.0062 & 0.2239 \end{bmatrix}$$

The error in the location of the zeros is 32.7% for the first complex conjugate pair, and 46.4% for the second complex conjugate pair. Some of the zeros of the matrix parameters estimated for the individual realizations have a larger error; the maximum error is 91.8% for the complex conjugate pair estimated at $0.48 \pm j 0.46$. These large errors are evident in Figure 5-6, a scatter plot of the forty zeros estimated in the ten realizations. All estimated sets of zeros are plotted in a single set of axes since all the true zeros are at the same location, $z = 0.5$. Error statistics for the estimated zeros are presented in Tables 5-1 and 5-2. All estimated zeros are inside the unit circle, as evidenced in Figure 5-6.

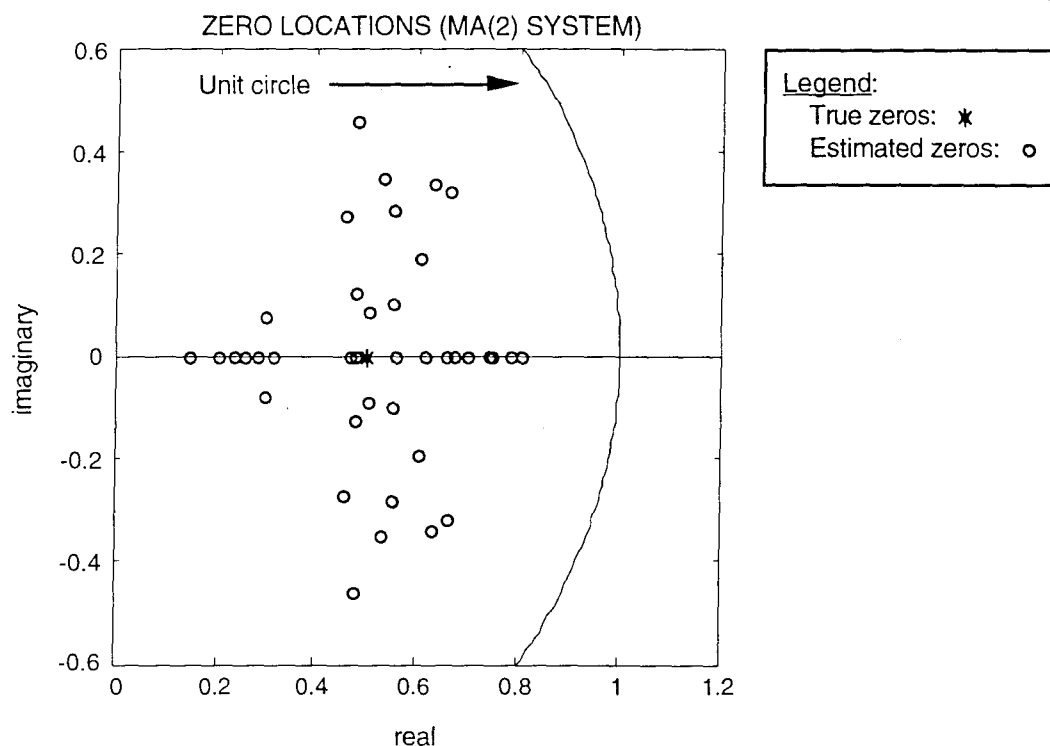


Figure 5-6. Scatter plot for the zeros of all ten realizations in Example 5-1 (Method II).

Example 5-2. The true MA(2) parameters are (with $B_0 = I_2$):

$$B_1^H = \begin{bmatrix} -1.8 & 0 \\ 0 & -1.8 \end{bmatrix} \quad \text{zeros: } \{0.9, 0.9, 0.9, 0.9\}$$

$$B_2^H = \begin{bmatrix} 0.81 & 0 \\ 0 & 0.81 \end{bmatrix}$$

Method I Estimates (single realization):

$$B_1^H = \begin{bmatrix} -1.8100 & 0.0222 \\ -0.0035 & -1.8237 \end{bmatrix} \quad \text{zeros: } \{0.856, 0.909 \pm j 0.145, 0.969\}$$

$$B_2^H = \begin{bmatrix} 0.8313 & -0.0052 \\ -0.0108 & 0.8457 \end{bmatrix}$$

The error in the locations of the zeros is 4.9% for the first real-valued zero, 16.1% for the complex conjugate pair, and 7.7% for the second real-valued zero.

Method II Estimates (average of ten realizations):

$$B_1^H = \begin{bmatrix} -1.7070 & -0.0047 \\ 0.0243 & -1.6572 \end{bmatrix} \quad \text{zeros: } \{0.826 \pm j 0.260, 0.856 \pm j 0.304\}$$

$$B_2^H = \begin{bmatrix} 0.8209 & -0.0003 \\ -0.0148 & 0.7542 \end{bmatrix}$$

The error in the locations of the zeros is 30.0% for the first complex conjugate pair, and 34.1% for the second complex conjugate pair. The zeros of several of the matrix parameters estimated for the individual realizations have a larger error, and eleven (out of forty) zeros are non-minimum-phase. This is evidenced in Figure 5-7, which is a scatter plot of the forty zeros estimated in the ten realizations. The largest error is 56.7%, and corresponds to a non-minimum-phase zero at 1.41. Figure 5-7 is in

the same scale as Figure 5-6. Notice that the dispersion of zeros is about the same in both figures.

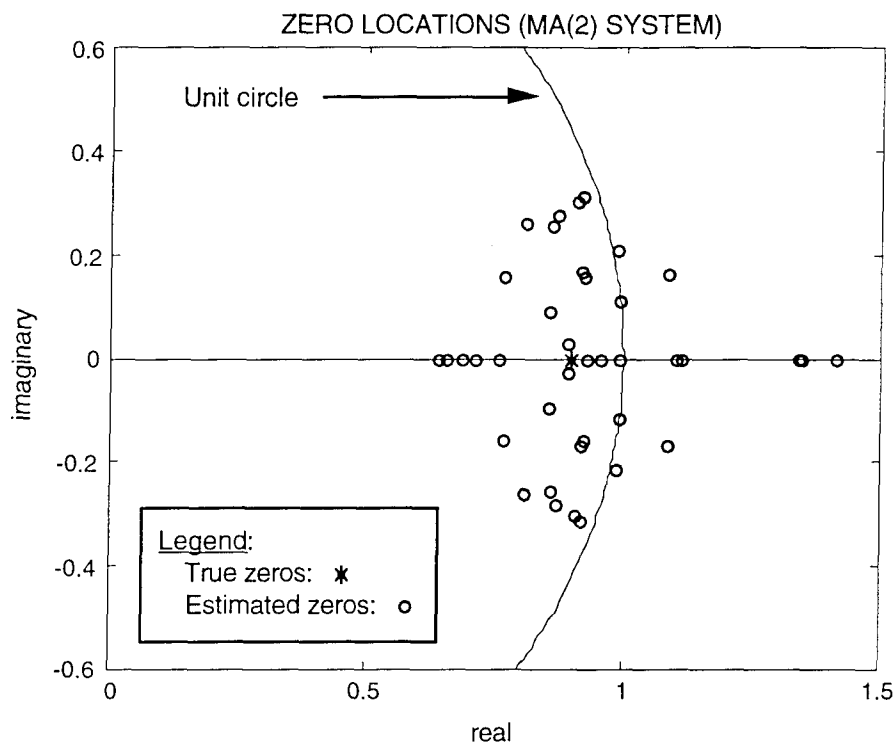


Figure 5-7. Scatter plot for the zeros of all ten realizations in Example 5-2 (Method II).

Example 5-3. The true MA(2) parameters are (with $B_0 = I_2$):

$$B_1^H = \begin{bmatrix} -2.2 & 0 \\ 0 & -2.2 \end{bmatrix}$$

zeros: {1.1, 1.1, 1.1, 1.1}

$$B_2^H = \begin{bmatrix} 1.21 & 0 \\ 0 & 1.21 \end{bmatrix}$$

Notice that this MA system is non-minimum phase (HOS-based methods can identify non-minimum phase systems, whereas covariance-based methods cannot). As mentioned earlier, non-minimum phase systems

result in unstable innovations filters. This example is presented to demonstrate the identification capabilities of HOS-based methods in a more general context.

Method I Estimates (single realization):

$$B_1^H = \begin{bmatrix} -2.2411 & 0.0297 \\ -0.0119 & -2.2144 \end{bmatrix} \quad \text{zeros: } \{1.027, 1.110 \pm j 0.173, 1.21\}$$

$$B_2^H = \begin{bmatrix} 1.2535 & -0.0089 \\ 0.0215 & 1.2493 \end{bmatrix}$$

The error in the locations of the zeros is 6.6% for the first real-valued zero, 15.8% for the complex conjugate pair, and 10.0% for the second real-valued zero. All estimated zeros are non-minimum phase.

Method II Estimates (average of ten realizations):

$$B_1^H = \begin{bmatrix} -2.0595 & -0.0213 \\ 0.0409 & -2.0469 \end{bmatrix} \quad \text{zeros: } \{1.006 \pm j 0.316, 1.047 \pm j 0.356\}$$

$$B_2^H = \begin{bmatrix} 1.1852 & 0.0079 \\ -0.0244 & 1.1480 \end{bmatrix}$$

The error in the location of the zeros is 30.0% for the first complex conjugate pair, and 32.7% for the second complex conjugate pair. The zeros of various parameter estimates for the individual realizations have a larger error; the largest error is 67.1%, and corresponds to a real-valued zero at 1.84. This is evidenced in Figure 5-8, which is a scatter plot of the forty zeros estimated in the ten realizations. Note that out of the forty estimated zeros, eleven are estimated incorrectly to be inside the unit circle.

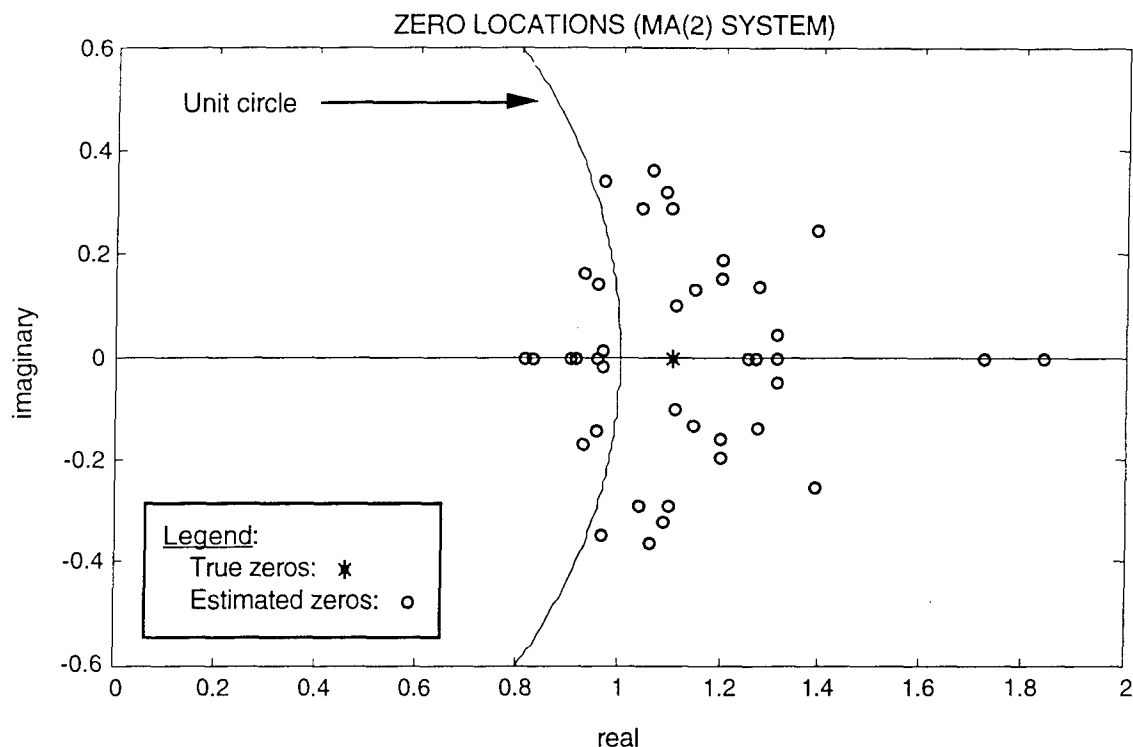


Figure 5-8. Scatter plot for the zeros of all ten realizations in Example 5-3 (Method II).

Comments. The statistics for the zeros of the parameter estimates of the ten realizations in Method II for the three examples are listed in Table 5-1. These results indicate that "slow" zeros (close to the unit circle) are estimated more accurately than "fast" zeros. This feature is common to all identification algorithms (Román and Davis, 1993). Figures 5-6 through 5-8 suggest that the magnitude of the estimated zeros is biased towards a magnification error.

Table 5-2 lists the errors in the zeros of the parameters estimated via Methods I and II for the three MA(2) examples. In all three examples the single realization method generated better zero estimates than the averaging method. This observation admits the following explanation. In the single realization method all

the averaging takes place in the estimation of the cumulants, prior to processing with the parameter identification algorithm. In the averaging method part of the averaging takes place after processing with the parameter identification algorithm. The identification algorithm propagates the input errors, and the post-processing averaging is less effective. Thus, for the MA algorithm, it is preferable to use more accurate cumulant estimates than to use post-algorithm averaging.

	TRUE ZERO (REPEATED)	MINIMUM ERROR (%)	MAXIMUM ERROR (%)	ERROR MEAN (%)	ERROR STD. DEV. (%)	ERROR MEDIAN (%)
EX. 5-1	0.5	4.7	91.8	46.9	21.9	48.3
EX. 5-2	0.9	3.4	56.7	24.0	11.9	23.5
EX. 5-3	1.1	9.3	67.1	23.5	11.6	19.7

Table 5-1. Error statistics for the zeros of all ten realizations in the three MA examples (Method II).

	ERRORS USING METHOD I (%)	ERRORS USING METHOD II (%)
EXAMPLE 5-1	22.4, 13.0, 15.4, 27.4	32.7, 32.7, 46.4, 46.4
EXAMPLE 5-2	4.9, 16.1, 16.1, 7.7	30.0, 30.0, 34.1, 34.1
EXAMPLE 5-3	6.6, 15.8, 15.8, 10.0	30.0, 30.0, 32.7, 32.7

Table 5-2. Zero estimate errors for the three MA(2) examples using both methods.

5.2.2 Raghuveer AR Identification Algorithm

The AR algorithm generates non-minimum-phase poles less often than the MA algorithm (the values referred to as "poles" are the roots of the polynomial $\alpha(z)$, as defined in Equation (2-40)). This is evidenced in Examples 5-4 and 5-5 for an AR(2) model with true poles located at the same values as the zeros in Examples 5-1 and 5-2, respectively. In order to allow direct comparisons, the true AR(2) parameters are selected equal to the true MA(2) parameters in the respective examples. Also, the normalized error in the estimate of the i th pole, denoted as δp_i , is defined analogous to δz_i in Equation (5-1).

Example 5-4. The true AR(2) parameters are the same as the true MA(2) parameters of Example 5-1; that is, $A_2 = B_2$, $A_1 = B_1$, and $A_0 = 1_2$. Also, the true poles are located at $\{0.5, 0.5, 0.5, 0.5\}$.

Method I Estimates (single realization):

$$A_1^H = \begin{bmatrix} -1.0065 & 0.0060 \\ 0.0026 & -1.0029 \end{bmatrix} \quad \text{poles: } \{0.501 \pm j 0.048, 0.504 \pm j 0.066\}$$

$$A_2^H = \begin{bmatrix} 0.2586 & -0.0001 \\ -0.0023 & 0.2528 \end{bmatrix}$$

The error in the first complex conjugate pole pair is 9.6%, and the error in the second complex conjugate pole pair is 13.1%.

Method II Estimates (average of ten realizations):

$$A_1^H = \begin{bmatrix} -0.9108 & -0.0048 \\ -0.0051 & -0.9147 \end{bmatrix} \quad \text{poles: } \{0.454 \pm j 0.164, 0.459 \pm j 0.145\}$$

$$A_2^H = \begin{bmatrix} 0.2313 & -0.0023 \\ 0.0005 & 0.2332 \end{bmatrix}$$

The error in the first complex conjugate pole pair is 34.1%, and the error in the second complex conjugate pole pair is 30.1%. These errors are slightly larger than the mean error for all forty matrix parameters estimated for the individual realizations, which is 21.7% for the complex conjugate pole pair estimated at $0.49 \pm j 0.53$ (see Table 5-3). From Table 5-3, the maximum error is 44.8%, and corresponds to the pole estimated at 0.28. A scatter plot of the forty poles estimated for the ten realizations is presented in Figure 5-9. Notice that the dispersion in Figure 5-9 is significantly less than the dispersion in Figure 5-6. Notice also that the complex-valued pole estimates appear along a circle of magnitude 0.5.

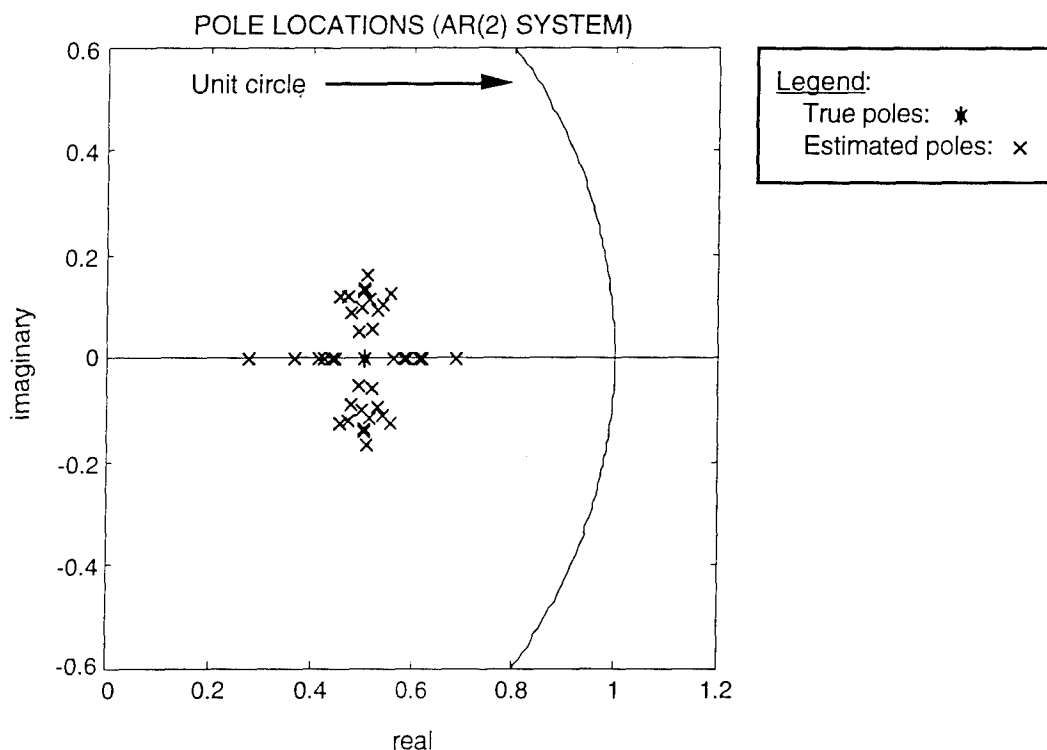


Figure 5-9. Scatter plot for the poles of all ten realizations in Example 5-4 (Method II).

Example 5-5. The true AR(2) parameters are the same as the true MA(2) parameters of Example 5-2; that is, $A_2 = B_2$, $A_1 = B_1$, and $A_0 = I_2$. Also, the true poles are located at $\{0.9, 0.9, 0.9, 0.9\}$.

Method I Estimates (single realization):

$$A_1^H = \begin{bmatrix} -1.7975 & 0.0070 \\ 0.0121 & -1.8044 \end{bmatrix} \quad \text{poles: } \{0.870, 0.921, 0.906 \pm j 0.038\}$$

$$A_2^H = \begin{bmatrix} 0.8075 & -0.0071 \\ -0.0119 & 0.8151 \end{bmatrix}$$

The two real-valued poles have an error of 3.3% and 2.3%, respectively, and the error in the complex conjugate pole pair is 4.3%.

Method II Estimates (average of ten realizations):

$$A_1^H = \begin{bmatrix} -1.6350 & -0.0248 \\ 0.0099 & -1.6432 \end{bmatrix} \quad \text{poles: } \{0.813 \pm j 0.269, 0.826 \pm j 0.253\}$$

$$A_2^H = \begin{bmatrix} 0.7355 & 0.0242 \\ -0.0108 & 0.7439 \end{bmatrix}$$

The error in the first complex conjugate pole pair is 31.4%, and the error in the second complex conjugate pole pair is 29.3%. Figure 5-10 is a scatter plot of the forty poles estimated for the ten realizations. The poles of the estimated individual matrix parameters have smaller error than the poles of the averaged matrix parameters given above. In fact, the maximum error is 13.5% for the pole estimated at 0.78 (see Table 5-3). This is possibly due to the fact that the poles are a nonlinear function of the averaged matrix parameters. From Figure 5-10, the poles of all ten sets of estimated matrix parameters are minimum-phase.

And the dispersion in Figure 5-10 is much less than in Figures 5-7 (MA case) and 5-9. Additionally, in this example the dispersion does not exhibit a pattern.

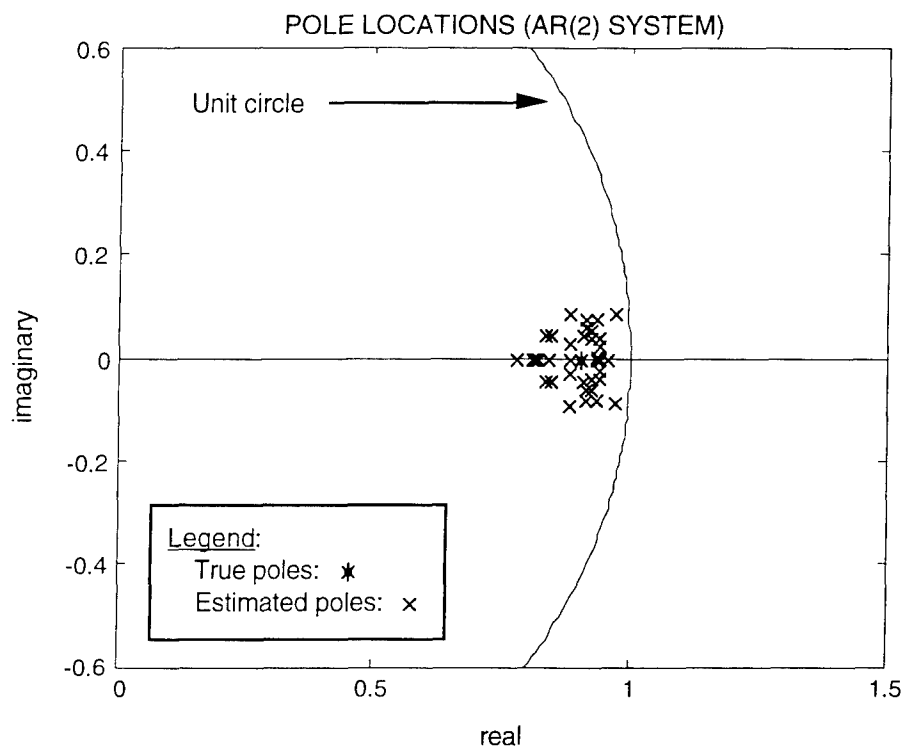


Figure 5-10. Scatter plot for the poles of all ten realizations in Example 5-5 (Method II).

Comments. The statistics for the poles of the parameter estimates of the ten realizations in Method II for Examples 5-4 and 5-5 are listed in Table 5-3. These results also indicate that "slow" poles (close to the unit circle) are estimated more accurately than "fast" poles, as is the case for the zeros. The magnitude error bias observed in the MA cases is present also in these AR cases using Raghuveer's algorithm, but to a significantly lesser degree.

Table 5-4 lists the errors in the poles of the parameters estimated via Methods I and II for the two AR(2) examples. In both examples the single realization method generated better pole estimates than the averaging method, which admits the same explanation as in the MA case. Thus, for the AR algorithm it is preferable also to use more accurate cumulant estimates than to use post-algorithm averaging.

	TRUE POLE (REPEATED)	MINIMUM ERROR (%)	MAXIMUM ERROR (%)	ERROR MEAN (%)	ERROR STD. DEV. (%)	ERROR MEDIAN (%)
EX. 5-4	0.5	10.8	44.8	21.7	7.7	22.5
EX. 5-5	0.9	2.2	13.5	7.1	2.6	6.7

Table 5-3. Error statistics for the poles of all ten realizations in the two AR examples (Method II).

	ERRORS USING METHOD I (%)	ERRORS USING METHOD II (%)
EXAMPLE 5-4	9.6, 9.6, 13.1, 13.1	34.1, 34.1, 30.1, 30.1
EXAMPLE 5-5	3.3, 2.3, 4.3, 4.3	31.4, 31.4, 29.3, 29.3

Table 5-4. Pole estimate errors for the two AR(2) examples using both methods.

Direct comparison of Figures 5-6 and 5-7 with Figures 5-9 and 5-10, and of Tables 5-1 and 5-2 with Tables 5-3 and 5-4 indicates that the AR algorithm generates much better estimates than the MA algorithm considering all relevant performance measures.

Effect of Additive Gaussian White Noise on AR Estimates. The effect of additive Gaussian noise is considered in Example 5-6. The example is for a specific set of conditions using Raghuveer's AR algorithm, but the results are representative of parameter identification performance in noise for AR and MA algorithms.

The normalized error defined via Equation (5-1) is useful in the determination of dynamic system response effects. An alternative error definition is required to assess parameter estimation performance. A useful error measure is defined as follows. Let $\underline{c}_{i;k}$ denote the i th column of \underline{A}_k^H , and let $\hat{\underline{c}}_{i;k}$ denote its estimate obtained using Raghuveer's AR algorithm. The normalized average column error, denoted as $\underline{\delta c}$, is defined as

$$(5-2) \quad \underline{\delta c} = \frac{1}{JL} \sum_{i=1}^J \sum_{k=1}^L \frac{|\underline{c}_{i;k} - \hat{\underline{c}}_{i;k}|}{|\underline{c}_{i;k}|}$$

This error is converted to a percent error by multiplication by 100%. In the example, $\underline{\delta c}$ is computed for each realization as a function of noise level.

Example 5-6. The signal is a two-channel AR(2) process with (four) repeated poles at 0.5 and zero coupling between channels, as in Example 5-4. Gaussian white noise is added to the AR(2) process. Sequence duration is 5×10^4 time samples for each realization. Raghuveer's AR parameter estimation algorithm is used to identify the AR matrix parameters. The normalized average column percent error is plotted in Figure 5-11. Notice that for $\text{SNR} > 7$ dB the identification error is close to its noise-free value (the error is less than 1% off the noise-free asymptote). This is a consequence of the insensitivity of third-order cumulants to additive Gaussian noise. The error increases dramatically for $\text{SNR} < 7$ dB. The SNR value at which the plot

starts to deviate from the noise-free asymptote is a function of sequence duration also.

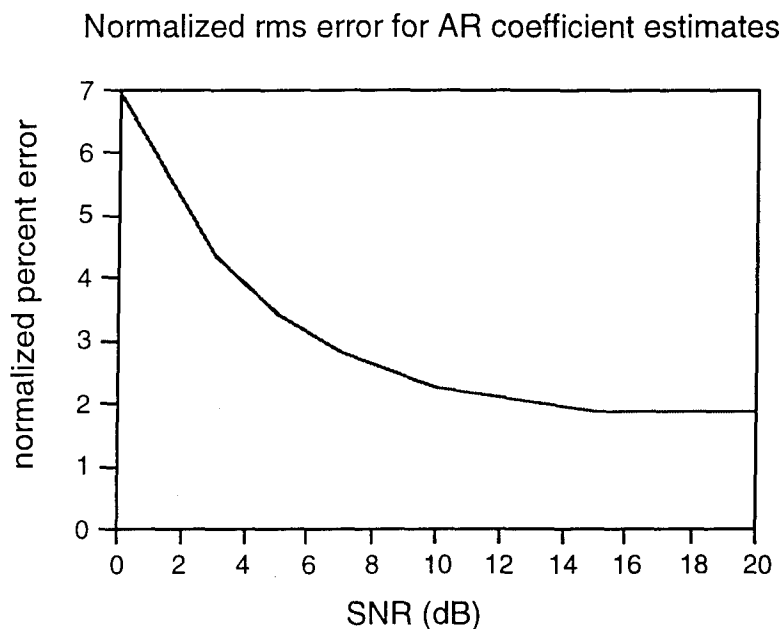


Figure 5-11. Normalized average column error for AR matrix parameters as a function of SNR (additive Gaussian noise).

5.2.3 Residual Time Series ARMA Identification Method

The residual time series ARMA identification method did not produce good results in most of the cases considered in Phase I. Simulation-based analyses indicate that the AR algorithm generates good matrix parameter estimates, while the MA algorithm generates poor estimates. As evidenced in Section 5.2.1, the MA algorithm generates non-minimum-phase estimates in many cases, even in the identification of the parameters of a true minimum-phase MA process. In the residual method the situation is complicated further by the fact that the MA algorithm has to deal with limited-duration residuals (from the AR inverse filter) that are not a true MA process (unless the identified AR parameters are the true parameters).

An alternative approach is to fit a higher-order AR model to the ARMA sequence. This approach has been considered by Michels (1991) for Case (2-20d), the multichannel Gaussian case. Preliminary results obtained by SSC suggest that such an approach is preferable over the residual method in the non-Gaussian case (see, for example, the results in Section 5.1).

5.3 Pseudo-Innovations Sequence Analyses

The capability of the HOS-based detection methodology to discriminate between the two hypotheses was established in Phase I. Simulation analyses were carried out for non-Gaussian colored sequences in additive white noise generated using the linear-nonlinear method, with the log function as the zero-memory nonlinearity. GWN was added to the GCP prior to applying the log to the sequence. The results show that the output of the H_0 filter is white when the null hypothesis is true, $\{\underline{x}(n) = \underline{c}(n) + \underline{w}(n)\}$, and the output of the H_0 filter is colored when the alternative hypothesis is true, $\{\underline{x}(n) = \underline{s}(n) + \underline{c}(n) + \underline{w}(n)\}$. Similarly, the output of the H_1 filter is white when the alternative hypothesis is true, $\{\underline{x}(n) = \underline{s}(n) + \underline{c}(n) + \underline{w}(n)\}$, and the output of the H_1 filter is colored when the null hypothesis is true, $\{\underline{x}(n) = \underline{c}(n) + \underline{w}(n)\}$. Given these observations, an appropriate detection rule (such as the approximate rule considered in Section 3.4) can discriminate between the two hypotheses based on the differences in the auto-correlation of the pseudo-innovations. A representative sample of this type of result is provided in Example 5-7. Detailed analyses will be carried out in Phase II to quantify detection performance.

Example 5-7. Both clutter and signal were generated using the linear-nonlinear method. Specifically, the clutter is a two-channel AR(2) process driven by GWN, and the signal is also a two-

channel AR(2) process driven by GWN. The true AR(2) matrix parameters for clutter and signal are (these are the real part of the complex-valued model parameters in [Román and Davis, 1993]):

CLUTTER

$$A_1^H = \begin{bmatrix} -1.0430 & 0.0 \\ 0.0 & -1.0430 \end{bmatrix}$$

$$A_2^H = \begin{bmatrix} 0.4900 & 0.0 \\ 0.0 & 0.4900 \end{bmatrix}$$

SIGNAL

$$A_1^H = \begin{bmatrix} 1.6290 & 0.0 \\ 0.0 & 1.6290 \end{bmatrix}$$

$$A_2^H = \begin{bmatrix} 0.8099 & 0.0 \\ 0.0 & 0.8099 \end{bmatrix}$$

GWN was added to the AR sequences to generate null and alternative hypotheses data, as appropriate, at an SNR level of 0 dB. The addition of GWN converts the sequence into an ARMA sequence. A sequence duration of 1,024 time samples (after initial transients decay) was selected. The Gaussian-distributed data (including the additive noise) was transformed using the logarithm transformation as described in Section 3.3. This completes the data generation step according to the linear-nonlinear method (Section 5.1). An alternative procedure is to add the GWN after the log is applied to the AR data. This should result in better performance.

Raghuveer's AR identification algorithm was used to generate AR matrix parameter estimates for a sixth-order AR model for the null hypothesis case (clutter + noise). Figure 5-12 presents the auto-correlation function of the pseudo-innovations $\underline{\varepsilon}(n|H_0)$, the residual at the output of the sixth-order H_0 filter driven with H_0 data. The residual is uncorrelated, as expected. Figure 5-13 presents the auto-correlation function of the residual at the output of the sixth-order H_0 filter driven with H_1 data. As expected, the residual in Figure 5-13 is correlated over several lags. This difference is the mechanism by which discrimination between the two hypotheses takes place.

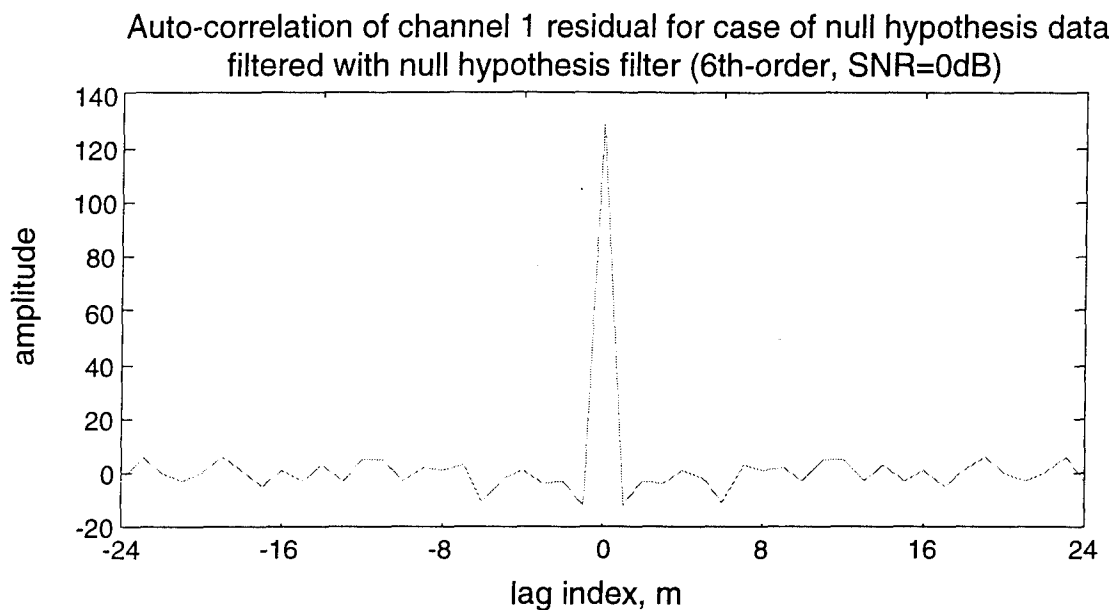


Figure 5-12. Central segment of pseudo-innovations auto-correlation (H_0 data filtered with H_0 filter) for Example 5-7.

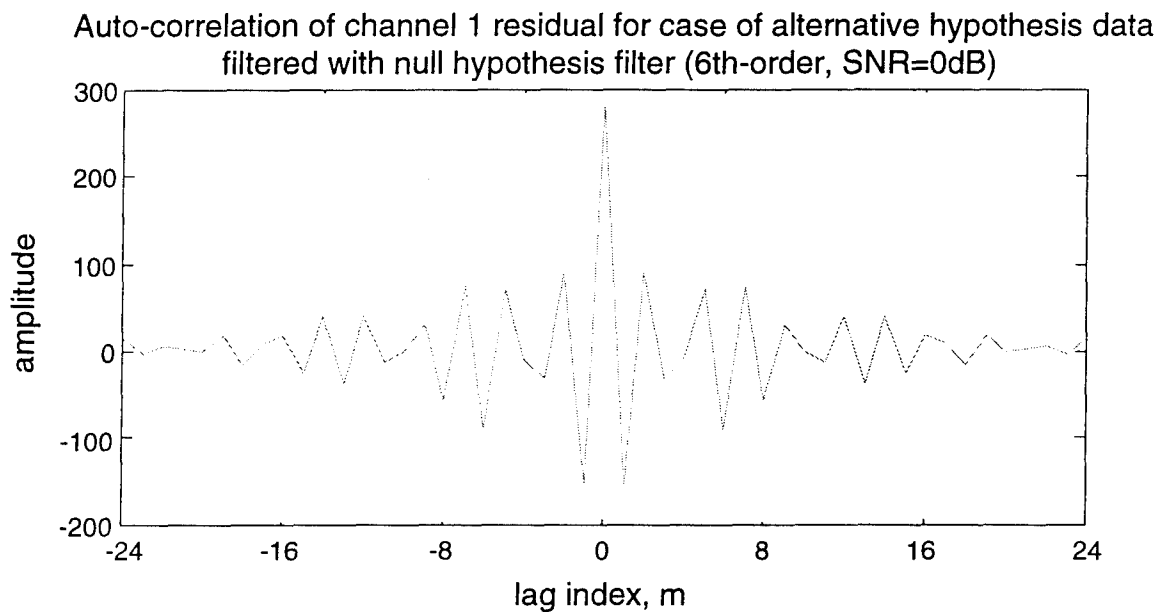


Figure 5-13. Central segment of pseudo-innovations auto-correlation (H_1 data filtered with H_0 filter) for Example 5-7.

6.0 CONCLUSIONS AND RECOMMENDATIONS

In this program the feasibility of using higher-order cumulants for radar target detection was established in a general context, as well as in the specific context of surveillance radar applications. With respect to surveillance radar, SSC identified several operational scenarios where non-Gaussian targets are present in a non-Gaussian clutter environment. Additionally, at least two different candidate problems of interest to RL were identified: radar arrays and pre-detection radar fusion. Emphasis was placed in surveillance radar arrays, which include the space/time processing application. In this context, a new methodology for model-based multichannel detection was formulated using third-order cumulants to identify the model parameters for models in the time series class. This methodology builds on the work of Metford (1984) and of Michels (1991) by the significant inclusion of higher-order statistics.

The SSC methodology can be applied for single-cell detection, which corresponds to the cases wherein the temporal statistics of the radar return are non-Gaussian. The methodology can be applied also for global detection, wherein the spatial statistics of the radar return are non-Gaussian. In these applications the use of third-order cumulants to identify model parameters provides immunity to additive Gaussian noise and interference sources because all higher-order cumulants are zero for Gaussian-distributed processes.

Simulation-based analyses were carried out to validate key aspects of the methodology, and to establish the feasibility of an HOS-based approach to model-based multichannel detection. Results obtained to date suggest the capability to discriminate between target-present and target-absent hypotheses using the suboptimal

and approximate detection rule proposed by Metford (1984) for non-Gaussian signals.

In Phase I several key technical issues were addressed, and candidate resolution approaches were identified. Those issues are discussed in this report, and are summarized in Table 6-1. Most of those issues will be addressed further during Phase II.

Several technical tasks have been identified also for further research and development in Phase II. These tasks are summarized next.

Processor Requirements Definition. Determination of the potential of the SSC methodology for radar system applications requires the establishment of requirements for the radar problems of interest at RL. This includes space/time processing in a surveillance radar array system, and fusion of data from multiple distinct radar systems. Similarly, requirements must be identified for non-defense applications of interest.

Additional Analyses and Detailed Algorithm Formulation. The analyses listed below are required in order to generate a detailed algorithm definition and to assess the SSC methodology in the context of the applications requirements. These analyses support the technical issues listed in Table 6-1.

- Alternative matrix parameter identification algorithms (such as the multichannel M-slice algorithm for ARMA parameter estimation) will be analyzed to select the one which best satisfies the trade-offs associated with performance and other relevant criteria.

ISSUE	COMMENTS	CANDIDATE RESOLUTION APPROACHES
Possible symmetry of marginal PDF of the quadrature components.	Not an issue in the cases (if any) where the marginal PDF of the quadrature components is asymmetric. (The marginal PDF is unknown for most non-Gaussian quadrature components.)	A. Apply zero-memory nonlinear transformation to the quadrature components. B. Use formulation based on fourth-order cumulants.
Non-minimum phase model parameter estimates.	<ul style="list-style-type: none"> Major issue only for MA models. Impact on ARMA models needs to be assessed further. 	A. Average estimates over several resolution cells. B. Use AR (or possibly ARMA) models only. C. Use non-causal formulation.
Complex-valued probabilistic representation is restrictive.	Restrictions are enhanced for non-Gaussian sequences.	A. Use PDF representation based on concatenated real-valued vectors.
Detection rule for non-Gaussian sequences.	Sub-optimal approximations may provide satisfactory performance.	A. Use Metford's approximate detection rule for non-Gaussian sequences. B. Use non-parametric detection rule.
Non-Gaussian multichannel data generation for performance evaluation.	<ul style="list-style-type: none"> Generation of temporal multichannel processes with specified multivariate PDF is an unsolved problem. Linear filtering of a non-Gaussian process induces Gaussianity or symmetry in the PDF. This increases the size of the data base required to obtain satisfactory cumulant estimates. 	A. Apply zero-memory nonlinear transformation to the quadrature components. B. Use SIRP-based data generation for global domain detection problems. C. Investigate alternative techniques such as extension of the Liu and Munson (1982) approach to vector processes.

Table 6-1. List of key technical issues and candidate resolution approaches.

- Giannakis and Delopoulos (1990) have demonstrated that the covariance sequence can be estimated from the third-order cumulants. Thus, it is possible to define an identification approach which combines the insensitivity to additive Gaussian noise offered by third-order cumulants with the robustness of covariance-based model identification methods for parametric models (Michels, 1991; Román and Davis, 1993). This combined approach will be investigated, with emphasis on the accuracy of the HOS-based covariance sequence estimate.
-
- Model order selection criteria for on-line and off-line decisions will be evaluated and the preferred criterion will be adopted. Criteria to be evaluated include approaches based on the singular values of higher-order normal matrices for AR and ARMA models, and approaches based on matrix norms applied to third-order cumulants for MA models.
- The performance of the Metford (1984) detection rule for non-Gaussian signals needs to be established. Alternative detection rules will be identified and considered as appropriate. One option is to use non-parametric detection methods with the pseudo-innovations sequence (Table 6-1). Another option is frequency-domain detection of moving targets using the bispectrum (the Fourier transform of the third-order cumulant sequence).
- Identification and detection performance will be compared with that of other methods. This includes covariance-based methods using time series as well as state space models.
- Key implementation parameters will be established for the selected application(s). This includes the minimum required

channel output sequence duration, and the order of the two whitening filters.

Real-Time Processor Architecture Design. A real-time architecture should be developed for the methodology formulated in Phase I, including identification of candidate hardware. Such an architecture should meet the requirements identified early in Phase II for the radar and non-defense applications. The very large scale integration (VLSI) systolic architecture developed by Liu and Jen (1992) for the IBDA of Metford and Haykin (1985) provides a point of departure since the methodology of Phase I is related to the IBDA.

The major computational task of the methodology formulated in Phase I is estimation of the third-order cumulants. Fortunately, the estimators for cumulants exhibit a highly parallel structure. Stellakis and Manolakos (1993) have developed a two-stage VLSI architecture to estimate the third-order cumulants of a real-valued scalar sequence which may be extended to the multichannel case (their architecture is applicable also to the estimation of fourth-order cumulants). In Phase II SSC will pursue extension of the Stellakis-Manolakos architecture to the multichannel case, and explore alternative architectures.

REFERENCES

- B. D. O. Anderson and J. B. Moore
(1979) Optimal Filtering, Prentice-Hall, Inc., Englewood Cliffs, NJ.
- D. R. Brillinger and M. Rosenblatt
(1967) "Computation and Interpretation of kth-Order Spectra," in Spectral Analysis of Time Series, B. Harris (editor), J. Wiley & Sons, Inc., New York, NY, pp. 189-232.
- N. C. Currie (editor)
(1989) Radar Reflectivity Measurement: Techniques And Applications, Artech House, Norwood, MA.
- J. J. Dongarra, C. B. Moler, J. R. Bunch, and G. W. Stewart
(1979) LINPACK User's Guide, Society for Industrial and Applied Mathematics (SIAM), Philadelphia, PA.
- V. N. Faddeeva
(1959) Computational Methods of Linear Algebra, Dover Publications, Inc., New York, NY.
- G. B. Giannakis, Y. Inouye, and J. M. Mendel
(1989) "Cumulant based identification of multichannel moving-average models," IEEE Transactions on Automatic Control, Vol. 34, No. 7 (July), pp. 783-787.
- J. W. Goodman
(1984) Statistical Optics, J. Wiley & Sons, Inc., New York, NY.

N. R. Goodman

- (1963) "Statistical analysis based on a certain multivariate complex Gaussian distribution (an introduction)," Annals of Mathematical Statistics, Vol. 34 (March), pp. 152-177.

N. A. J. Hastings and J. B. Peacock

- (1974) Statistical Distributions - A Handbook for Students and Practitioners, J. Wiley & Sons, Inc., New York, NY.

S. Haykin, B. W. Currie, and S. B. Kesler

- (1982) "Maximum entropy spectral analysis of radar clutter," Proceedings of the IEEE, Vol. 70, No. 9 (September), pp. 953-962.

A. G. Jaffer, M. H. Baker, W. P. Ballance, and J. R. Staub

- (1991) Adaptive Space-Time Processing Techniques for Airborne Radars, RL Technical Report No. RL-TR-91-162, Rome Laboratory, Griffiss AFB, NY.

E. Jakeman and P. N. Pusey

- (1976) "A model for non-Rayleigh sea echo," IEEE Transactions on Antennas and Propagation, Vol. AP-24, No. 6 (November), pp. 806-814.

B. Jelonnek and K.-D. Kammeyer

- (1992) "Improved methods for the blind system identification using higher order statistics," IEEE Transactions on Signal Processing, Vol. 40, No. 12 (December), pp. 2947-2960.

I. I. Jouny and R. L. Moses

(1992) "The bispectrum of complex signals: definitions and properties," IEEE Transactions on Signal Processing, Vol. 40, No. 11 (November), pp. 2833-2836.

D. J. Lewinski

(1983) "Non-stationary probabilistic target and clutter scattering models," IEEE Transactions on Antennas and Propagation, Vol. AP-31, No. 3 (May), pp. 490-498.

C. -M. Liu and C. -W. Jen

(1992) "A parallel adaptive algorithm for moving target detection and its VLSI array realization," IEEE Transactions on Signal Processing, Vol. 40, No. 11 (November), pp. 2841-2848.

B. Liu and D. C. Munson, Jr.

(1982) "Generation of a random sequence having a jointly specified marginal distribution and autocovariance," IEEE Transactions on Acoustics, Speech, and Signal Processing, Vol. ASSP-30, No. 6 (December), pp. 973-983.

A. L. Maffett

(1989) Topics for a Statistical Description of Radar Cross Section, J. Wiley & Sons, Inc., New York, NY.

J. I. Marcum and P. Swerling

(1960) "Studies of target detection by pulsed radar," IRE Transactions on Information Theory, Vol. IT-6, No. 2 (April), pp. 59-267.

S. L. Marple, Jr.

(1987) Digital Spectral Analysis With Applications, Prentice-Hall, Inc., Englewood Cliffs, NJ.

J. M. Mendel

(1991) "Tutorial on higher-order statistics (spectra) in signal processing and system theory: theoretical results and some applications," Proceedings of the IEEE, Vol. 79, No. 3 (March), pp. 278-305.

P. A. S. Metford

(1984) An Innovations Approach to Discrete-Time Detection Theory With Application to Radar, Ph. D. dissertation, Electrical Engineering Department, McMaster University, Hamilton, Ontario, Canada.

P. A. S. Metford and S. Haykin

(1985) "Experimental analysis of an innovations-based detection algorithm for surveillance radar," IEE Proceedings, Vol. 132, Pt. F, No. 1 (February), pp. 18-26.

P. A. S. Metford, S. Haykin, and D. P. Taylor

(1982) "An innovations approach to discrete-time detection theory," IEEE Transactions on Information Theory, Vol. IT-28, No. 2 (March), pp. 376-380.

J. H. Michels

(1991) Multichannel Detection Using the Discrete-Time Model-Based Innovations Approach, RL Technical Report No. RL-TR-91-269, Rome Laboratory, Griffiss AFB, NY.

F. E. Nathanson

(1991) Radar Design Principles (second edition), McGraw-Hill, Inc., New York, NY.

L. M. Novak, M. B. Sechtin, and M. J. Cardullo

(1989) "Studies of target detection algorithms that use polarimetric radar data," IEEE Transactions on Aerospace and Electronic Systems, Vol. 25, No. 2 (March), pp. 150-165.

A. V. Oppenheim and R. W. Schaffer

(1975) Digital Signal Processing, Prentice-Hall, Inc., Englewood Cliffs, NJ.

A. Papoulis

(1984) Probability, Random Processes, and Stochastic Variables (second edition), McGraw-Hill, Inc., New York, NY.

M. C. Pease

(1965) Methods of Matrix Algebra, Academic Press, Inc., New York, NY.

R. S. Raghavan

(1991) "A method for estimating parameters of K-distributed clutter," IEEE Transactions on Aerospace and Electronic Systems, Vol. 27, No. 2 (March), pp. 238-246.

M. R. Raghuveer

(1986) "Multichannel bispectrum estimation," Proceedings of the Third Annual ASSP Workshop on Spectrum Estimation and Modeling, Boston, MA, pp. 21-24.

M. R. Raghuveer and C. L. Nikias

- (1985) "Bispectrum estimation: a parametric approach," IEEE Transactions on Acoustics, Speech, and Signal Processing, Vol. ASSP-33, No. 5 (October), pp. 1213-1230.

M. Rangaswamy

- (1992) Spherically Invariant Random Processes for Radar Clutter Modeling, Simulation, and Distribution Identification, Ph. D. dissertation, Electrical Engineering Department, Syracuse University, Syracuse, NY.

M. Rangaswamy, P. Chakravarthi, D. Weiner, L. Cai, H. Wang, and A. Ozturk

- (1993) Signal Detection in Correlated Gaussian and Non-Gaussian Radar Clutter, RL Technical Report No. RL-TR-93-79, Rome Laboratory, Griffiss AFB, NY.

M. Rangaswamy, D. Weiner, and J. H. Michels

- (1993) "Multichannel detection for correlated non-Gaussian random processes based on innovations," presented at the SPIE International Symposium on Optical Engineering and Photonics in Aerospace and Remote Sensing (Conference 1955), April 12-16, Orlando, FL.

J. R. Román and D. W. Davis

- (1993) State-Space Models for Multichannel Detection, RL Technical Report No. RL-TR-93-146, Rome Laboratory, Griffiss AFB, NY.

H. H. Rosenbrock

- (1970) State-space and Multivariable Theory, J. Wiley & Sons, Inc., New York, NY.

M. Sekine, T. Musha, Y. Tomita, T. Haggisawa, T. Irabu, and E. Kiuchi

- (1979) "On Weibull-distributed weather clutter," IEEE Transactions on Aerospace and Electronic Systems, Vol. AES-15, No. 6 (November), pp. 824-828.

W. L. Simkins

- (1981) RADC Clutter Model, RADC Report (November), Rome Laboratory, Griffiss AFB, NY.

M. L. Skolnik

- (1980) Introduction to Radar Systems (second edition), McGraw-Hill, Inc., New York, NY.

H. M. Stellakis and E. S. Manolakos

- (1993) "An architecture for the estimation of higher order cumulants," Proceedings of the IEEE International Conference on Acoustics, Speech, and Signal Processing (ICASSP), April 27-30, Minneapolis, MN, Vol. IV, pp. 220-223.

A. Swami, G. B. Giannakis, and J. M. Mendel

- (1989) "A unified approach to modeling multichannel ARMA processes," Proceedings of the IEEE International Conference on Acoustics, Speech, and Signal Processing (ICASSP), Glasgow, Scotland, United Kingdom, pp. 2182-2185.

J. B. Thomas

- (1969) An Introduction to Statistical Communication Theory, J. Wiley & Sons, Inc., New York, NY.

L. Tong, Y. Inouye, and R. Liu

- (1992) "A finite-step global convergence algorithm for the parameter estimation of multichannel MA processes," IEEE Transactions on Signal Processing, Vol. 40, No. 10 (October), pp. 2547-2558.

S. Watts

- (1987) "Radar detection prediction in K-distributed sea clutter and thermal noise," IEEE Transactions on Aerospace and Electronic Systems, Vol. AES-23, No. 1 (January), pp. 40-45.

D. B. Williams and D. H. Johnson

- (1993) "Robust estimation of structured covariance matrices," IEEE Transactions on Signal Processing, Vol. 41, No. 9 (September), pp. 2891-2906.

F.-C. Zheng, S. McLaughlin, and B. Mulgrew

- (1993) "Blind equalization of nonminimum phase channels: Higher order cumulant based algorithm," IEEE Transactions on Signal Processing, Vol. 41, No. 2 (February), pp. 681-691.

Rome Laboratory
Customer Satisfaction Survey

RL-TR-_____

Please complete this survey, and mail to RL/IMPS,
26 Electronic Pky, Griffiss AFB NY 13441-4514. Your assessment and
feedback regarding this technical report will allow Rome Laboratory
to have a vehicle to continuously improve our methods of research,
publication, and customer satisfaction. Your assistance is greatly
appreciated.
Thank You

Organization Name: _____ (Optional)

Organization POC: _____ (Optional)

Address: _____

1. On a scale of 1 to 5 how would you rate the technology
developed under this research?

5-Extremely Useful 1-Not Useful/Wasteful

Rating_____

Please use the space below to comment on your rating. Please
suggest improvements. Use the back of this sheet if necessary.

2. Do any specific areas of the report stand out as exceptional?

Yes___ No_____

If yes, please identify the area(s), and comment on what
aspects make them "stand out."

3. Do any specific areas of the report stand out as inferior?

Yes___ No___

If yes, please identify the area(s), and comment on what aspects make them "stand out."

4. Please utilize the space below to comment on any other aspects of the report. Comments on both technical content and reporting format are desired.

***MISSION
OF
ROME LABORATORY***

Mission. The mission of Rome Laboratory is to advance the science and technologies of command, control, communications and intelligence and to transition them into systems to meet customer needs. To achieve this, Rome Lab:

- a. Conducts vigorous research, development and test programs in all applicable technologies;
- b. Transitions technology to current and future systems to improve operational capability, readiness, and supportability;
- c. Provides a full range of technical support to Air Force Materiel Command product centers and other Air Force organizations;
- d. Promotes transfer of technology to the private sector;
- e. Maintains leading edge technological expertise in the areas of surveillance, communications, command and control, intelligence, reliability science, electro-magnetic technology, photonics, signal processing, and computational science.

The thrust areas of technical competence include: Surveillance, Communications, Command and Control, Intelligence, Signal Processing, Computer Science and Technology, Electromagnetic Technology, Photonics and Reliability Sciences.



DEPARTMENT OF THE AIR FORCE
AIR FORCE RESEARCH LABORATORY (AFRL)

15 Jun 04

MEMORANDUM FOR DTIC-OCQ

ATTN: Larry Downing
Ft. Belvoir, VA 22060-6218

FROM: AFRL/IFOP

SUBJECT: Distribution Statement Change

1. The following documents (previously limited by SBIR data rights) have been reviewed and have been approved for Public Release; Distribution Unlimited:

ADB226867, "Multichannel System Identification and Detection Using Output Data Techniques", RL-TR-97-5, Vol 1.

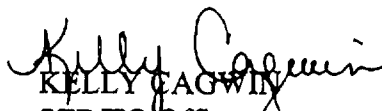
ADB176689, "Multichannel System Identification and Detection Using Output Data Techniques", RL-TR-93-141.

ADB198116, "Multichannel Detection Using Higher Order Statistics", RL-TR-95-11.

ADB232680, "Two-Dimensional Processing for Radar Systems", RL-TR-97-127.

ADB276328, "Two-Dimensional Processing for Radar Systems", AFRL-SN-RS-TR-2001-244.

2. Please contact the undersigned should you have any questions regarding this memorandum. Thank you very much for your time and attention to this matter.


KELLY CAGWIN
STINFO Officer
Information Directorate
315-330-7094/DSN 587-7094